INVESTIGATIONS OF THE ELECTRODE-SOLUTION INTERFACE IN MICROHETEROGENEOUS SOLUTIONS INVOLVING SURFACTANTS

By

STACEY E. BOYETTE

A DISSERTATION PRESENTED TO THE GRADUATE SCHOOL
OF THE UNIVERSITY OF FLORIDA IN PARTIAL FULFILLMENT
OF THE REQUIREMENTS FOR THE DEGREE OF
DOCTOR OF PHILOSOPHY

UNIVERSITY OF FLORIDA

1991

ACKNOWLEDGEMENTS

Praise God for giving me the ability and the opportunity to pursue a higher education. May I serve Him well.

Thanks go to my parents and my brother, Rodney, who have suffered and celebrated with me from childhood to adulthood. Their love and support is invaluable.

Thanks go to my friends scattered up and down the East coast who are too many to name but too precious not to mention.

Special thanks go to the chemistry faculty at Georgia Southern University for their friendship and encouragement throughout this past year. I look forward to working with them next year.

Last of all, thanks go to the members, past and present, of the small but powerful Toth group, especially S.A. Myers, Mike Freund, Allan Witkowski, Shi-Min Zhu, Liakat Bodalbhai, and Dr. Anna Brajter-Toth.

The funding for my work came from a variety of sources, including U.S. Army Chemical Research, Development, and Engineering Center, the Division of Sponsored Research at the University of Florida, the National Institutes of Health, and Battelle (Research Triangle Park, NC).

TABLE OF CONTENTS

LIST OF TABLES

LIST OF FIGURES

Abstract of Dissertation Presented to the Graduate School
of the University of Florida in Partial Fulfillment of the
Requirements for the Degree of Doctor of Philosophy

INVESTIGATIONS OF THE ELECTRODE-SOLUTION INTERFACE IN MICROHETEROGENEOUS SOLUTIONS INVOLVING SURFACTANTS

By

Stacey E. Boyette

August, 1991

Chairman: Dr. Anna Brajter-Toth
Major Department: Chemistry

The purpose of this research was to develop new modified carbon electrode surfaces for the detection of small biological molecules. Carbon electrodes are frequently used in electroanalytical chemistry, and rough pyrolytic graphite (RPG) and glassy carbon (GC) electrodes were chosen for this work. Graphite electrodes, like other solid electrodes, are prone to memory effects and frequently exhibit poor sensitivity or poor reproducibility. Many methods have been developed to improve the reactivity of graphite electrodes by direct modification of the electrode surface, such as pretreatment methods, resurfacing techniques, and surface coating procedures. In this work, a new method of indirect modification of the electrode surface by manipulating the solution environment was developed.

Surfactants, at concentrations above and below CMC, were used to modify analyte solutions. No systematic studies of the effects of surfactants on probe responses have been reported, although the use of surfactants in electrochemistry is not a new concept. The objective of this work was to provide a systematic study which would allow predictions of the effects of a given surfactant on a particular probe response.

The effects of surfactants on the electrochemistry of dopamine, hydroquinone, 2,6-diamino-8-purinol (DAPOL), and 3,4-dihydroxyphenylacetic acid (DOPAC) were investigated at RPG and GC electrodes. All of these probes undergo two electron/two proton oxidation in the same potential window and have known adsorption properties on graphite surfaces. At pH 7, two of the probes, hydroquinone and DAPOL, are neutral, while the other two probes, dopamine and DOPAC, are charged. Dopamine is positively charged and DOPAC is negatively charged. To investigate interactions at the electrode-solution interface, anionic (sodium dodecyl sulfate (SDS)), cationic (hexadecyltrimethylammonium bromide (CTAB)), and nonionic (Triton X-100) surfactants were used.

Surfactants adsorb at RPG and GC surfaces and attractive interactions between probe molecules and adsorbed surfactants enhance probe responses at both electrodes. Interactions between specific probe-surfactant pairs observed from the electrochemistry were verified and quantified by micellar HPLC results.

CHAPTER I

INTRODUCTION

Theories of Graphite Activity

Graphite surfaces have found many applications in analytical chemistry. Consequently, the characterization of graphite surfaces has become a major topic of interest, especially with respect to the relationship between structure and reactivity. Graphite electrodes, including glassy carbon and pyrolytic graphite, are widely used in electroanalysis, although the specific parameters controlling electrode activity are not well understood. Graphite electrodes generally have low residual currents and are very useful over a large potential range; however, the apparent rate of heterogeneous charge-transfer is slower for most compounds at carbon electrodes than at metal electrodes [1-3]. Various pretreatment methods have been devised to increase the electrochemical activity of graphite surfaces, including heating [2-6], laser irradiation [7-12], exposure to radio frequency plasmas [13-15], polishing [3,5-7,16-18], and chemical [19,20], and electrochemical [1,3,7,9,21-28] procedures. Many explanations for the improvement in electrochemical response of carbon electrodes following pretreatment have been formulated; some indicate changes in physical properties of the carbon surface, such as surface roughness and edge plane density, while others deal with the chemistry of the electrode surface. Although the

activation mechanism appears to be different for each pretreatment method, it is evident that cleanliness of the electrode surface plays a crucial role in graphite electrode activity [3,4,16,18,29]. Impurities are known to adsorb onto electrode surfaces and contribute to the deactivation of the surface [8,10,16,18]. One common effect of pretreatment methods is to remove contaminants and clean the electrode surface as part of the activation process [4,5,7-10,12,16,18,21,25].

It is frequently proposed that electrode activation is due to an increase in active sites [3,4,6,30], although what constitutes active sites remains undefined. Electron Spectroscopy for Chemical Analysis (ESCA) studies of heat-treated [2], highly polished [18], electrochemically pretreated [21], and RF plasma treated [13,14] carbon electrodes have shown an increased oxygen concentration or oxygen-to-carbon ratio on the electrode surface as compared to corresponding untreated electrodes. Results such as these, along with electrochemical observations, at carbon surfaces have led many researchers to implicate surface oxygen functionalities, such as carboxyl and quinoidal groups, in the activation of carbon electrodes [13-15,18,27,31-34]. However, it has been shown that heat treatments at high temperatures eliminates surface redox functionalities while activating the electrode surface [4,6]; thus, surface functionalities are not necessary for rapid electron transfer. Consistent with increased oxygen concentrations at activated electrodes, researchers have observed the formation of graphite oxide layers on electrochemically pretreated carbon electrodes [1,25,28], which can selectively activate the electrode surface based on permeability and/or ion-exchange properties.

Poon and McCreery [12] have demonstrated that laser treatment can remove the effects of electrochemical pretreatment of glassy carbon and suggest that this implies removal of an oxygen-rich surface film. Likewise, Hershenhart, McCreery, and Knight [8] have reported that intense pulsed laser radiation of electrodes removes polymeric or adsorbed films while creating an active surface.

Laser and other pretreatment methods may activate graphite surfaces by increasing the edge plane density [3,9,11,22,29,35]. It has been reported that graphite edge orientation is necessary for fast electron transfer [3,9]. Graphitic edge planes are hydrophilic while the basal plane orientation is hydrophobic [3,36]. Indirect evidence for electrode activation due to an increase in edge planes can be found in reported correlations between accelerated electron transfer rates and increased hydrophilicity (and wettability) upon pretreatment [5,20,21,31,37]. Direct evidence for graphite activation via increased edge plane density can be found in Raman and electrogenerated chemiluminescence studies of highly ordered pyrolytic graphite (HOPG) [9,22,29,35]. Raman studies of HOPG show a correlation between the intensity of a band at 1360 cm^{-1}, which is proportional to density of edge planes, and electron transfer activation [9,22,29]. High intensity of the 1360 cm^{-1} band corresponds to larger heterogeneous rate constants for laser and electrochemically pretreated electrodes [9,22,29]. Electrogenerated chemiluminescence studies of HOPG show enhanced electron-transfer kinetics at regions rich in edge plane defects compared with regions of undisturbed basal plane HOPG [35]. The electron-transfer rate constant for luminol oxidation differed by more than two

orders of magnitude between the two types of regions [35]. The activation theories involving high surface oxygen concentrations and edge plane orientation are not in direct conflict, since it appears that edge planes are the sites for the formation of oxygen functionalities [3,33,36] and for the nucleation and rapid growth of graphite oxides [23,34]. In light of the many different surface pretreatments that effectively activate a variety of carbons, it seems obvious that no single mechanism or property of carbon surfaces can explain all of the observed electrochemical behaviors [5,38]. More than likely it is a combination of effects that leads to the activation of pretreated graphite electrodes to heterogeneous charge transfer [28,31,34,38].

Purpose of Proposed Work

The focus of the work presented in this report is not direct characterization of active graphite electrodes, but rather exploitation of that activity for the detection of small biological molecules. However, it is expected that the results of this work will provide insight into the electron transfer and mass transfer processes occurring at the electrode surface. High electrochemical reactivity for different types of electron transfer systems such as outer-sphere systems including ferri/ferrocyanide [2-4,9,10,16-19,22,25], ferrocene [18], and ruthenium and cobalt hexamines [1,19], and inner-sphere systems including ascorbic acid [1-5,8,10,12,18,31,39], hydroquinone [10,12,18,25,28], and catechols [1,5,9,10,12,18,24,27,28,38,39] such as dopamine, 3,4-dihydroxyphenylacetic acid (DOPAC), and 4-methylcatechol, can be observed on active (or activated) graphite surfaces. Sensitive electrochemical responses on graphite electrodes are frequently accompanied by adsorption [1,7,24-28,40-42]. As

a result, the relationship between adsorption and electrochemical activity has attracted much attention [6,7,27,41]. One way to investigate the relationship between probe adsorption and electrode activity is to study the electrochemistry of adsorbing compounds while controlling the electrode-solution interface. The electrode-solution interface may be controlled and manipulated by either modifying the electrode surface itself or by modifying the solution environment of the analyte. In the work presented here, a new method combining both approaches of controlling the electrode-solution interface is used; the electrochemistry of adsorbing compounds on graphite surfaces is investigated in solutions containing surfactants and micelles.

Surfactants and Micelle Systems in Electrochemistry

Effects of Surfactants and Micelles on Electrochemical Parameters

The use of surfactants and micelles in electroanalytical chemistry has been well documented in several reviews [43-47]. The concentration and nature of surfactant used in electroanalysis can affect the shape of the electrochemical wave, the half-wave potential, electron transfer rates at the electrode, diffusion and transfer coefficients, limiting currents, and the stability of intermediate species [44,45]. Low concentrations of surfactants have been used for years as maxima suppressors or selective masking agents in polarographic analysis [44,45,47-49]. At higher concentrations, above the critical micelle concentration (CMC), micelles are formed which have the ability to solubilize water-insoluble or sparingly soluble species in aqueous media. Largely due to their solubilizing power, micelles have

been used in conjunction with ferrocene to form mediator-titrants [50,51], as stabilizers for electrochemically generated ion radical intermediates [52-57], and to improve the electrochemistry of organic compounds in aqueous media [58-60]. Ohsawa and Aoyagui [59] demonstrated that it is even possible to determine the formal standard potential of a water-insoluble substance in aqueous media using micellar electrochemistry in conjunction with solubility measurements.

Practical Considerations in Micellar Electrochemistry

Although micelles are considered to be relatively simple models for enzymatic and membrane environments [45,55], they present a rather complex electrochemical situation. Two fundamental processes must be considered when discussing electrochemistry in micellar solutions: 1) interaction of analytes and reaction products with micelles, and 2) interaction of surfactants with the electrode surface. This situation becomes further complicated if the analyte (or reaction product) adsorbs at the electrode surface. For example, in their studies of the reductive electrochemistry of methyl viologen (MV^{2+}) on glassy carbon, Kaifer and Bard [55] found that the product of one-electron reduction of MV^{2+}, the MV cation radical ($MV^{+\cdot}$), adsorbs on glassy carbon in the presence of the negatively charged surfactant, sodium dodecyl sulfate (SDS), at concentrations below the CMC due to interaction with SDS molecules adsorbed on the electrode surface. However, at SDS concentrations above the CMC, adsorption of $MV^{+\cdot}$ is eliminated due to solubilization of $MV^{+\cdot}$ in SDS micelles in solution.

Solubilized species may reside in various regions of a micelle [44-46,61], some penetrate far into the hydrophobic core, some remain near the micelle-solution interface around the hydrophilic head groups, and others may orient themselves somewhere between these two extremes. Although much of the literature indicates a trend of preferential interaction of ions and ion radicals with oppositely charged micelles [52-57,62], neither the stability nor the electrochemistry of these species in micellar aggregates can be predicted based solely on electrostatic considerations [55]. The strength of interactions between electroactive species and micelles [54,62], the structure [55,60,62] and size [60] of the micelle, as influenced by supporting electrolyte and solubilized species, and the ability of the electroactive species to move in and out of the micelles [44,53,54], will all influence the observed electrochemical response.

Methods of Quantitating Analyte-Micelle Interactions

Several methods for quantitating the strength of interactions between analyte molecules and micelles have been reported, including fluorescence and phosphorescence quenching [63-66], electrochemistry in micellar media [44,59,67], and micellar liquid chromatography [68,69]. Luminescence quenching techniques are based on a correlation between the magnitude of quenching observed in the presence of micelles and the entrance and exit rate constants for probes and/or quenchers in micelles, which are related to the micelle-solute equilibrium association constants (i.e., binding constants) [63-66]. Binding constants determined from luminescence quenching data have been reported for a variety of systems including

neutral arenes in ionic micelles [63] and transition metal dications in anionic micelles [65]. Electrochemical methods for determining binding constants between probes and micelles depend on the relationship between shifts in half-wave potentials ($E_{1/2}$) in micellar solutions compared to those in aqueous solutions and are determined by the extent of probe-micelle interactions [44,59,67]. The mathematical relationship between $E_{1/2}$ and association constants of electroactive species with micelles, developed by Ohsawa et al. [59,67], will be discussed later.

Micellar liquid chromatography techniques for determining binding constants are based on the correlation between changes in mobile phase micelle concentration and changes in probe retention, as measured by capacity factors [68-70]. Arunyanart and Cline-Love have used micellar liquid chromatography to determine micelle-solute binding constants for a series of uncharged aromatic solutes [68] and charged aromatic compounds, such as organic acids and bases, which participate simultaneously in other equilibria [69]. Foley [70] has compiled over 150 solute-micelle association (binding) constants for a variety of neutral compounds and phenylthiohydantoin-amino acids based on micellar liquid chromatography data. In the work reported here, in addition to the electrochemical measurements, micellar chromatographic techniques were used to investigate the extent of interaction between the probe molecules and micelles.

Surfactant Adsorption at Solid-Liquid Interfaces

Interfacial Parameters

Aside from interactions between surfactants and probes, the interactions between surfactants and the electrode surface must also be considered when dealing with electrochemistry in surfactant media. A characteristic feature of surfactants is their tendency to adsorb at solid-liquid interfaces [56,61]. Surfactant adsorption has been studied to determine: 1) the concentration of surfactant at the interface, since it is a measure of coverage; 2) the orientation of a surfactant at the interface, since it indicates whether the interface becomes more hydrophilic or more hydrophobic as a result of surfactant adsorption; and 3) energy changes, ΔG, ΔH, and ΔS, in the system, resulting from adsorption, since they provide insight into the type and mechanism of surfactant interactions at the interface [61].

Adsorption Mechanisms

Possible mechanisms by which surfactants may adsorb onto solid substrates from aqueous solutions are: 1) ion-exchange; 2) ion pairing; 3) hydrogen bonds or Lewis acid - Lewis base reaction; 4) adsorption by π-π overlap; 5) adsorption by London-van der Waals dispersion forces; and 6) hydrophobic bonding [61].

Surfactant Molecules at Hydrophilic Surfaces

Surfactants are amphiphilic molecules consisting of a hydrophobic portion (tail group) and a hydrophilic portion (head group). If an electrode surface is hydrophilic or has charge opposite to that of the surfactant head group, the surfactant will bind with the hydrophilic head group oriented toward the surface

(Figure 1). At low surface coverage, the hydrocarbon tail groups may coil [61], bend, or orient skewed to the electrode surface [71] to obtain the most energetically favorable configuration (Figure 1(a)). For alkylbenzene sulfonates on mineral oxide surfaces, it has been reported that terminal carbons on tail groups having 10 carbons or more may strongly interact with the surface in addition to the electrostatic attraction between the charged head group and the surface [72]. As adsorption and surface coverage increase on hydrophilic surfaces, head groups become more closely packed and hydrocarbon chains align perpendicular, for the most part, to the electrode surface (Figure 1(b)) [71-74]. Once the binding sites on the surface are saturated with surfactant molecules, adsorption may continue through the formation of two-dimensional surfactant aggregates called hemimicelles (Figure 1(c)) [61,71,72,75-78]. In the formation of hemimicelles, oncoming surfactant molecules adsorb with reversed orientation and overlap with already adsorbed surfactants due to the hydrophobic interactions between tail groups (*normal* hemimicelles) [61,71].

Surfactant Molecules at Hydrophobic Surfaces

If an electrode surface is hydrophobic, surfactant molecules will adsorb onto the surface with the hydrophobic tail groups toward the surface and the head groups toward the aqueous phase (Figure 2) [61]. At low surface coverage, surfactant molecules may be parallel to the surface, slightly tilted from the surface, or L-shaped (Figure 2(a)). As adsorption increases, surfactant molecules align more and more perpendicular to the surface with the head groups oriented toward the solution (Figure 2(b)) [61,78]. The formation of *reverse* hemimicelles of 1-decanol at the

Figure 1: Surface model for the adsorption of surfactant molecules at hydrophilic surfaces, such as RPG in aqueous media, for: a) low surface coverage, b) increased surface coverage, and c) hemimicelle formation.

a)

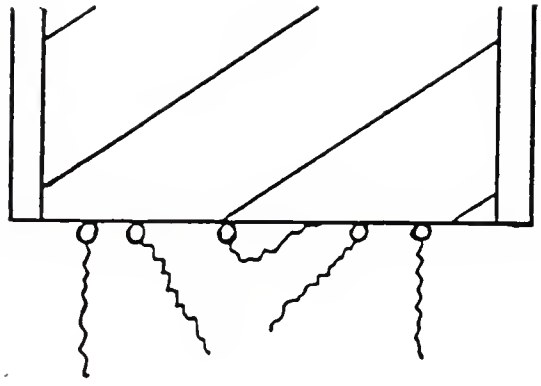

b)

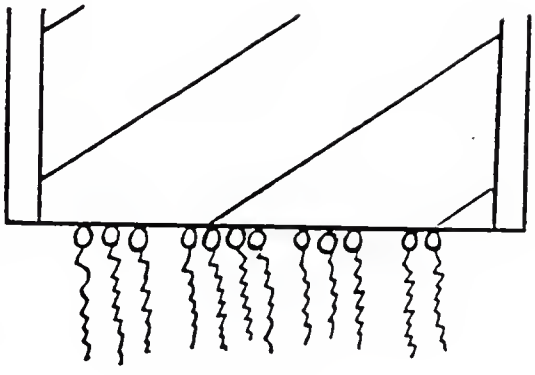

c)

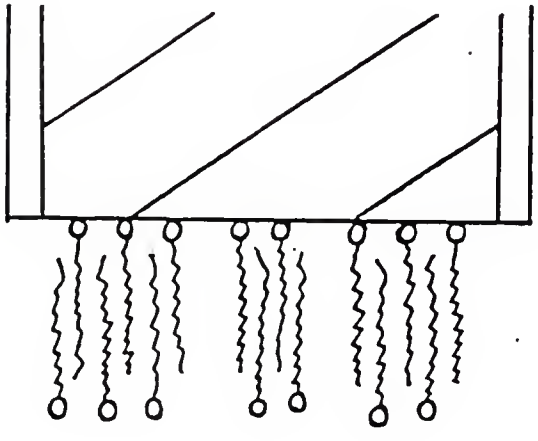

Figure 2: Surface model for the adsorption of surfactant molecules at hydrophobic surfaces, such as GC in aqueous media, for: a) low surface coverage, b) increased surface coverage, and c) the unlikelihood of reverse hemimicelle formation.

a)

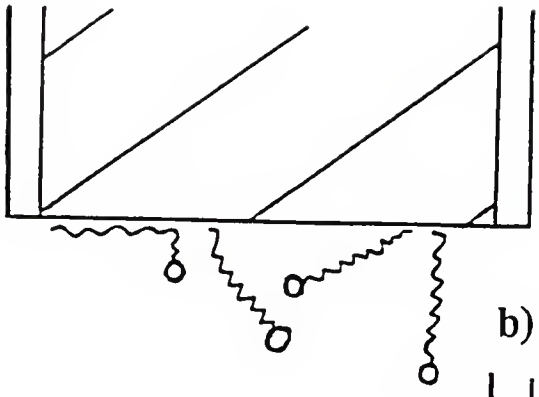

b)

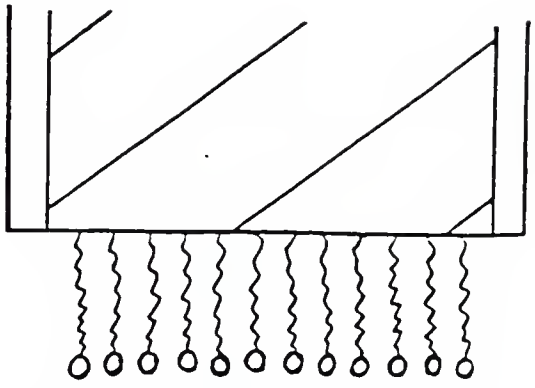

c)

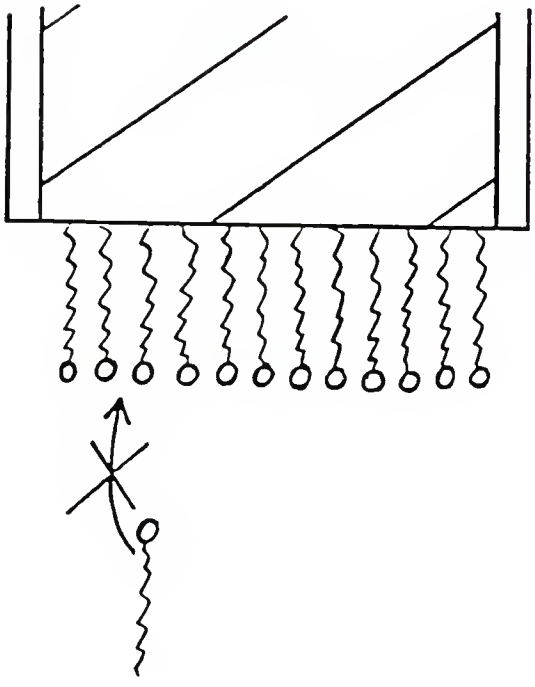

heptane/carbon black interface, due to strong polar interactions between head groups, has been reported by Zhu and Gu [79]. However, in aqueous solutions, the formation of reverse hemimicelles is unlikely, especially for charged surfactants, since head groups will not attract and will interact with the aqueous environment (Figure 2(c)).

At surfactant concentrations above the critical micelle concentration, normal micelles, three-dimensional aggregates with the head groups oriented outward from a hydrophobic core (aqueous media), would also be expected to bind to hydrophilic surfaces (in addition to hemimicelles), while reverse micelles, with tail groups oriented outward from a hydrophilic core (organic media), would be expected to bind to hydrophobic surfaces.

When surfactants and micelles adsorb at the solution-electrode interface, changes occur in the interfacial tension, the double-layer structure, and the rate of electron transfer at the electrode [43,44,47]. Several reports have appeared [48,49,55-58,60,73,74,80,81] which discuss the formation of adsorbed layers on electrode surfaces in surfactant and micellar solutions and the effects these films have on electrochemical responses. The effects on surfactants of electrochemistry have been studied for a wide variety of redox couples and surfactants at different electrodes, in various potential windows, and for a variety of surfactant concentrations in aqueous and nonaqueous media. The nonsystematic nature of these studies makes it impossible to deduce any broad conclusions about electrochemistry in the presence of surfactants. Systematic investigations of the

effects of surfactants on the electrical double layer as well as on the kinetics and thermodynamics of electron transfer processes are needed before the predictions of surfactant effects on the electrochemistry of a given probe will be possible.

Systems Studied

In this work, the electrochemical oxidation of four small biological molecules was investigated at graphite electrodes in aqueous surfactant and micellar media. Micellar liquid chromatography was performed to verify and quantify probe-micelle interactions observed in the electrochemical work.

Probes

The four probes studied were dopamine (DA), 3,4-dihydroxyphenylacetic acid (DOPAC), 2,6-diamino-8-purinol (DAPOL), and hydroquinone (HQ) (Figure 3). These four probes were chosen on the basis of size, structure, biological significance, and similarities in electrochemical behavior on carbon surfaces. All four probe molecules have molecular weights below 250 g/mole. By choosing small molecules, it was hoped that problems typical for large biological molecules, such as slow heterogeneous electron transfer, would be avoided. These four probes are structurally different and provide examples of a positively charged probe (DA), a negatively charged probe (DOPAC), and two neutral probes (DAPOL and HQ) at pH 7 (Figure 3). Each of the probes is of biological significance: dopamine is a central nervous system neurotransmitter [20,24], DOPAC is a metabolite of dopamine [20], DAPOL is a biological degradation product of 2,6-diaminopurine (a growth inhibitor of bacterial and mammalian cells) [42], and hydroquinone

Figure 3: Structure of probe molecules at pH 7.

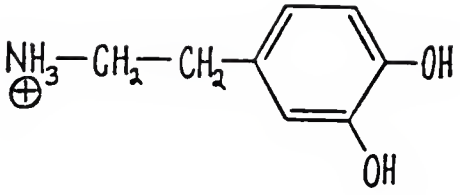

Dopamine
3-hydroxytyramine
pK_a=8.92

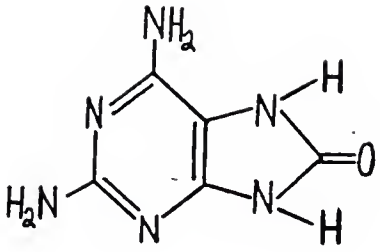

DAPOL
2,6-diamino-8-purinol
$pK_{a1}\approx 2.0$; $pK_{a2}=10$

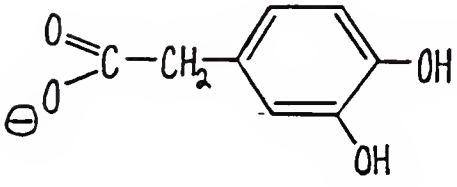

DOPAC
3,4-dihydroxyphenylacetic acid
$pK_{a1}=4.22$; $pK_{a2}=9.58$; $pK_{a3}=12.15$

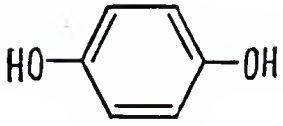

Hydroquinone
1,4-dihydroxybenzene
$pK_{a1}=9.91$; $pK_{a2}=12.04$

derivatives participate in electron transport in living organisms ranging from fungi to vertebrates [82]. Therefore, the detection of these molecules is of interest to the chemist and biochemist alike. Electrochemically, all four probes undergo a two electron/two proton oxidation in the same potential window [2,18,25,42,82] and have known adsorption properties on graphite [2,27,28,42].

Surfactants

The surfactants used to modify the electrochemical behavior of the probe molecules were chosen based on their charges. Since we have anionic, cationic, and neutral probes, we selected representative anionic, cationic, and nonionic surfactants to investigate analyte-surfactant interactions and their effect on the observed electrochemistry. Sodium dodecyl sulfate (SDS), cetyltrimethylammonium bromide (CTAB), and Triton X-100 (Figure 4) were chosen as the anionic, cationic, and nonionic modifiers, respectively.

Electrodes

The electrochemistry was studied at rough pyrolytic graphite (RPG) and glassy carbon (GC) electrodes. RPG and GC provide two structurally [7,30,34,83,84] and electrochemically (as prepared here) [5-7,16,21,30] different graphite surfaces for the evaluation of probe responses and surfactant effects on probe responses. RPG is a polycrystalline form of carbon manufactured by depositing carbon from the vapor phase onto a substrate [34]. RPG is characterized by a high degree of orientation of carbon layers and shows high electrical conductivity in the plane parallel to the surface of deposition (edge plane) and low conductivity in the plane

Figure 4: Structure of surfactant molecules.

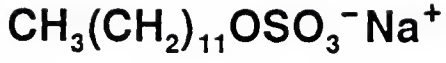

SDS
sodium dodecyl sulfate

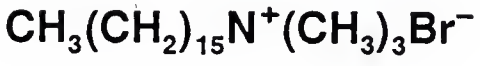

CTAB
cetyltrimethylammonium bromide

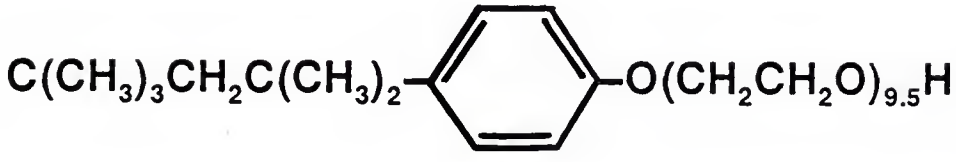

Triton X-100
octyl phenoxy polyethanol

perpendicular to the surface of deposition (basal plane) [30,34]. Amorphous GC is formed by the pyrolysis of phenolic polymers [83] and consists of tangled aromatic ribbon molecules with strong intra-ribbon carbon-carbon bonds cross-linked by highly strained (i.e., weaker) inter-ribbon carbon-carbon bonds [30,83]. Activated graphite surfaces, such as the silicon carbide-polished RPG used here, exhibit hydrophilic character [5,20,21,31,37] and high electrochemical reactivity [7,30]. Unactivated graphite surfaces, such as the alumina-polished GC used here, exhibit hydrophobic character [5,37,85] and low electrochemical reactivity [5-7,16,21,30].

Presented here is a systematic study of the effects of surfactant and micellar systems on the electrochemical behavior of four structurally different probes. The results provide new insights into the role of surfactant, micelle, and electrode surface interactions in the electrochemistry of small adsorbing biological molecules and provide information which may lead to improved electrochemical analysis of these species.

CHAPTER II

EXPERIMENTAL SECTION

Reagents

A pH 7 phosphate buffer of ionic strength 1.0 M was prepared from anhydrous dibasic sodium phosphate, Na_2HPO_4 (Mallinckrodt, Inc.) and monobasic sodium phosphate, NaH_2PO_4 x H_2O (Mallinckrodt, Inc.; Fisher Scientific Co.) in deionized-distilled water. The pH of the phosphate buffer was measured using a Corning pH Meter 130. Adjustments of pH of the buffer solution were made by adding small amounts of either phosphoric acid, H_3PO_4 (Mallinckrodt Chemical Works), or sodium hydroxide, NaOH (Fisher Scientific Co.), as needed. The pH 7 phosphate buffer (μ=1.0) was diluted to ionic strengths of 0.5 M for use in electrochemical experiments and 0.05 M for use in micellar HPLC and UV spectroscopy experiments. All experiments were run at room temperature, 25 ($\pm$1)°C.

The probe compounds, 3-dihydroxytyramine hydrochloride (dopamine) (Sigma Chemical Co.), 3,4-dihydroxyphenylacetic acid (DOPAC) (Sigma Chemical Co.), 2,6-diamino-8-purinol hemisulfate monohydrate (DAPOL) (Aldrich Chemical Co.), and hydroquinone (HQ) (Chem Service, Westchester, PA), and the surfactants, sodium lauryl sulfate (SDS) (Fisher Scientific Co.), hexadecyltrimethylammonium

bromide (CTAB) (Sigma Chemical Co.), and Triton X-100 (Sigma Chemical Co.), were used as received. The pK_a values for the probe molecules are:

Probe	pK_{a1}	pK_{a2}	pK_{a3}	REF.
dopamine	8.92			[86]
DOPAC	4.22	9.58	12.15	[87]
DAPOL	2.0	10.0		[7]
hydroquinone	9.91	12.04		[88]

The CMC's and aggregation numbers for SDS, CTAB, and Triton X-100 in water at 25(±1)°C are:

	SDS	CTAB	Triton X-100
CMC (mM):	2.25* [55]	1.3 [47]	0.24 [89]
Agg. #:	62 [47]	78.0 [47]	140.0 [90]

*determined in 50 mM NaCl.

Electrochemical Apparatus and Procedures

Electrode Preparation

Rough pyrolytic graphite (RPG) and glassy carbon (GC) electrodes were made by sealing a ca. 0.05 cm^2 piece of RPG or a ca. 3 mm diameter rod of GC in glass tubing with epoxy (Hysol Aerospace and Industrial Products Division). GC electrodes were initially polished on 600-grit silicon carbide paper (Mark V Laboratory) using a Buehler Ecomet I Polisher-Grinder before being polished by

hand to a glassy finish with gamma alumina suspensions of particle sizes finer than 0.1 μm (Gamal, Fisher Scientific) on an alpha A polishing cloth (Mark V Laboratory). The electrodes were resurfaced prior to each measurement. After the final polish, GC electrodes were ultrasonicated for 5-10 min in doubly distilled water, and gently wiped with a Kimwipe. RPG electrodes were resurfaced on 600-grit silicon carbide paper using the Buehler Ecomet I Polisher-Grinder, rinsed with deionized-distilled water, and gently wiped with a Kimwipe.

Electrochemical Methods

Electrode areas were determined using chronocoulometry with a Bioanalytical Systems electrochemical analyzer, BAS 100, with a Houston Instruments DMP-40 Series Digital Plotter (Bausch & Lomb). The reference electrode was an Saturated Calomel Electrode (SCE) (Fisher Scientific Co.) and the counter electrode was a 0.8 cm square Pt ribbon (Sargent). The potential was stepped from 0.400 to 0.0 V vs SCE at a pulse width of 250 ms. Electrode areas were determined in solutions of 4.0 mM potassium ferricyanide, $K_3Fe(CN)_6$ (Fisher Scientific Co.), in 1.0 mM potassium chloride, KCl (Fisher Scientific Co.), using a diffusion coefficient of $D_o = 7.63 \times 10^{-6}$ cm^2/s [91]. Solutions were deaerated for at least 5 min with nitrogen and kept under nitrogen atmosphere during chronocoulometric experiments. Measurements were taken immediately after placing resurfaced RPG and GC electrodes in solution. The electrode areas determined by chronocoulometry were $(3.5 - 5.2) \times 10^2$ cm^2 for RPG electrodes and $(4.0 - 7.5) \times 10^{-2}$ cm^2 for GC electrodes.

Cyclic voltammetry was performed using an EG & G Princeton Applied Research - Model 173 Potentiostat/Galvanostat, EG & G PARC - 175 Universal Programmer, and a Houston Instruments Omnigraphic 2000 Recorder (Bausch & Lomb). The working electrodes were RPG and GC electrodes, the counter electrode was a Pt wire electrode, and the reference electrode was an SCE with a 4% agar/KCl salt bridge. All probe solutions consisted of a single analyte dissolved in a pH 7 phosphate buffer (μ = 0.5 M) plus one of the following: 1) a single surfactant at concentrations below the CMC and 2) a single surfactant at concentrations above the CMC. Electrode response as a function of time, t_{dip}, was studied by varying the length of time that the electrode was exposed to solution at an open circuit before activating the cell. Cyclic voltammograms (CVs) were taken at exposure times of 0, 2, 5 and 10 min at a scan rate of 200 mV/s in the potential window -0.5 V to +0.75 V, encompassing the formal potentials for all probes which lie between -0.12 V and +0.40 V at both RPG and GC electrodes. Voltammetric peak currents obtained from exposure time studies were normalized for electrode area and probe concentration. Electrode response as a function of scan rate was investigated at scan rates of 5, 20, 50, 100, 200, and 500 mV/s in the potential window -0.5 V to +0.75 V for all probes on RPG and for DAPOL on GC. Measurements were made at scan rates of 10, 20, 50, 100, and 200 mV/s in the same potential window as above for DA, DAPOC, and HQ on GC. Scan rate studies were run at t_{dip} = 0 min unless otherwise stated. All sample solutions were deaerated for at least 5 min with nitrogen and kept under nitrogen atmosphere

during electrochemical experiments. All potentials are reported vs SCE and at room temperature, 25(±1)°C.

Fundamentals of Electrochemical Measurements

Electrochemical parameters, such as cyclic voltammetric anodic peak currents (i_{pa}), separation of cathodic and anodic peak potentials (ΔE_p, where $\Delta E_p = E_{pc} - E_{pa}$, with E_{pc} and E_{pa} representing the cathodic and anodic peak potentials, respectively), and slopes of log i_{pa} (anodic peak current) vs log v (scan rate), were measured at different electrode exposure times to the analyte solution, t_{dip}, in order to study electrode reactivity, electron transfer kinetics, and surface interactions.

Peak current measurements at different electrode exposure times to the analyte solution are of interest since changes in peak current (i.e., sensitivity) with exposure time are indicative of analyte adsorption onto the electrode surface [7,8,92]. Decreases in peak current (i.e., deactivation of the electrode surface) with increasing exposure time are associated with adsorption, such as physisorption, i.e., relatively weak, long-range adsorption, of a probe onto the electrode surface and chemisorption, i.e., strong, specific adsorption, which is indicated by an initial increase in peak current with exposure time [7,8,92].

Measurements of ΔE_p values provide insight into the processes controlling heterogeneous electron transfer (i.e., diffusion or adsorption) and the reversibility of those processes. According to theory for reversible (fast) heterogeneous electron transfer [92], ΔE_p values for a diffusion controlled process will be 59/n (mV), where n is the number of electrons transferred per mole, and ΔE_p for an adsorption

controlled process will be 0. If the electron transfer kinetics are slow (i.e., quasi-reversible or irreversible), larger than predicted ΔE_p values will be obtained (i.e., $\Delta E_p > 59/n$ (mV) for a diffusion controlled process and $\Delta E_p > 0$ (mV) for adsorption controlled process). The probe molecules studied here undergo $2e^-/2H^+$ oxidation [5,7,42,82], so that ΔE_p values of approximately 30 mV are expected if the oxidation is reversible and strictly diffusion controlled.

Slope values for plots of log i_{pa} (anodic peak current) vs log v (scan rate) indicate to what degree probe molecules adsorb at the electrode surface. According to theory for a diffusion controlled electron transfer process [92], the equation defining cyclic voltammetric peak current for a reversible system is:

$$i_p = (2.69 \times 10^5) n^{3/2} A D_o^{1/2} v^{1/2} C_o^* \qquad (1)$$

and for an irreversible system is:

$$i_p = (2.99 \times 10^5) n(\alpha n_a)^{1/2} A C_o^* D_o^{1/2} v^{1/2} \qquad (2)$$

where n is the number of electrons per mole oxidized or reduced, A is the area of the electrode (cm^2), D_o is the diffusion coefficient (cm^2/sec), v is the scan rate (V/s), C_o^* is the bulk concentration of the electroactive species (mol/cm^3), α is the transfer coefficient, and n_a is the number of electrons in the rate-determining step. The equation defining peak current for an adsorption controlled electron transfer process [92] for a reversible system is:

$$i_p = \frac{n^2 F^2}{4RT} v A \Gamma_o \qquad (3)$$

and for an irreversible system is:

$$i_p = \frac{n\alpha n_a F^2 A v \Gamma_o}{2.718RT} \quad (4)$$

where Γ_o is the surface excess of the electroactive species (mol/cm^2), F is the Faraday constant, R is the ideal gas constant, and T is the absolute temperature (K). Based on these equations, plots of log i_{pa} vs log v should be linear and have slopes values of 0.5 for diffusion (since $i_p \alpha v^{1/2}$) and 1.0 for adsorption (since $i_{pa} \alpha v$) independent of electrochemical kinetics.

Determination of Equilibrium Binding Constants (K_{eq}) from Electrochemical Data

Differences between the formal potentials observed for probe responses in phosphate buffer and those observed in micellar media are indicative of differences in the strength of binding of the reduced and oxidized probes with surfactant aggregates. The formal potential for a probe, E°', is calculated from the equation:

$$E^{o'} = \frac{E_{pc} + E_{pa}}{2} \quad (5)$$

where E_{pc} and E_{pa} represent the cathodic and anodic peak potentials, respectively. The equilibria for binding of the reduced and oxidized forms of a probe to a surfactant aggregate can be expressed as:

$$Ox(aq) + M \rightleftharpoons Ox\text{-}M \qquad K_o \quad (6)$$

$$Red(aq) + M \rightleftharpoons Red\text{-}M \qquad K_R \quad (7)$$

and the electrochemical reactions are:

$$Ox(aq) + e^- \rightleftharpoons Red(aq) \qquad E^{o'}_{aq} \tag{8}$$

$$Ox\text{-}M + e^- \rightleftharpoons Red\text{-}M \qquad E^{o'}_{M} \tag{9}$$

where Ox and Red represent the oxidized and reduced forms of the probe, respectively, Ox-M represents the oxidized form of the probe bound to a surfactant aggregate, Red-M represents the reduced form of the probe bound to a surfactant aggregate, and M represents a surfactant aggregate which may be a micelle or a hemimicelle. In the case presented here, probe molecules are expected to interact with surfactant molecules adsorbed onto the electrode surface in the form of hemimiclles. A scheme similar to the one reported by Kaifer and Bard [55] can be used to more clearly illustrate the relationship between the equilibria expressed in equations 6-9:

$$\begin{array}{ccc} Ox(aq) + e^- & \rightleftharpoons & Red(aq) \\ +M \;\; \Updownarrow & & \Updownarrow \;\; +M \\ Ox\text{-}M + e^- & \rightleftharpoons & Red\text{-}M \end{array}$$

At a given potential, E, the Nernst equation for the redox reaction in phosphate buffer (denoted by aq) and the redox reaction in micellar media (denoted by M) can be written:

$$E = E^{o'}_{aq} + \left(\frac{RT}{nF}\right)\ln\left(\frac{[Ox_{aq}]}{[Red_{aq}]}\right) \tag{10}$$

and

$$E = E^{o'}_{m} + \frac{RT}{nF} \ln \frac{[Ox\text{-}M]}{[Red\text{-}M]} \tag{11}$$

equations (10) and (11) can be combined to yield:

$$E^{o'}_{M} - E^{o'}_{aq} = \frac{RT}{nF} \ln \frac{[Ox_{aq}]}{[Red_{aq}]} - \frac{RT}{nF} \ln \frac{[Ox\text{-}M]}{[Red\text{-}M]} \tag{12}$$

which can be rearranged as follows:

$$E^{o'}_{M} - E^{o'}_{aq} = \frac{RT}{nF} \ln \left\{ \frac{[Ox_{aq}]}{[Red_{aq}]} \frac{[Red\text{-}M]}{[Ox\text{-}M]} \right\}, \tag{13}$$

$$E^{o'}_{M} - E^{o'}_{aq} = \frac{RT}{nF} \ln \left\{ \frac{[Ox_{aq}]}{[Ox\text{-}M]} \frac{[Red\text{-}M]}{[Red_{aq}]} \frac{[M]}{[M]} \right\} \tag{14}$$

and

$$E^{o'}_{M} - E^{o'}_{aq} = \frac{RT}{nF} \ln \left\{ \frac{[Ox_{aq}][M]}{[Ox\text{-}M]} \frac{[Red\text{-}M]}{[Red_{aq}][M]} \right\} \tag{15}$$

The equilibrium constants for the binding of the probe forms to a surfactant aggregate are defined as:

$$K_R = \frac{[Red\text{-}M]}{[Red_{aq}][M]} \qquad \text{for the reduced form and} \qquad (16)$$

$$K_o = \frac{[Ox\text{-}M]}{[Ox_{aq}][M]} \qquad \text{for the oxidized form} \qquad (17)$$

which can be substituted into equation (15) to obtain the relationship between changes in formal potential and binding constants:

$$E^{o'}_M - E^{o'}_{aq} = \frac{RT}{nF} \ln \frac{K_R}{K_o} \qquad (18)$$

The probe molecules studied in this work undergo a two electron/two proton oxidation and reduction, so that equation (18) becomes:

$$E^{o'}_M - E^{o'}_{aq} = \frac{RT}{2F} \ln \frac{K_R[H^+]^2}{K_o[H^+]^2}. \qquad (19)$$

Since the pH is constant throughout the redox reaction, the proton concentration terms can be neglected yielding:

$$E^{o'}_M - E^{o'}_{aq} = \frac{RT}{2F} \ln \frac{K_R}{K_o} \qquad (20)$$

Differences between the formal potentials observed for probe responses in phosphate buffer, $E^{o'}_{aq}$, and those observed in micellar media, $E^{o'}_{M}$, provide a means of evaluating the strength of interaction of the oxidized probe with surfactant aggregates relative to the strength of interaction of the reduced probe with surfactant aggregates. The probe molecules studied in this work are purchased in the reduced form, so that the K_{eq} calculated from HPLC data, which will be discussed in this chapter in the Micellar Chromatography Theory Section, are the binding constants for the reduced form of the probe, K_R. Shifts in formal potential, $E^{o'}_{M} - E^{o'}_{aq}$, obtained from the electrochemical data indicate the strength of probe interactions with surfactant aggregates in the form of hemimicelles, while equilibrium constants obtained from HPLC data indicate the strength of probe interactions with micelles. The strength of probe binding with a surfactant is thermodynamically independent of the structure of the aggregate, however the number of surfactant molecules in an aggregate may affect the amount of probe that interacts with the aggregate. Assuming that the aggregation number for a hemimicelle is the same as that for a micelle, shifts in formal potential, $E^{o'}_{M} - E^{o'}_{aq}$, and the binding constants for the reduced probe, K_R, can be used to calculate the binding constant for the oxidized probe, K_o, from equation (25). Since K_o can only be calculated relative to K_R in this work, the absolute numerical values of K_o and K_R are less important than the relative values of K_o and K_R for comparing strengths of interactions of the oxidized and reduced probes with surfactant aggregates.

Chromatographic Apparatus and Procedures

HPLC System

A Macintosh computer-controlled Rainin gradient HPLC system (Rainin Instruments Co., Inc.) with ultraviolet-visible detection was used to perform micellar chromatography. A Rheodyne sample injection valve (20 µl sample loop), a Spectroflow 757 Absorbance Detector (Applied Biosystems Inc.), and a Fisher Recordall Series 5000 chart recorder (Houston Instruments) were included in the HPLC set-up. The columns used for these experiments were reversed-phase Microsorb 5 µm C18 columns (15 cm x 4.6 mm i.d.) with guard columns (1.5 cm x 4.6 mm i.d.) (Rainin Instruments Co., Inc.). A precolumn (15 cm x 4.6 mm i.d.) packed with silica gel (Adsorbosil Silica, 200/425 Mesh) was located between the pumps and the sample injector to saturate the mobile phase with silica and minimize dissolution of analytical column packing. A filter between the injector and the analytical column was used to protect the guard column and the analytical column from precolumn silica particles which may be drawn out by mobile phase. All experiments were performed at a flow rate of 1.0 ml/min with the column at room temperature, 25(±1)°C.

Choice of Detector Wavelength Maxima

Ultraviolet (UV) spectra for each probe were recorded on a Tracor Northern TN-6500 diode array spectrophotometer to determine absorbance maxima and the stability of probe solutions. HPLC detector wavelength settings were chosen based on these spectra. Solutions used to record UV spectra contained a single probe in

pH 7 phosphate buffer (0.05 M) and a single surfactant at a concentration above CMC. The phosphate-SDS buffer solutions contained 0.050 M SDS and the phosphate-CTAB solutions contained 6.0 mM CTAB. Solutions were prepared just prior to initial data acquisition and were studied over a period of time up to 5 hrs. From the UV spectra obtained, a detector wavelength of 280 nm was selected for the detection of dopamine, DOPAC, and HQ and a wavelength of 246 nm was selected for the detection of DAPOL.

Procedures in Micellar Chromatography

Micellar mobile phase solutions were prepared by dissolving SDS and CTAB in deionized-distilled water. SDS mobile phases which contained 0.020, 0.040, 0.060, and 0.080 M SDS were prepared. CTAB mobile phases which contained 2.00, 4.01, 6.00, 8.00, and 10.1 mM CTAB were prepared. All mobile phases were filtered through 0.45 μm Nylon 66 membrane filters (Alltech Associates, Inc.). SDS mobile phases were filtered three times before use and the CTAB mobile phases were filtered twice to ensure that all sizable particles were removed from solution. HPLC sample solutions were prepared fresh daily and contained a single probe in pH 7 phosphate buffer (0.05 M) and either 0.050 M SDS or 6.0 mM CTAB.

SDS and CTAB micellar HPLC was performed on two separate columns. Initial attempts at performing micellar HPLC with mobile phase surfactant concentrations slightly above CMC were plagued by irreproducible retention times for consecutive probe solution injections. Retention times continually increased for injections of probes known to interact with the C18 stationary phase. These changes

in retention times were interpreted as indicating adsorption of surfactant molecules from the mobile phase onto the stationary phase which eventually leads to complete coverage (i.e., saturation) of the stationary phase with surfactant molecules. In chromatography, analyte molecules partition between the mobile phase and the stationary phase. In the case presented above, the stationary phase is constantly being altered by surfactant adsorption onto the column, while the properties (e.g., surfactant concentration) of the mobile phase remain constant. As the amount of surfactant adsorbed on the column increases, the retention times of probes that interact with this surfactant increase due to an increase in "surfactant" stationary phase sites. In the case of probes that interact with the C18 stationary phase, retention times decrease as surfactant adsorption increases due to a decrease in available C18 stationary phase sites. Gradual increases in column pressure during the above experiments also indicated that the column was being "loaded" with surfactant molecules. As surfactant molecules adsorb onto the stationary phase, the inside diameter of the column is decreased, causing an increase in column back pressure. In order to obtain reproducible results, it was decided that columns should be saturated with the mobile phase surfactant prior to experiments. The column to be used with SDS mobile phases was saturated with SDS molecules by flushing the column with a 0.060 M SDS solution in 10% methanol until reproducible retention times for HQ injections were obtained (over 120 mL of this solution were passed through the column). The column to be used with CTAB mobile phases was saturated with CTAB molecules by flushing the column with a

10.07 mM CTAB aqueous solution until reproducible retention times for DAPOL injections were obtained (over 120 mL of this solution were passed through the column). HQ and DAPOL are not strongly retained on the SDS and CTAB columns, respectively, so that injections of these samples provide a quick check for column saturation.

Solubility experiments showed that CTAB was soluble in methanol and sparingly soluble in water while SDS was soluble in water and insoluble in methanol. Thus, column loading with CTAB occurs on a reasonable scale in terms of time and materials in an aqueous solution, while it is necessary to add methanol to the SDS "loading" mobile phase to ensure efficient saturation of the column with SDS. While using the columns daily, the SDS column was rinsed with and stored in methanol overnight and the CTAB column was rinsed with and stored in water overnight. The SDS column was not flushed with water between experiments since this procedure would remove some of the loaded SDS from the column. The CTAB column was not flushed with methanol between experiments for the same reason. It is usually undesirable to store columns in water for extended periods of time, especially when buffers are used, since this provides an environment favorable for the growth of microbes. However, storing columns in water that are used daily does not seem to degrade column performance over a two to three week experimental period. When the work on both columns was complete, the SDS column was flushed with large amounts of water and the CTAB column was flushed with large amounts of methanol in an effort to remove some of the surfactant molecules from

the columns. Total removal of the surfactants from the columns was not possible. Methanol was used for long term storage of both columns.

Micellar Chromatography Theory

In micellar HPLC, changes in probe retention with changes in mobile phase surfactant concentration can be used to determine the strength of the interactions between probes and micelles. The calculation of equilibrium constants for analyte-micelle interactions from micellar HPLC data depends on a linear relationship between the reciprocal of the capacity factor, 1/k′, and the strength of the mobile phase, as determined by the concentration of surfactant (i.e., micellar aggregates) in the mobile phase, $[M_m]$ [68,70]. As discussed in the previous section, the stationary phase in micellar chromatography is covered with surfactant molecules. Therefore, a probe that interacts with the surfactant will partition between the stationary phase and the mobile phase due to the presence of surfactant molecules in both phases. Since the column is saturated with surfactant, the concentration of surfactant molecules on the stationary phase will remain effectively constant throughout the experiment, while the mobile phase surfactant concentration may be changed by changing mobile phase concentration. Changes in probe retention with changes in mobile phase strength (i.e., concentration) are due to an increase or decrease in the number of sites of interaction (i.e., micelles) in the mobile phase. The magnitude of the change in retention time (in the form of 1/k′) with increasing mobile phase strength (i.e., molar concentration of surfactant in the mobile phase, $[M_m]$) provides a measure of probe-micelle interaction.

Three reversible equilibria are involved in reversed-phase micellar chromatography [68,70]: 1) interaction between probe in bulk mobile phase, P_m, and stationary phase sites, S_s, to form the complex PS_s; 2)interaction between probe in bulk mobile phase, P_m, and surfactant molecules in micellar aggregates in the mobile phase, M_m, to form the complex PM_m; and 3) transfer of probe in a complex with a micelle, PM_m, to stationary phase sites to form the complex PS_s.

$$P_m + S_s \overset{K_1}{\rightleftharpoons} PS_s \tag{21}$$

$$P_m + M_m \overset{K_2}{\rightleftharpoons} PM_m \tag{22}$$

$$PM_m + S_s \overset{K_3}{\rightleftharpoons} PS_s + M_m \tag{23}$$

The subscripts denote the location of a species in the mobile phase (m) and the stationary phase (s). K_1 and K_2 are the respective binding constants for the probe with the stationary phase and the mobile phase, while K_3 describes the exchange equilibrium for the probe between the mobile and stationary phases.

The capacity factor is a measure of probe retention and is given by $k' = (t_R - t_m)/t_m$, where t_R is the retention time for a given probe and t_m is the retention time of the solvent. The capacity factor can be expressed in terms of the above equilibria as:

$$k' = \frac{\phi[S_s]K_1}{(1 + K_2[M_m])}, \qquad (24)$$

where ϕ is the phase ratio (i.e., the ratio of the volume of stationary phase to the volume of the mobile phase in the column) and $[M_m]$, expressed in moles/Liter, is calculated from the equation $[M_m]$ = [surfactant] - CMC [68,70]. Notice that K_3 is absent from equation (24). It is assumed that probes bind to stationary phase sites as shown in equation (21). The interaction between probe-micelle complexes and the stationary phase as shown in equation (23) is considered to be negligible [68,70]. Therefore, equilibrium (23) is not significant in the retention mechanism of probe molecules. Equation (24) can be linearized as:

$$1/k' = \frac{[M_m]K_2}{\phi[S_s]K_1} + \frac{1}{\phi[S_s]k_1} \qquad (25)$$

A plot of $1/k'$ vs $[M_m]$ should yield a straight line with a slope of $K_2/\phi[S_s]K_1$ and an intercept of $1/\phi[S_s]K_1$ from which K_2 can be calculated. K_2 (eqn. 22) is defined as the binding constant for the interaction between the analyte and a single surfactant molecule that is part of a micellar aggregate in the bulk mobile phase. Therefore, the equilibrium constant for the interaction between the analyte and the entire

micelle, K_{eq}, is calculated by multiplying K_2 by the aggregation number for the given surfactant.

$$K_{eq} = K_2 \times \text{Agg. } \# \qquad (26)$$

CHAPTER III

ELECTROCHEMICAL BEHAVIOR OF PROBE MOLECULES ON GRAPHITE ELECTRODES

The focus of this work is the study of surfactant effects on the reactivity of graphite electrodes for small biological materials. In order to elucidate the effects of surfactants on the electrochemical behavior of analyte molecules, it was necessary to first characterize the response of the analytes in the absence of surfactants. Therefore, the electrooxidation of dopamine (DA), DOPAC, DAPOL, and hydroquinone (HQ) was investigated at rough pyrolytic graphite (RPG) and glassy carbon (GC) electrodes in pH 7 phosphate buffer.

The electrochemical results obtained here confirm other reports that these molecules adsorb from pH 7 buffered aqueous solutions on activated graphite electrode [2,7,24-28,42] and do not adsorb on unactivated graphite electrodes [5,7]. Cyclic voltammetric experiments on RPG electrodes yielded sharp, symmetrically shaped peaks, small separations between cathodic and anodic peak potentials (ΔE_p), and slopes of log i_{pa} vs log v significantly above 0.5, all of which indicate probe adsorption on the electrode [92]. Cyclic voltammetric experiments on GC electrodes yielded broad peaks, large ΔE_p values, and slopes of log i_{pa} vs log v slightly below 0.5, all of which indicate slow electron transfer with no adsorption. The

electrochemical behavior of the probe molecules on these two surfaces is discussed in further detail below.

Results and Discussion for Rough Pyrolytic Graphite

In Figures 5a, 6a, 7a, and 8a, representative cyclic voltammograms are shown which illustrate the peak shapes indicative of adsorption [92] and give a qualitative look at ΔE_p and sensitivity of probe responses on RPG. Cyclic voltammograms of DAPOL (Figure 5a) show two oxidation peaks. It has been reported [84] that the first oxidation peak (I_a) is controlled by a combination of diffusion and adsorption, while the second oxidation peak (II_a) is controlled by relatively strong adsorption (ΔG_{Red} = -8.3 kcal/mol) of the reactant. Quantitative results and discussion of the electrochemistry of DAPOL in this report will concern the first oxidation peak unless otherwise specified, since the peaks observed for the other three probes are controlled by the same combination of diffusion and adsorption as the processes at this peak. Dopamine (Fig. 6a), DOPAC (Fig. 7a), and hydroquinone (Fig. 8a) exhibit one sharp oxidation peak and the corresponding reduction peak in the potential window studied.

Probe Adsorption

Slope values of log i_{pa} vs log v plots for the probe molecules on RPG in pH 7 phosphate buffer (0.5M) are shown in Table 1. Slope values for all four probe molecules are significantly larger than 0.5 (Table 1), the theoretical value for strictly diffusion controlled electron transfer, indicating contributions from adsorption to probe responses. As shown in Table 1, the responses of DAPOL and hydroquinone

Figure 5: Cyclic voltammograms of 0.2 mM DAPOL at RPG vs SCE in pH 7 phosphate buffer (μ=0.5M) containing: a) no surfactant, b) 3.080 mM CTAB, c) 9.36 mM SDS, and d) 2.253 mM Triton X-100; exposure time to analyte solution t_{dip} = 0 min; v = 200 mV/s; 20μA scale; electrode area (RPG) = 4.4 ($\pm$1.2) x 10^{-2} cm^2.

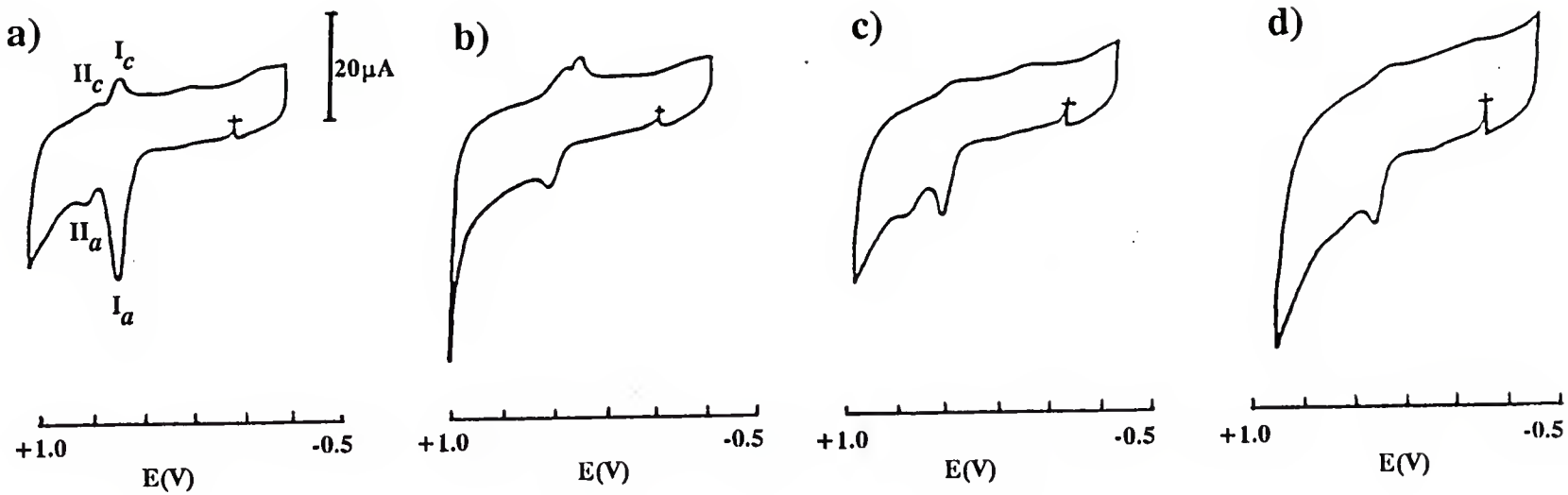
a)
I_c
II_c
20μA
II_a
I_a
+1.0
-0.5
E(V)
b)
+1.0
-0.5
E(V)
c)
+1.0
-0.5
E(V)
d)
+1.0
-0.5
E(V)

Figure 6. Cyclic voltammograms of 0.5 mM dopamine at RPG vs SCE in pH 7 phosphate buffer (μ = 0.5 M) containing: a) no surfactant, b) 3.043 mM CTAB, c) 9.26 mM SDS, and d) 3.196 mM Triton X-100; exposure time to analyte solution t_{dip} = 0 min; v = 200 mV/s; 20 μA scale; electrode area (RPG) = 4.4 ($\pm$1.2) x 10^{-2} cm^2.

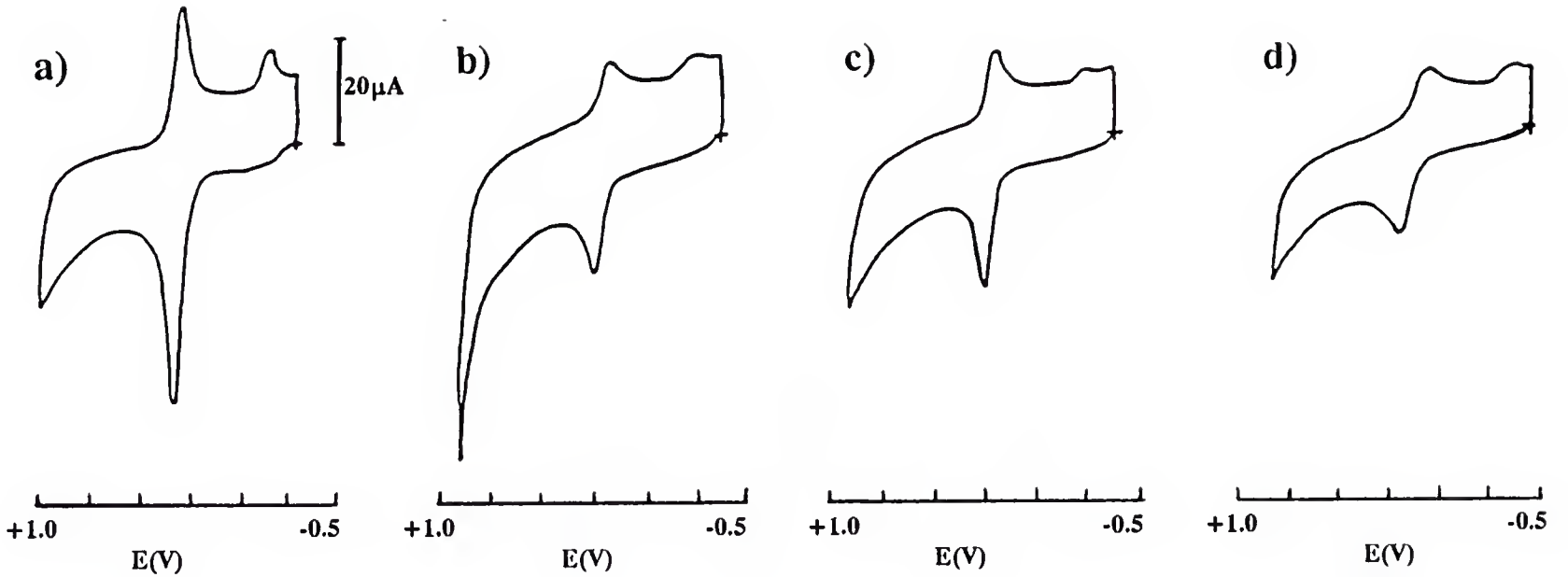
a)
20μA
+1.0
-0.5
E(V)
b)
+1.0
-0.5
E(V)
c)
+1.0
-0.5
E(V)
d)
+1.0
-0.5
E(V)

Figure 7. Cyclic voltammograms of 0.5 mM DOPAC at RPG vs SCE in pH 7 phosphate buffer (μ = 0.5 M) containing: a) no surfactant, b) 3.147 mM CTAB, c) 9.71 mM SDS, and d) 2.624 mM Triton X-100; exposure time to analyte solution t_{dip} = 0 min; v = 200 mV/s; 20 μA scale; electrode area (RPG) = 4.4 ($\pm$1.2) x 10^{-2} cm^2.

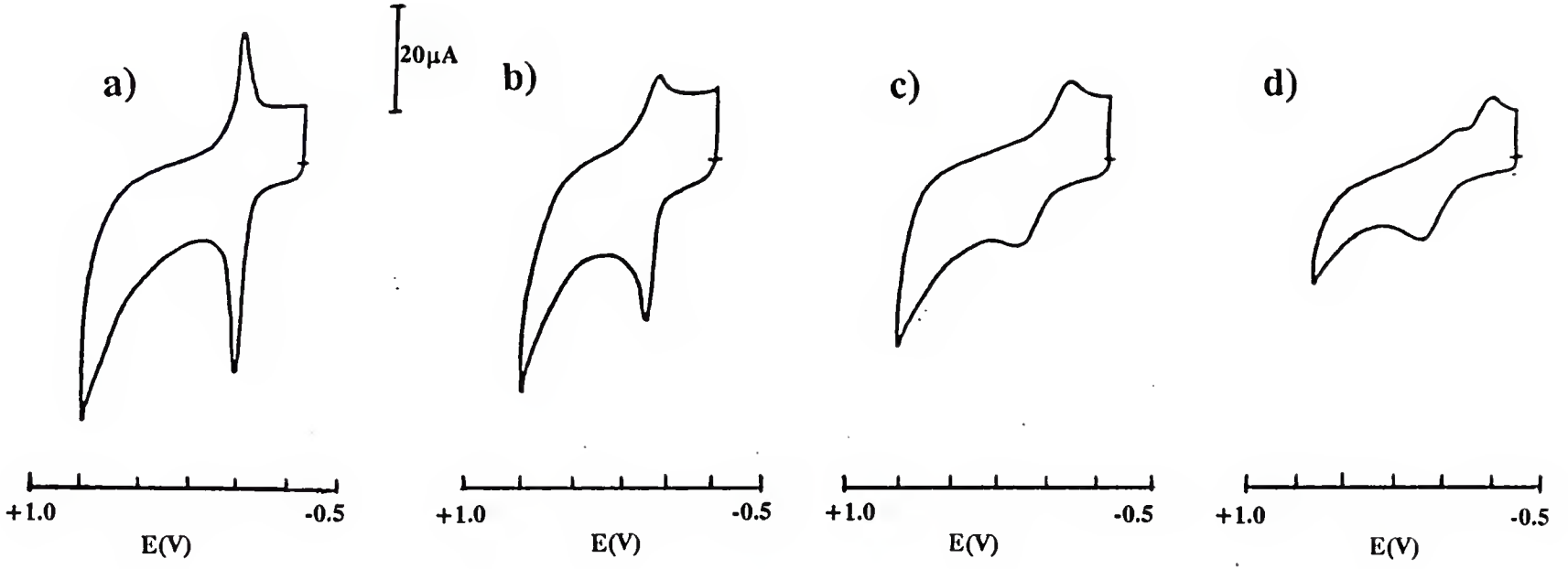
a)
20μA
b)
c)
d)
+1.0
-0.5
E(V)
+1.0
-0.5
E(V)
+1.0
-0.5
E(V)
+1.0
-0.5
E(V)

Figure 8. Cyclic voltammograms of 0.3 mM hydrdoquinone at RPG vs SCE in pH 7 phosphate buffer (μ = 0.5 M) containing: a) no surfactant, b) 3.013 mM CTAB, c) 9.47 mM CTAB, and d) 3.421 mM Triton X-100; exposure time to analyte solution t_{dip} = 0 min; v = 200 mV/s; 20 μA scale; electrode area (RPG) = 4.4 ($\pm$1.2) x 10^{-2} cm^2.

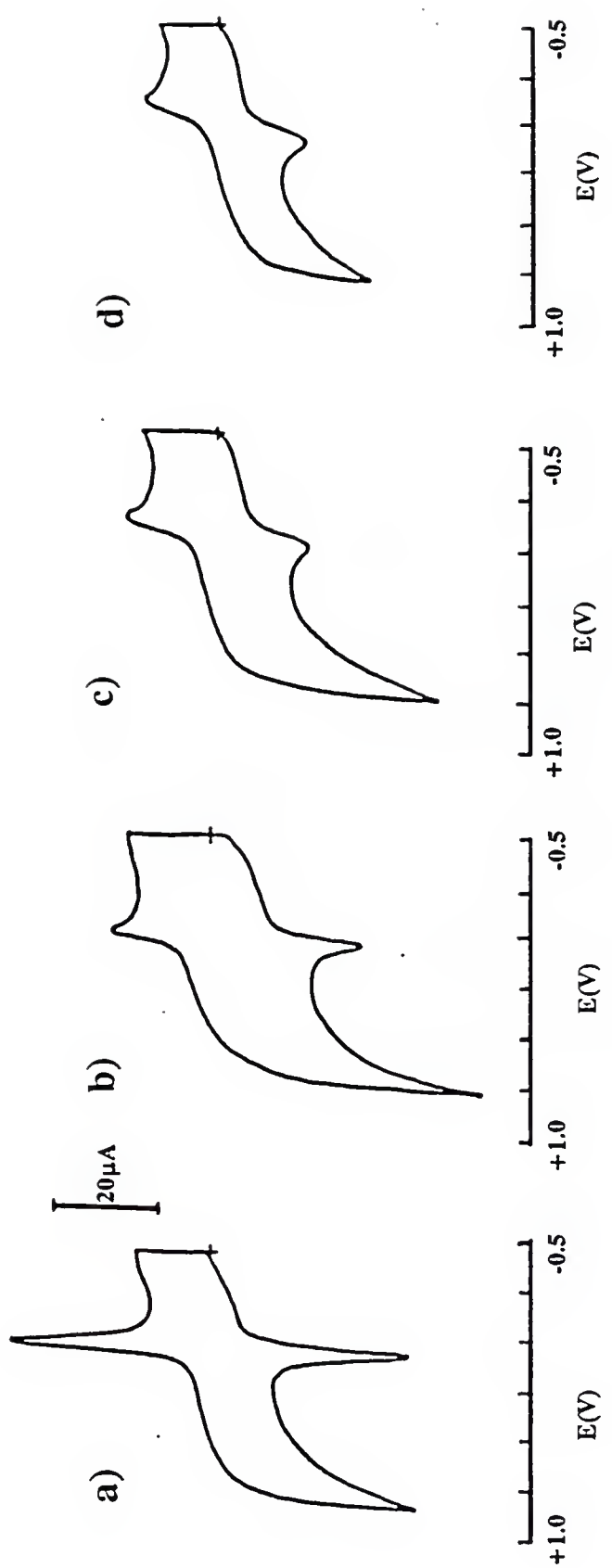
a)
b)
c)
d)
20μA
+1.0
-0.5
E(V)

Table 1. SCAN RATE STUDIES: Slopes of log peak current vs log scan rate plots at RPG electrodes in the presence of surfactant concentrations above CMC[a]; t_{dip} = 0 min.

Solution	Dopamine[b]	DAPOL[b]	Hydroquinone[b]	DOPAC[b]
Buffer[c]	0.62(±0.01)	0.72(±0.01)	0.69(±0.02)	0.65(±0.02)
SDS[a]	0.56(±0.02)	0.64(±0.02)	0.44(±0.01)	0.46(±0.01)
CTAB[a]	0.51(±0.03)	0.59(±0.03)	0.58(±0.02)	0.57(±0.02)
Triton X-100	0.47(±0.01)	0.57(±0.01)	0.46(±0.01)	0.45(±0.01)

[a]Surfactant concentrations above CMC: 10 mM SDS, 3mM CTAB, 3mM Triton X-100.
[b]Probe concentrations: 0.5 mM dopamine, 0.2 mM DAPOL, 0.3mM hydroquinone, 0.5 mM DOPAC.
[c]All solutions in phosphate buffer, pH 7.0, μ = 0.5 M.

(HQ) exhibit the strongest adsorption character (i.e., largest slope values of log i_{pa} vs log v plots) on RPG.

Electron Transfer Kinetics

The ΔE_p values for the probes under same conditions as in Table 1 are shown in Table 2. The ΔE_p values for the probe molecules, all of which undergo $2e^-/2H^+$ oxidation, [5,7,42,82] are very close to 30 mV (Table 2), implying reversible, diffusion controlled electron transfer. However, the slopes of log i_{pa} vs log v plots discussed above show that adsorption is involved in the electrochemical processes for these probes on RPG. The fact that ΔE_p values are larger than 0 (the theoretical value for fast, adsorption controlled electron transfer) indicates that the observed electron transfer is a quasi-reversible (i.e., slower than theoretical) process. Very large ΔE_p values would indicate very slow (i.e., irreversible) electron transfer. As shown in Table 2, DAPOL exhibits the fastest electron transfer kinetics of all the probes at t_{dip} = 0 min (i.e., $\Delta E_p = 14(\pm 4)$ mV), while the kinetics for DOPAC are also very fast (i.e., $\Delta E_p = 25(\pm 5)$ mV).

Electrode Reactivity

When anodic peak currents, i_{pa}, of the probes are normalized for the geometric electrode area and for the probe concentration (Figure 9), different normalized responses are obtained for different probe molecules even though the oxidation of all probes is a two electron process and the kinetics of oxidation of all probes are similar and relatively fast, which can be concluded from similar peak-to-peak separations shown in Table 2. A number of reports [1,18,19,36,38] have shown

Table 2: Anodic to cathodic peak-to-peak potential separations (ΔE_p in mV) at RPG electrodes[a] in the presence of surfactant concentrations above CMC[b]; v = 200 mV/s.

t_{dip}[c] (min)	Surfactant[b]	Dopamine	DAPOL[d]	Hydro-quinone	DOPAC
0	N	32 (±8)	14 (±4)	30 (±4)	25 (±5)
2	O	43 (±5)	26 (±4)	32 (±2)	22 (±2)
5	N	35 (±5)	30 (±0)	30 (±4)	28 (±12)
10	E	40 (±0)	30 (±8)	40	30
0	C	68 (±4)	--	50 (±0)	33 (±5)
2	T	75 (±4)	--	53 (±5)	37 (±5)
5	A	87 (±5)	--	70 (±8)	37 (±9)
10	B	85	--	70	30
0	S	50 (±0)	--	123 (±5)	263 (±5)
2	D	50 (±0)	--	130 (±0)	290 (±8)
5	S	53 (±5)	--	148 (±8)	308 (±6)
10		50	--	140	350
0	Triton	128 (±6)	--	190 (±8)	310 (±36)
2	X-100	130 (±29)	--	190(±22)	325 (±23)
5		123 (±5)	--	183 (±5)	360 (±16)
10		150	--	210	320

[a]All solutions in phosphate buffer, pH 7.0, μ = 0.5 M.
[b]Surfactant concentrations above CMC: 10mM SDS, 3 mM CTAB, 3 mM Triton X-100.
[c]t_{dip} - exposure time of electrode to analyte solution at an open circuit.
[d]ΔE_p values for the first oxidation peak of DAPOL (Peak I_a).

Figure 9: Normalized peak current (i_{pa}/ACo) vs exposure time to analyte solution (t_{dip}) for the four probes at RPG electrodes; pH 7 phosphate buffer (μ = 0.5 M); v = 200 mV/s; Probe concentrations: 0.2 mM DAPOL, 0.5 mM dopamine (DA), 0.3 mM hydroquinone (HQ), and 0.5 mM DOPAC.

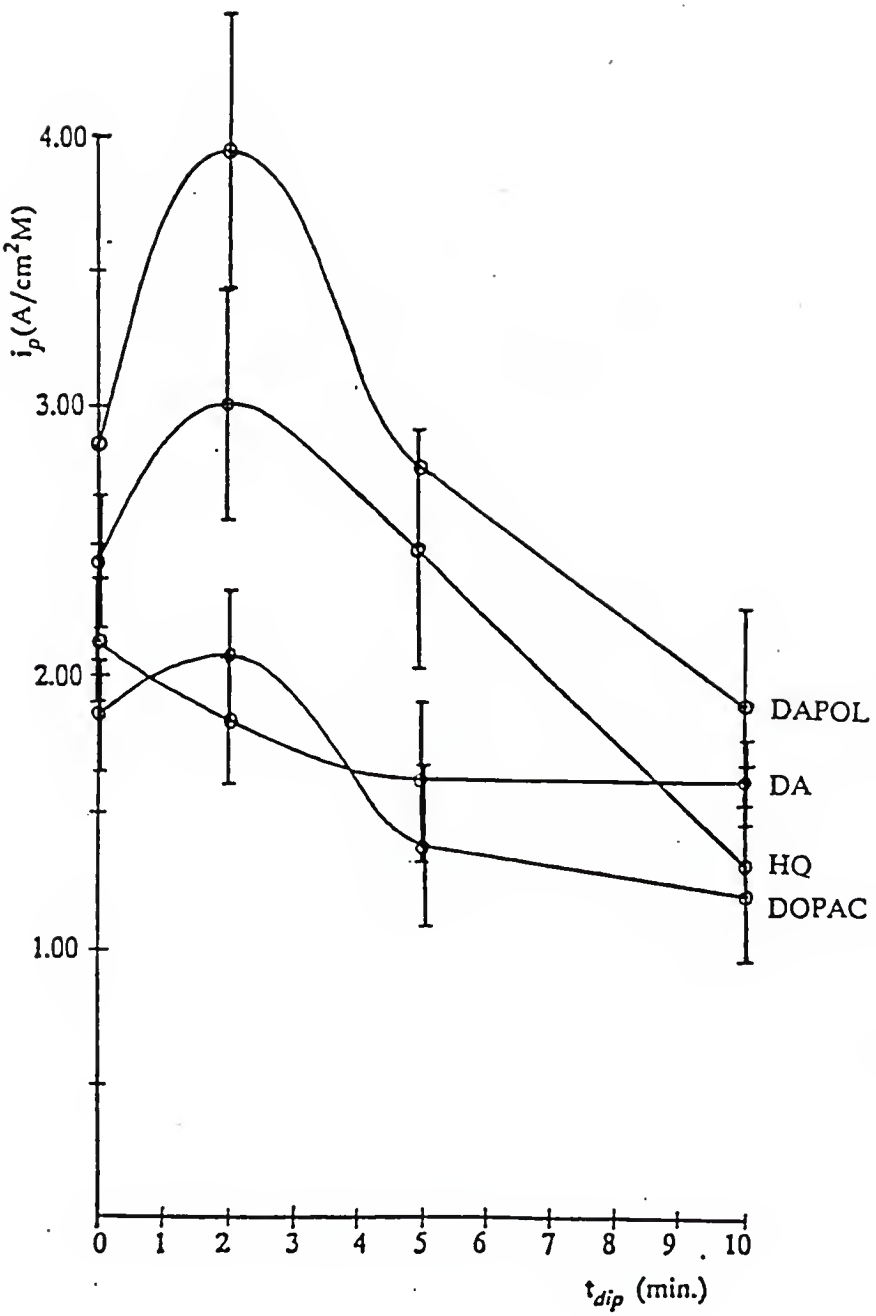
4.00
3.00
2.00
1.00
i_p(A/cm^{2}M)
0
1
2
3
4
5
6
7
8
9
10
t_{dip} (min.)
DAPOL
DA
HQ
DOPAC

a relationship between the charge of a molecule and its electrochemical reactivity on highly polished and electrochemically treated graphite surfaces. Kovach, Deakin, and Wightman [1] studied the electrochemistry of anionic and cationic species at electrochemically oxidized carbon fiber electrodes and found that cations adsorb onto the electrode and yield larger than predicted (i.e., by geometric area) currents while anions showed no adsorptive behavior and yielded smaller than predicted currents. These observations were explained on the basis of an insulating surface oxide layer formed on the electrode during electrochemical treatment which has cation-exchange capabilities [1]. Saraceno and Ewing [38] studied the electron transfer reactions for a series of catechols at electrochemically treated ultrasmall carbon ring electrodes and observed charge-selective enhancement of oxidation rates. Voltammetric measurements for cationic catechols were found to be less reproducible but more Nernstian than those obtained for anionic catechols [38]. To explain these results, Saraceno and Ewing [38] suggested a surface model involving charge-specific sites on the electrode which are somehow involved in the electron transfer process, perhaps as specific adsorption or ion-exchange sites. In the studies presented here, charge does not appear to be an important factor since both the cationic and the anionic probes exhibit similar (almost within standard deviation) ΔE_p and i_{pa} values on polished RPG electrodes (Table 2, Figure 9). In fact, the neutral probes, DAPOL, exhibits stronger adsorption (Table 1) and higher sensitivity (Figure 9) than both the cationic and the anionic probes. Hance and Kuwana [6] have reported that the method of electrode pretreatment largely determines the

extent of probe adsorption. However, pretreatment procedures used here are the same for all experiments and do not provide an explanation for differences in sensitivity of response from probe to probe. Differences in diffusion coefficient values cannot explain the differences in normalized peak currents since the diffusion coefficients for the probes are very similar.

Probe	D_o x 10^6 (cm^2/s)	Conditions	Ref.
DA	6.0_5 ($\pm$0.25)	0.1 M (pH 7.4) phosphate buffer	[93]
DOPAC	5.9_3 ($\pm$0.17)	0.1 M (pH 7.4) phosphate buffer	[93]
DAPOL	6.04 ($\pm$0.02)	0.5 M (pH 7.0) phosphate buffer	[94]
HQ	8.5	0.1 M KCl, 0.0005 M H_2SO_4	[95]
	7.4	0.1 M KNO_3	[95]

A plausible explanation for differences in probe responses on RPG is that the adsorbing molecules pack differently on the electrode surface, i.e., effectively different areas are available for the reactions of different probes. This explanation is consistent with the observation of different slope values of log i_{pa} vs log v for each of the four probes (Table 1) and different kinetics (Table 2).

Peak currents of all probes change with the time of exposure of the electrode to the analyte solution (t_{dip}) (Figure 9). The responses of all probes, with the exception of the second oxidation peak of DAPOL, are initially high and/or increase initially but decrease when exposure time exceeds 5 min. The decreasing responses of dopamine (DA) and DOPAC level off (i.e., reach steady state) between exposure

times of 5 and 10 min. while the responses of DAPOL and hydroquinone (HQ) are still decreasing at exposure times of 10 min. (Figure 9). Kepley and Bard [28] studied the deactivation of electroactivated graphite and concluded that deactivation occurs due to extensive electrochemical reduction of an active surface graphite oxide layer formed during electrochemical pretreatment. The loss of activity observed in our studies was faster than the reductive deactivation of graphitic oxide observed by Kepley and Bard [29]. The loss of activity in our studies is also faster than the deactivation of laser pretreated GC electrodes observed by Poon and McCreery [10] and of polished GC electrodes as observed by Hu, Karweik, and Kuwana [16], where adsorption of impurities was blamed for deactivation. Changes in sensitivity with time indicate that the effective surface area available for reaction of probes is changing with time. Subtraction of background current measured with time in the absence of analytes did not eliminate the observed changes in sensitivity indicating that degradation of response is directly related to the presence of analyte in solution. The shape of the i_{pa} vs t_{dip} curves (Figure 9), the magnitude of the change in sensitivity with time (Figure 9), and the electron transfer kinetics (Table 2) depend on the probe confirming that the differences in probe response are due to different available surface areas (i.e., different probe packing) for reactions of different probes. It is likely that probe packing at the electrode surface blocks a fraction of the active area. The exact shape of the i_{pa} vs t_{dip} curves (Figure 9) also depends on the ionic strength and pH of solution and attempts were made to keep the solution conditions constant.

The observed decrease in effective electrode area (i.e., loss of activity) at RPG electrodes is relatively fast as shown in Figure 9 and such deactivation of graphite has been associated with adsorption [7,8]. Deactivation of RPG occurs without significant effects on the electrochemical kinetics (as measured by ΔE_p) of the analyte which remain relatively fast (Table 2). Similar behavior has been observed on other types of graphite where the rate of electron transfer remained immune to considerable adsorption [7]. Large changes in sensitivity with time, such as those observed for DAPOL and hydroquinone, indicate that physical adsorption similar to the intercalation observed by Kepley and Bard [28] on electroactivated graphite may be responsible for the observed loss of activity. For physisorption, long-range interactions between the electroactive species and the surface affect the electrochemical response by increasing the concentration of the species at the electrode surface and perturbing the potential distribution (i.e., distribution of ions) near the electrode surface [92]. Intercalation is a type of physisorption where a species becomes incorporated into the electrode surface environment perhaps by uptake into an oxide layer on the surface or into defect sites in the electrode surface. In physisorption, as observed for the first DAPOL oxidation peak and for each of the other probes, the adsorbed electroactive species "blocks" the active sites on the electrode from the electroactive species in the bulk solution, thus decreasing the response of the electrode to the bulk analyte, while the electrochemical kinetics of the adsorbed species remain fast (Table 2). The slight decrease in electron transfer kinetics observed with time for DAPOL and DOPAC in the absence of

surfactants (Table 2) confirms that active sites are being blocked by adsorbed probes.

The response of the second oxidation peak of DAPOL (II_a) increases rapidly with exposure times up to t_{dip} = 2 min where the rate of increase decreases yielding a characteristic specific adsorption (i.e., chemisorption) isotherm (Figure 10a) [92]. In chemisorption, the electroactive species is preconcentrated at the electrode surface in a tightly bound layer [92] so that approaching probe molecules interact with the electrode surface relatively uninhibited by the presence of the adsorbed species. Therefore, sensitivity of response is sustained at a high level even in the presence of adsorption.

Conclusions

In summary, probe molecules adsorb at RPG electrodes with different efficiencies and yield sensitive responses that are characteristic of quasi-reversible, mixed adsorption-diffusion controlled heterogeneous electron transfer.

Results and Discussion for Glassy Carbon

Electrode Reactivity

Figure 11 shows representative cyclic voltammograms of hydroquinone (HQ) on RPG and GC electrodes. Qualitative comparison of these curves, in terms of peak shape, sensitivity of response, and ΔE_p, can be generalized to describe the response of all probes on RPG and GC surfaces. For example, oxidation and reduction peaks obtained on GC are smaller and much broader than those observed on RPG and ΔE_p values obtained on GC are much larger than those observed on

Figure 10: Normalized peak current (i_{pa}/ACo) vs exposure time (t_{dip}) for the second oxidation peak (II_a) of DAPOL: a) in the absence of surfactants, b) in SDS concentrations above CMC, c) in SDS concentrations below CMC; phosphate buffer, pH 7, μ = 0.5 M; v = 200 mV/s.

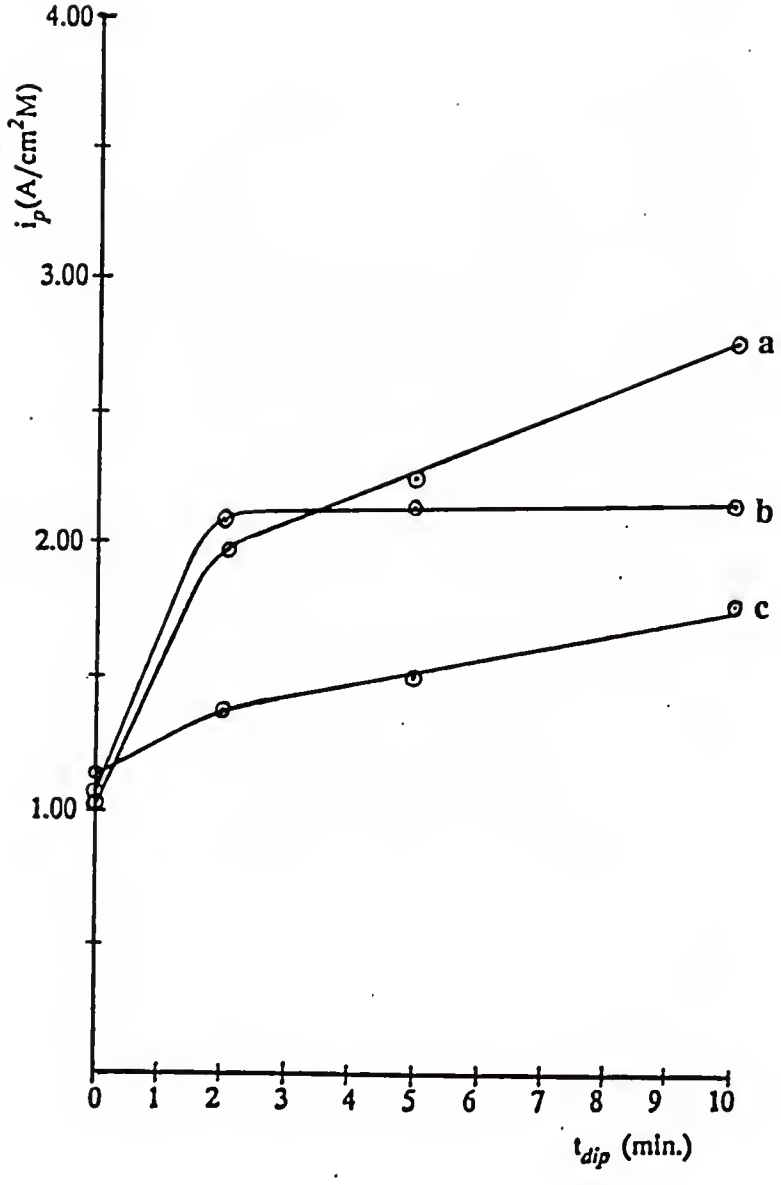
4.00
3.00
2.00
1.00
i_p(A/cm^{2}M)
a
b
c
0
1
2
3
4
5
6
7
8
9
10
t_{dip} (min.)

Figure 11: Cyclic voltammograms of 0.3 mM hydroquinone at RPG (0.0382 cm^2) and GC (0.0728 cm^2) vs SCE in pH 7 phosphate buffer (μ = 0.5 M); Exposure time to analyte solution t_{dip} = 0 min; v = 200 mV/s; 20 μA scale.

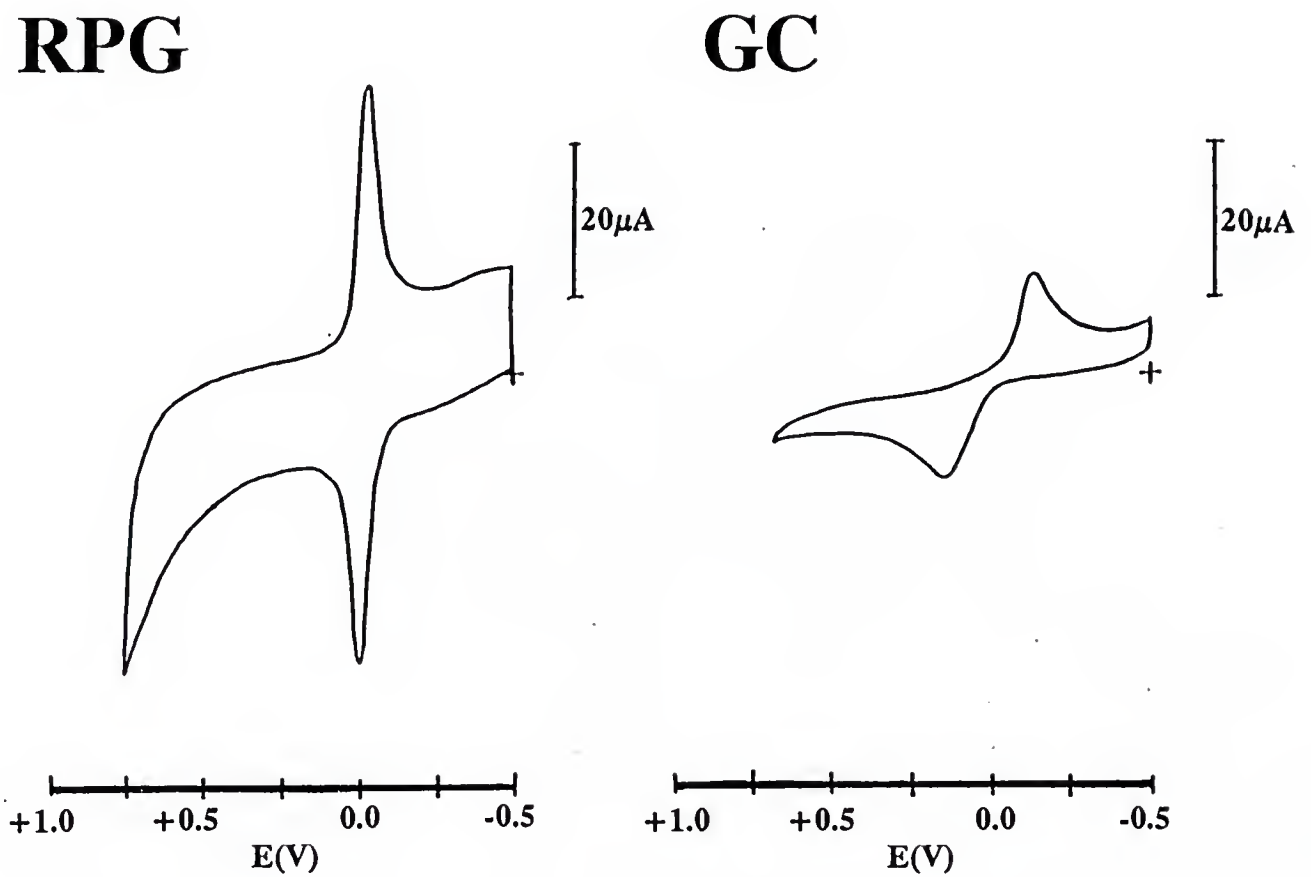
RPG
20μA
+1.0
+0.5
0.0
-0.5
E(V)
GC
20μA
+1.0
+0.5
0.0
-0.5
E(V)

RPG for all probe molecules. Quantitatively, normalized anodic peak currents ($Acm^{-2}M^{-1}$) on GC electrodes are approximately one-fourth as large as those obtained on RPG electrodes (Figures 9 and 12). This result is consistent with previous reports that GC, as prepared here, is a less active surface than RPG [7,30,96]. Probe responses on GC show very little, if any, change with time (Figure 12) indicating no slow adsorption of these probes on GC. Also, the second oxidation peak of DAPOL on RPG corresponding to strongly adsorbed DAPOL is not observed on GC. Scan rate studies (Table 3) confirm that the responses of all probes at GC electrodes are diffusion controlled.

Probe Adsorption

Slope values for the plots of log i_{pa} vs log v of the probe molecules on GC in pH 7 phosphate buffer (0.5 M) are shown in Table 3. Scan rates ranged from 5-500 mV/s for DAPOL and from 10-200 mV/s for DA, DOPAC, and HQ. Slope values for all probes are below 0.5, the theoretical value for diffusion controlled processes, confirming that the probes do not adsorb on GC electrodes. The equations used to relate peak current and scan rate (equations 1-4) are based on the assumptions that the entire electrode surface is active and that the heterogeneous electron transfer kinetics of the analyte molecule are fast or do not change within the scan rate window [92]. The fact that the slope values are less than theoretically predicted for diffusion controlled processes indicates that one or all of these assumptions fails (i.e., only a portion of the entire electrode area is active and/or the heterogeneous electron transfer kinetics of analytes are sufficiently slow to cause

Figure 12: Normalized peak current (i_{pa}/ACo) vs exposure time to analyte solution (t_{dip}) for the four probes at GC electrodes; pH 7 phosphate buffer (μ = 0.5 M); v = 200 mV/s; probe concentrations: 0.5 mM dopamine (DA), 0.3 mM hydroquinone (HQ), 0.2 mM DAPOL, and 0.5 mM DOPAC.

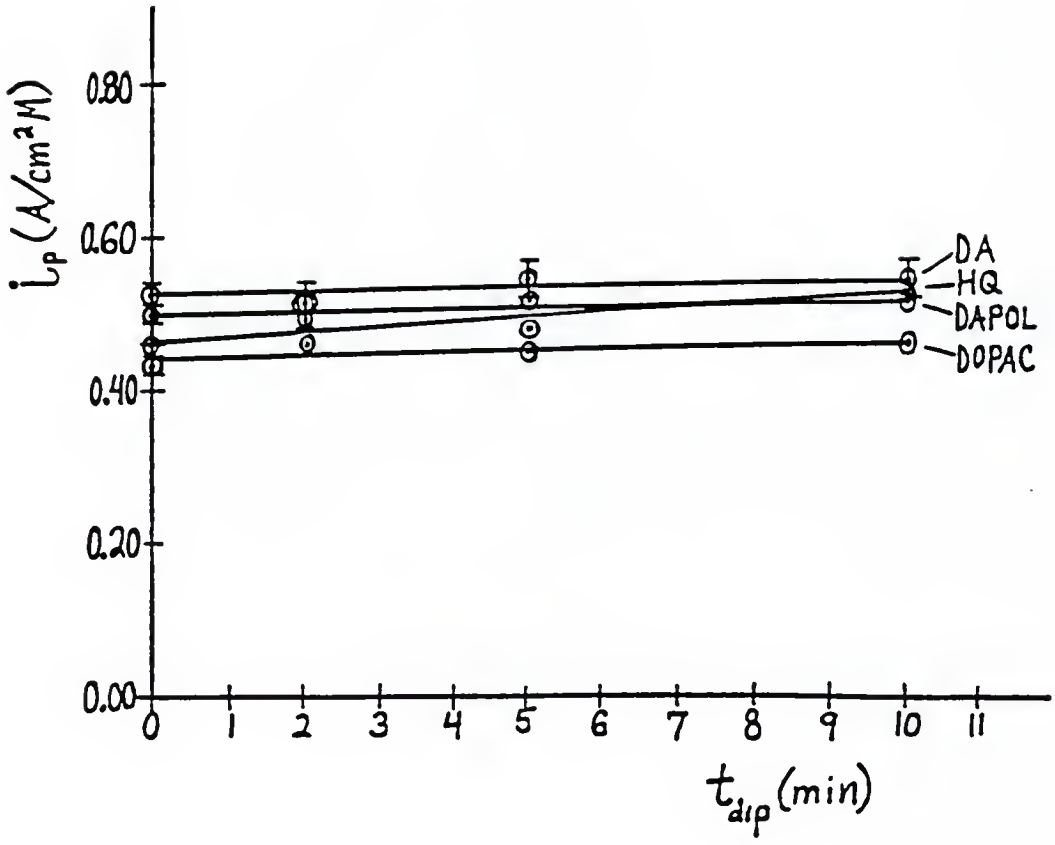
i_p (A/cm²M)
0.80
0.60
0.40
0.20
0.00
0
1
2
3
4
5
6
7
8
9
10
11
t_{dip} (min)
DA
HQ
DAPOL
DOPAC

Table 3: SCAN RATE STUDIES: Slopes of log peak current vs log scan rate plots at polished GC electrodes in the presence of surfactant concentrations above[a] and below[b] CMC; t_{dip} = 0 min.

Solution	Dopamine[c]	DAPOL[c]	Hydroquinone[c]	DOPAC[c]
Buffer[d]	0.40 (±0.01)	0.48 (±0.01)	0.45 (±0.03)	0.44 (±0.03)
SDS[a]	0.40 (±0.02)	0.47 (±0.01)	0.50 (±0.01)	0.47 (±0.01)
SDS[b]	0.42 (±0.01)	0.48 (±0.00)	0.44 (±0.03)	0.47 (±0.01)
CTAB[a]	0.39 (±0.02)	0.46 (±0.01)	0.40 (±0.01)	0.45 (±0.01)
CTAB[b]	0.42 (±0.02)	0.45 (±0.01)	0.40 (±0.01)	0.49 (±0.01)

[a]Surfactant concentrations above CMC; 10mM SDS, 3mM CTAB, 3mM Triton X-100.
[b]Surfactant concentrations below CMC; 1mM SDS, 0.3mM CTAB, 0.106mM Triton X-100.
[c]Probe concentrations: 0.5mM dopamine, 0.2mM DAPOL, 0.3mM hydroquinone, 0.5mM DOPAC.
[d]All solutions in phosphate buffer, pH 7.0, μ = 0.5 M.

deviations from linearity in the plots of log i_{pa} vs log v at fast scan rates). Slow kinetics are confirmed by ΔE_p values as discussed below.

Electron Transfer Kinetics

The ΔE_p values for the probes on GC in pH 7 phosphate buffer (0.5 M) are shown in Table 4. The ΔE_p values for DAPOL are not listed, since the reduction peak for DAPOL on GC is not well defined. The ΔE_p values for DA, DOPAC, and HQ are much larger than 30 mV, the expected value for a two electron, diffusion controlled process, indicating slow electron transfer kinetics for the probes at GC. DOPAC exhibits the slowest kinetics of all probes on GC. These results are consistent with the results of Deakin et al. [5] who studied the oxidation of substituted catechols at alumina-polished (i.e., unactivated) and heat treated (i.e., activated) GC electrodes. Deakin et al. [5] obtained voltammetric peak shapes and reduced heterogeneous rate constants indicative of electrochemically quasi-reversible processes and found that responses for DOPAC were more irreversible than those for other catechols studied.

Conclusions

In summary, GC is a less active surface than RPG yielding responses for all probes which exhibit poor sensitivity and are characteristic of slow heterogeneous electron transfer with no contribution from adsorption.

Table 4: Anodic to cathodic peak-to-peak potential separations (ΔE_p in mV) at polished GC electrodes[a] in the presence of surfactant concentrations above CMC[b]; v = 200 mV/s.

t_{dip}[c] (min)	Surfactant[b]	Dopamine	DAPOL[d]	Hydro-quinone	DOPAC
0	N	133(±21)	--	310(±29)	366(±69)
2	O	191(±5)	--	300(±18)	333(±57)
5	N	150(±22)	--	280	390
10	E	150(±22)	--	315	350
0	C	285(±7)	--	147(±9)	175(±0)
2	T	277(±5)	--	130(±0)	150(±0)
5	A	270	--	130	160
10	B	275	--	130	170
0	S	163(±5)	--	363 (±9)	537 (±9)
2	D	150(±0)	--	355 (±4)	547 (±5)
5	S	160	--	370	560
10		160	--	365	550

[a]All solutions in phosphate buffer, pH 7.0, μ = 0.5 M.
[b]Surfactant concentrations above CMC; 10mM SDS, 3 mM CTAB, 3 mM Triton X-100.
[c]t_{dip} - exposure time of electrode to analyte solution at an open circuit.
[d]ΔE_p values cannot be obtained - reduction peak not observed on GC.

CHAPTER IV

RESPONSE OF HYDROPHILIC ELECTRODES IN SURFACTANT SOLUTIONS ABOVE THE CRITICAL MICELLE CONCENTRATION

In electroanalysis it is desirable to control the electrode-solution interface so that the most sensitive and most precise measurements possible are obtained. The electrode-solution interface may be manipulated (i.e., controlled) by either modifying the electrode surface or by modifying the probe solution. The electrode surface may be altered by using various pretreatment methods, by coating the electrode surface with a polymer, by depositing thin films or monolayers on the electrode surface, or by varying the form of the electrode material (e.g. solid carbon vs carbon paste electrodes). Solution modification may be achieved by varying the pH of solution, varying the ionic strength of solution, using solution additives, or changing solvents completely. In the work presented here, the electrode-solution interface was modified using surfactants as solution additives.

Effects of pH and Ionic Strength

Throughout this work it was observed that anodic peak currents and peak potentials varied for different preparations of a given probe solution in pure phosphate buffer. All probe solutions were thought to be similarly prepared, i.e., with the same probe concentration, same pH, and same ionic strength, however, various batches of phosphate buffer (prepared by different laboratory personnel)

were used to make up probe solutions. Slight variations in phosphate buffer composition can lead to deviations in probe response, therefore, the pH and ionic strength of the buffer were investigated as possible sources of the observed variations in probe responses. A narrow range of pH and ionic strength values was investigated since all buffer preparations were similarly prepared to be approximately pH 7 and ionic strength 1.0 M. Anodic peak current and peak potential measurements were found to be sensitive to both pH (Table 5) and ionic strength (Table 6). In the pH and ionic strength ranges studied, definite trends in the change of peak potential with increasing pH and ionic strength were observed, while no patterns for the change in peak current with increasing pH or ionic strength could be discerned (Tables 5 and 6). For dopamine, anodic peak potentials become slightly less positive (i.e., shift by approximately -15 mV) as ionic strength is increased from 0.1 M to 1.0 M while marked shifts in the negative direction (i.e., approximately -45 mV per pH unit) are observed with increasing pH (in the range from pH 6-8). The observation of a negative shift in anodic peak potentials with increasing pH is consistent with the Nernst equation for a $2e^-/2H^+$ oxidation which predicts a possible potential shift of up to -60 mV per pH unit for reversible electron transfer. An effort was made to use phosphate buffer of the same ionic strength and the same pH throughout the course of this work, however there appear to be slight variations in buffer composition from one batch to another. Variations in buffer composition will affect electrochemical results, such as formal potentials and i_{pa} vs t_{dip} plots as shown in Figure 9.

Table 5. Average anodic peak potentials (E_{pa}) and normalized average anodic peak currents (i_{pa}/ACo) for pH studies at RPG electrodes of 0.54 mM dopamine in phosphate buffer (μ = 0.5); v = 200 mV/s.

pH	t_{dip} (min)	E_{pa} (mV)	i_{pa} ($Acm^{-2}M^{-1}$)
6.0	0	170(±8)	1.85(±0.35)
	2	180(±0)	2.38(±0.06)
	5	177(±5)	2.21(±0.49)
	10	190	2.32
7.0	0	127(±5)	2.16(±0.29)
	2	135(±7)	2.33(±0.32)
	5	137(±5)	2.46(±0.16)
	10	130	2.56
7.4	0	100(±4)	2.47(±0.19)
	2	113(±5)	3.06(±0.24)
	5	107(±2)	2.39(±0.29)
	10	120	1.52
8.1	0	78(±2)	1.93(±0.31)
	2	70(±0)	2.36(±0.28)
	5	81(±5)	2.67(±0.16)
	10	92(±2)	1.79(±0.29)

Table 6. Average anodic peak potentials (E_{pa}) and normalized average anodic peak currents (i_{pa}/ACo) for ionic strength studies at RPG electrodes of 0.54 mM dopamine in phosphate buffer (pH 7); v = 200 mV/s.

μ(M)	t_{dip} (min)	E_{pa} (mV)	i_{pa} ($Acm^{-2}M^{-1}$)
0.1	0	12(±6)	1.61(±0.13)
	2	17(±9)	1.51(±0.23)
	5	17(±5)	1.45(±0.14)
	10	20	1.46
0.5	0	-6.7(±5)	1.54(±0.10)
	2	1.7(±2)	1.82(±0.37)
	5	-1.2(±2)	1.24(±0.31)
	10	0	1.56
1.0	0	-9.2(±8)	1.30(±0.12)
	2	-1.3(±4)	1.40(±0.30)
	5	-5.0(±4)	1.55(±0.20)
	10	0	1.22

Deactivation of RPG Surface

In this study, different surfactants were added to probe solutions at concentrations above the critical micelle concentration (CMC) in order to modify the electrode-solution interface in a controlled manner. Representative cyclic voltammograms for the responses of probe molecules in the presence of surfactant at RPG are shown in Figures 5b-d, 6b-d, 7b-d, and 8b-d. Effects on probe responses as observed from anodic peak currents (i_{pa}) in micellar solutions include: 1) decrease in the magnitude of the electrochemical response of all probes compared to that in phosphate buffer alone (Figures 5-8; Figure 13); 2) effective elimination of the changes in response with time (Figure 13); and 3) increase in the reproducibility (i.e., precision) of peak current (i_{pa}) measurements (as indicated by error bars) (Figure 13).

Electrode Reactivity

The normalized peak currents for all probes in the presence of high surfactant concentrations (i.e., above CMC) are smaller and more constant with time than those obtained in the absence of surfactants (Figures 9 and 13). One exception to this behavior is the response of the second oxidation peak (II_a) of strongly adsorbing DAPOL in the presence of SDS micelles which is more sensitive, at short exposure times, than the response in the absence of surfactant and which changes with time before levelling off around t_{dip} = 2 min to a value lower than that observed in the absence of surfactant (Figure 10a and Figure 10b). The response

Figure 13: Normalized peak current (i_{pa}/AC_o) vs exposure time (t_{dip}) for: a) dopamine (DA), b) DAPOL, c) DOPAC, and d) hydroquinone (HQ) at RPG electrodes in phosphate buffer (pH 7, μ = 0.5 M) and in the indicated surfactant at concentrations above CMC; v = 200 mV/s.

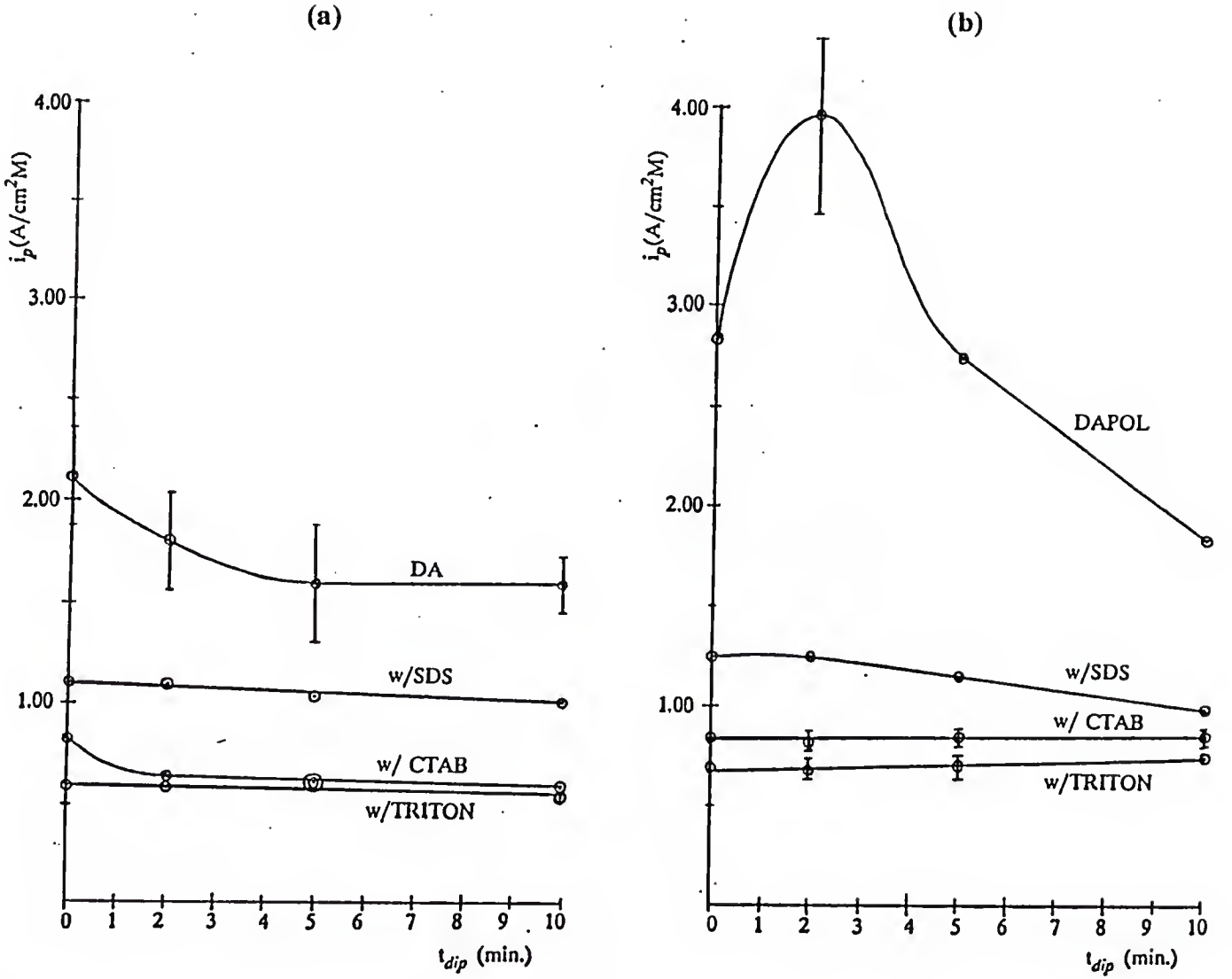
(a)
(b)
4.00
3.00
2.00
1.00
i_p(A/cm^{2}M)
DA
w/SDS
w/ CTAB
w/TRITON
DAPOL
0 1 2 3 4 5 6 7 8 9 10
t_{dip} (min.)

Figure 13: (continued) Normalized peak current (i_{pa}/AC_o) vs exposure time (t_{dip}) for: a) dopamine (DA), b) DAPOL, c) DOPAC, and d) hydroquinone (HQ) at RPG electrodes in phosphate buffer (pH 7, μ = 0.5 M) and in the indicated surfactant at concentrations above CMC; v = 200 mV/s.

(c)

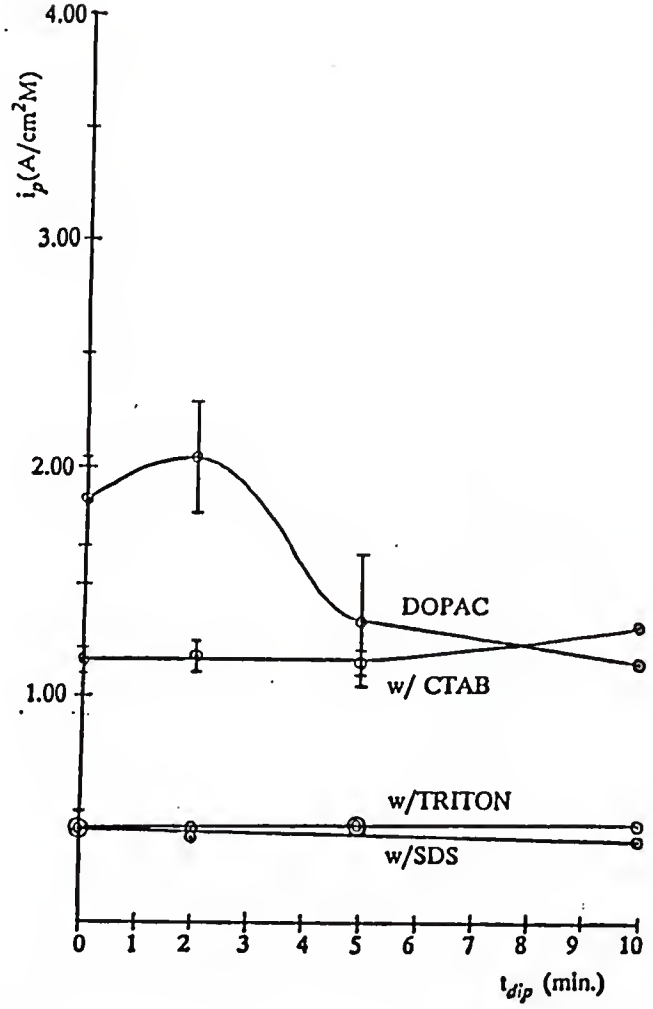
4.00
3.00
2.00
1.00
i_p(A/cm^{2}M)
DOPAC
w/ CTAB
w/TRITON
w/SDS
0 1 2 3 4 5 6 7 8 9 10
t_{dip} (min.)

(d)

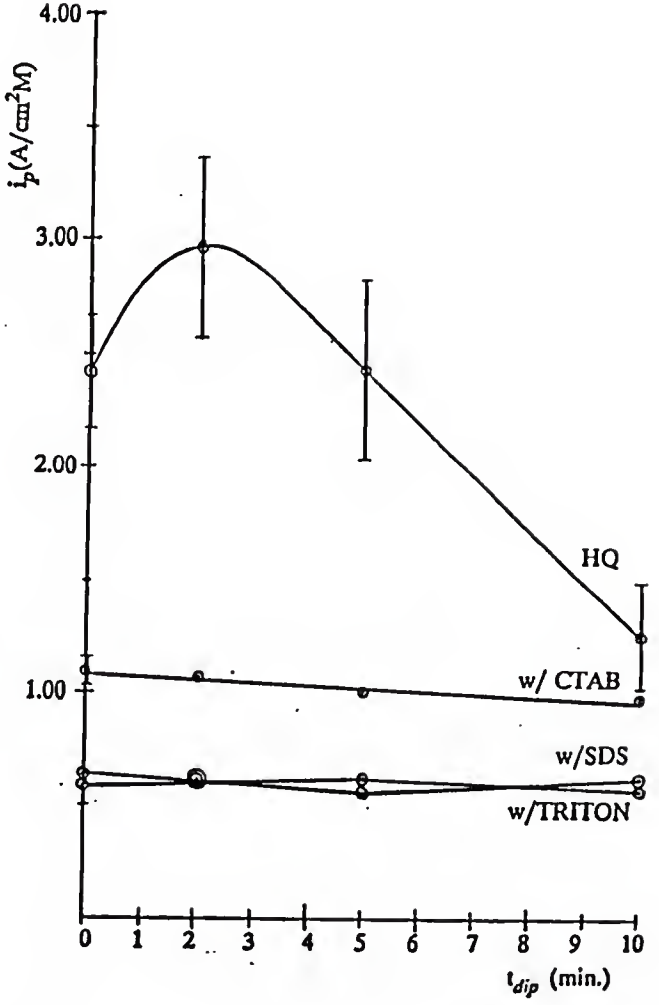
4.00
3.00
2.00
1.00
i_p(A/cm^{2}M)
HQ
w/ CTAB
w/SDS
w/TRITON
0 1 2 3 4 5 6 7 8 9 10
t_{dip} (min.)

of DAPOL peak II_a levels off around t_{dip} = 2 min in SDS micellar solutions while the response in the absence of surfactants is still increasing at t_{dip} = 2 min indicating that adsorption equilibrium is reached more quickly in the presence of SDS. In the presence of CTAB and Triton X-100, the second oxidation peak of DAPOL becomes distorted and can no longer be measured. These results indicate that time dependent physisorption and chemisorption of analytes on RPG are inhibited in the presence of micelles, with the exception of the second oxidation peak of DAPOL in the presence of SDS. The unique effect of SDS on the response of the strongly adsorbing molecule, DAPOL, suggests attractive interactions between the probe and the surfactant, since the probe saturates the electrode surface (i.e., reaches adsorption equilibrium) more quickly in the presence of surfactant than in the absence of surfactant. The elimination of changes in probe responses with time in micellar media (Figure 13) indicates that the activity of the electrode surface is constant with time and that probe adsorption is less prominent in the presence of micelles in solution. The dramatic increase in precision of measurement (in most cases (Figure 13)), in micellar media compared to that in pure phosphate buffer indicates that the electrode surface is more reproducible for probe response in the presence of high surfactant concentrations.

Probe Adsorption

The effects of high surfactant concentrations (i.e., above CMC) on the electrochemistry of the probes at RPG electrodes can also be seen from changes in the dependence of peak currents (i_{pa}) on scan rate (v) (Table 1) and from changes

in peak-to-peak separation (ΔE_p) (Table 2). The slopes of log i_{pa} vs log v for all probes in micellar media (Table 1) are significantly lower than those obtained in pH 7 phosphate buffer (0.5 M) indicating a decrease in adsorption. This observation is in agreement with the conclusion drawn from peak current measurements with time that probe adsorption is inhibited in the presence of micelles in solution, with the exception of DAPOL peak II_a in the presence of SDS. Some slope values fall below the theoretical value of 0.5 for diffusion controlled processes indicating either that less than the entire electrode area is active or that the heterogeneous electron transfer kinetics are slow and cause deviations from linearity in log i_{pa} vs log v plots at fast scan rates.

Electron Transfer Kinetics

The ΔE_p values (Table 2) for the probes in micellar media are larger than those observed in pure phosphate buffer. Such an increase in ΔE_p values can indicate a decrease in the rate of heterogeneous electron transfer or a decrease in probe adsorption on the electrode [92]. For cases in which responses are strictly diffusion controlled, increases in ΔE_p values clearly indicate a decrease in heterogeneous electron transfer kinetics. However, for cases in which probe adsorption is involved it becomes difficult to discern whether increases in ΔE_p values are due to decreases in probe adsorption or electron transfer kinetics. For the systems studied here, it has been shown (from slope values of log i_{pa} vs log v) that probe adsorption is decreased in the presence of micellar solutions, thus explaining the increases in ΔE_p values. However, it also seems likely (based on the slope values

for log i_{pa} vs log v that were below 0.5) that the rate of electron transfer may be diminished to some extent in the presence of high surfactant concentrations.

Surface Model

Several possible explanations for the observed decreases in electrode activity, in standard deviation of peak current measurements, in probe adsorption, and in electron transfer kinetics in micellar media must be considered. All of the above results imply that the RPG electrode surface is deactivated in solutions containing surfactant molecules at concentrations above CMC. Surfactants commonly adsorb at solid-liquid interfaces [56,61], and in this case it appears that surfactants adsorb at the electrode surface and effectively reduce the surface area available for the adsorption of probe molecules. The likelihood of surfactant adsorption is supported by the observations that the electrode surface conditions are more constant with time and are more reproducible (for a given exposure time) in the presence of surfactants than in pure phosphate buffer.

Surfactants may adsorb at solid surfaces in the form of surfactant monomers, micelles, or hemimicelles. Activated graphite surfaces are known to have hydrophilic character [5,20,21,31,37], which would favor adsorption of surfactant monomers with the hydrophilic head groups oriented toward the electrode surface and the tail groups oriented toward the solution (Figure 1a and b). The hydrophilicity of RPG would also favor the adsorption of surfactants onto the electrode surface in the form of normal micelles (i.e., three-dimensional aggregates with the hydrophilic head groups oriented outward from a hydrophobic core).

However, there have been no reports of micelle adsorption at solid surfaces indicating affinity of micellar aggregates for the solution (i.e., aqueous) phase. Several reports [61,71,75-78] have suggested the adsorption of surfactants onto hydrophilic surfaces in the form of hemimicelles (Figure 1c). Hemimicelles (normal) are two-dimensional aggregates which form due to hydrophobic interactions between surfactant hydrocarbon chains, so that surfactant head groups are oriented toward both the electrode and the solution with a hydrophobic region in the center (Figure 1c) [61,71,72]. Evidence for the adsorption of surfactants in the form of hemimicelles, such as attractive interactions between probe molecules and adsorbed surfactants and time-dependent surfactant effects at concentrations below CMC, will be discussed later in this text.

Attractive Interactions Between Probe Molecules and Adsorbed Surfactants

The observed electrochemical responses for the probes in the presence of surfactants at concentrations above CMC imply that attractive interactions occur between specific probe-surfactant pairs. For example, enhanced peak currents (Figure 13) for a given probe in the presence of one surfactant compared to those observed in the presence of other surfactants, e.g., dopamine in the presence of SDS (Figure 13a), indicate attractive interactions between the probe molecule and a specific surfactant. These attractive interactions may be due to electrostatic effects resulting from the net charges on the probe and surfactant molecules, electrostatic effects resulting from induced dipoles on the neutral probe molecules and the net charge on the surfactant molecules, and/or hydrophobic effects.

Electrode Reactivity

Evidence for attractive interactions is shown by an increased response of negative DOPAC in the presence of the positive surfactant, CTAB (compared to that in negatively charged SDS solutions) (Figure 13c) and by a similar increased response for positive dopamine in the presence of the negative surfactant, SDS (compared to that in CTAB solutions) (Figure 13a). Repulsive interactions were ruled out as a possible explanation for the observation of less sensitive responses for charged probes in the presence of like charged surfactants compared to those obtained in solutions of oppositely charged surfactants based on probe responses in the presence of neutral Triton X-100 (Figure 13a and c). Low responses similar to those obtained for negative DOPAC in the presence of negative SDS and for positive dopamine in the presence of positive CTAB are observed for these probes in the presence of neutral Triton X-100 (Figure 13a and c). These results indicate that the decrease in response for probes in the presence of like charged surfactants is not due to repulsive interactions between probes and adsorbed hemimicelles but is likely caused by deactivation of the graphite surface, as suggested above.

Increased responses for neutral hydroquinone (HQ) in the presence of positive CTAB (Figure 13d) and for neutral DAPOL (Peak I_a) in the presence of negative SDS (Figure 13b) may suggest attraction between probe and surfactant molecules due to an induced dipole in the neutral probe molecules or hydrophobic interactions between probe molecules and adsorbed surfactants. The response of the second oxidation peak of DAPOL is very poorly defined in the presence of

CTAB and Triton X-100 while it is well-defined and quantifiable in the presence of SDS. Based on the fact that Triton X-100 is the largest surfactant, i.e., has the most hydrophobic character, and that neutral probes show suppressed responses in the presence of Triton X-100, it appears that enhanced responses for neutral probes in the presence of adsorbed surfactants may be due to electrostatic rather than hydrophobic interactions. The effect of surfactant chain length may also be important.

Probe Adsorption

The effects of attractive interactions between specific probes and surfactants on electrochemical responses can be seen from larger slope values for log i_{pa} vs log v plots (Table 1) for probes in the presence of one surfactant compared to the slope values obtained in the presence of other surfactants. From slope values of log i_{pa} vs log v (Table 1), it appears that adsorption of HQ and DOPAC is eliminated in the presence of negative SDS, whereas dopamine and DAPOL exhibit adsorption character in this medium. The same type of observations can be made from slopes in positive CTAB micellar media, where adsorptive interactions for dopamine are negligible (i.e., slope of log i_{pa} vs log v = 0.51) and HQ, DOPAC, and DAPOL adsorption remains significant (Table 1). Triton X-100 deactivates the RPG electrodes for all probes except DAPOL, the response of which exhibits adsorption characteristics on RPG in all media studied here (Table 1). The variations in slope values of log i_{pa} vs log v with micellar media confirm attractive interactions for

dopamine and DAPOL with adsorbed SDS and for DOPAC and HQ with adsorbed CTAB.

Electron Transfer Kinetics

The effects of attractive interactions on heterogeneous electron transfer rates are evident from smaller ΔE_p values (Table 2) for probes in the presence of one surfactant compared to the ΔE_p values obtained in the presence of other surfactants. Small ΔE_p, similar to those obtained in the absence of surfactants, show that the heterogeneous electron transfer kinetics of DOPAC are essentially unaffected by the presence of CTAB at concentrations above CMC and that the kinetics of dopamine are not significantly altered by the presence of SDS at concentrations above CMC. The kinetics of dopamine are the least sensitive of all of the probe kinetics to the presence of surfactants at concentrations above CMC (Table 2), since the ΔE_p values for dopamine in all media are relatively small. Also, ΔE_p values for dopamine in the presence of SDS and CTAB are relatively small compared with the ΔE_p values for HQ and DOPAC in the presence of these surfactants indicating that dopamine interacts to some extent with positively charged CTAB as well as with negatively charged SDS. Attractive interactions of dopamine with SDS and CTAB are confirmed by slope values of log i_{pa} vs log v for dopamine in the presence of SDS and CTAB (Table 1) which are above 0.5, indicating adsorption like behavior in the presence of the adsorbed surfactants, while the slopes for other probe-surfactant combinations fall below 0.5, indicating no interaction of probes with the electrode surface. The most dramatic decrease in electron transfer rates (i.e., largest

increase in ΔE_p's) for all probes is observed in the presence of neutral Triton X-100 (Table 2), and low slope values of log i_{pa} vs log v similar to those obtained in like charged surfactants are obtained for all probes in the presence of Triton X-100 (Table 1). Large ΔE_p values and small slope values of log i_{pa} vs log v for all probes in the presence of Triton X-100 verify that repulsive interactions between probes and surfactants are not the source of the observed decrease in probe responses in micellar solutions since the nonionic surfactant alters the electrochemical kinetics and the adsorption behavior of the probes to the same degree as the surfactant with the same charge as the probes. Triton X-100 is much larger than SDS and CTAB, and chain length may contribute to the observed surfactant effects.

Conclusions

The results discussed above suggest that the situation at the RPG electrode surface in pH 7 phosphate buffered micellar media is the following: 1) surfactants adsorb at the electrode surface, most likely in the form of hemimicelles, and effectively deactivate the electrode; 2) specific probes interact with adsorbed surfactants and are attracted to the RPG surface; and 3) the probes which attractively interact with adsorbed surfactants exhibit responses indicative of fast electron transfer and adsorption behavior.

CHAPTER V

BINDING CONSTANTS FOR PROBE-MICELLE INTERACTIONS

Equilibrium Binding Constants (K_{eq}) Determined from HPLC Data

The strength of interactions between probes and micelles are measured quanitatively using micellar HPLC. Binding constants, K_{eq}, as defined by equations 22 and 26, are a direct measure of probe-micelle interactions that can be calculated from probe retention in micellar HPLC as measured by the capacity factor, k′, or the retention time, t_R, as described in equations 21-26. The strength of probe-micelle interactions directly reflects the strength of probe interactions with surfactant monomers and hemimicelles. In this work, the stationary phase is coated with surfactant monomers with head groups toward the mobile phase, as discussed in the Theory section, while the mobile phase contains *normal* micelles of the same surfactant. Therefore, probe retention involves partitioning of probe molecules between the stationary phase containing surfactant molecules (equation 21) and the micelles in the mobile phase (equation 22). The K_{eq} value for DAPOL in CTAB was predicted to be one-tenth as large as the K_{eq} value for HQ in CTAB since the retention times for DOPAC (t_R (avg) = 86.8 sec) were approximately one-tenth as long as those for HQ (t_R (avg) = 922 sec) in the CTAB micellar chromatography. The K_{eq} value for DAPOL in CTAB was predicted to be more than three times

larger than the K_{eq} for DA in SDS since DOPAC retention times in CTAB (t_R > 3 hrs) were at least three times as long as DA retention times in SDS (t_R (avg) ≈ 30 min) for relative concentrations of CTAB and SDS. The approximate values obtained from micellar HPLC for equilibrium constants, K_{eq}, for probe molecule interactions with micelles are listed in Table 7. It was not possible to calculate the equilibrium constants missing from Table 7 or marked as "predicted". Some probes interact too strongly with the mobile phase (i.e., probe peaks elute with the solvent peak) and exhibit no change in retention with changes in micelle concentration in the mobile phase, such as dopamine (DA) with CTAB, DOPAC with SDS, and DAPOL with CTAB (Table 7). Other probes interact too weakly with the mobile phase and do not elute within the time frame of our experiments (within 4 hours), even in the most concentrated mobile phase preparation, such as DOPAC in 10.1 mM CTAB. The strong retention of DOPAC on the CTAB-loaded column indicates that strong interactions occur between DOPAC and the adsorbed CTAB on the stationary phase and that higher concentrations of CTAB micelles are needed in the mobile phase to elute this probe. However, instrumental conditions, such as high column back pressure, restrict the use of higher concentrations of CTAB in the micellar mobile phases.

It was concluded that DOPAC and CTAB interact more strongly than DA and SDS. DA retention times on the SDS-loaded column were on the order of 45 min in the strongest SDS mobile phase used, while DOPAC retention times on the CTAB-loaded column were on the order of three hours in the strongest CTAB

Table 7. Micellar HPLC Data

Probe	Micelle	t_m[a](avg)(sec)	t_R[b](avg)(sec)	K_{eq}[c](M^{-1})
DA	SDS CTAB	70.6(±0.3) 64.7(±1.5)	1834(±618) 72.3(±0.7)	3×10^4 -----
DAPOL	SDS CTAB	69.8(±0.4) 73.6(±0.7)	161(±12) 86.8(±1.0)	4×10^2 2×10^2 (predicted)
HQ	SDS CTAB	71.2(±0.7) 64.4(±1.9)	120(±4.1) 922(±38)	2×10^2 2×10^3
DOPAC	SDS CTAB	70.2(±0.8) -----	75.7(±1.6) >10800[d]	----- 1×10^5 (predicted)

[a]t_m(avg) is the average solvent retention time over the range of mobile phase concentrations studied (i.e., 0.020 - 0.080 M SDS, 2.0 - 10.1 M CTAB).
[b]t_R(avg) is the average analyte retention time over the range of mobile phase concentrations studied (i.e., 0.020 - 0.080 M SDS, 2.0 - 10.1 M CTAB).
[c]Values calculated from equations 21-26.
[d]The DOPAC peak elutes after more than three hours on the CTAB-loaded column.

mobile phase. The conclusion that DOPAC-CTAB interactions are stronger than DA-SDS interactions is consistent with comparisons of plots of i_{pa} vs t_{dip} (Figure 13a and c) and changes with the addition of surfactants in ΔE_p (Table 2) for these probe-surfactant pairs. The i_{pa} vs t_{dip} curves for DOPAC (Figure 13c) show an enhanced response for DOPAC in the presence of CTAB compared to DOPAC responses in other surfactants which is very close to and intersects with (at exposure times greater than 5 min) the response curve of DOPAC in pure phosphate buffer. The i_{pa} vs t_{dip} curves for DA show a similar enhanced response for DA in the presence of SDS, but this response does not closely approach the response of DA in pure phosphate buffer. Furthermore, ΔE_p values (Table 2) for DOPAC in the presence of CTAB are very close to (i.e., within standard deviations at long exposure times) the ΔE_p values for DOPAC in pure phosphoate buffer, while ΔE_p values (Table 2) for DA in the presence of SDS are 10-18 mV larger than ΔE_p values obtained for DA in pure phosphate buffer. These observations indicate that DOPAC and CTAB interact more strongly than DA and SDS.

DOPAC elutes very close to the solvent front in the SDS mobile phases and DA elutes very close to the solvent front in CTAB mobile phases (Table 7). These results indicate little interaction of DOPAC with SDS molecules in the stationary phase (and thus with SDS micelles) and of DA with CTAB molecules in the stationary phase (and thus with CTAB micelles), which is consistent with the electrochemical results (i.e., plots of i_{pa} vs t_{dip}, slope values of log i_{pa} vs log v, and changes in ΔE_p). For example, plots of i_{pa} vs t_{dip} show that the least sensitive

response for DOPAC is obtained in the presence of SDS (Figure 13c) and that at less sensitive response for DA is obtained in the presence of CTAB than in pure phosphate buffer or in the presence of SDS (Figure 13a). Slope values of log i_{pa} vs log v (Table 1) for DOPAC in the presence of SDS and DA in the presence of CTAB are decreased from their value in pure phosphate buffer to near or below 0.5, indicating that probe adsorption is eliminated by the presence of surfactant in both cases. Elimination of adsorption behavior of probes in the presence of surfactants indicates that probe molecules are not attracted to surfactants which are adsorbed onto the electrode surface. Furthermore, increases in ΔE_p values (Table 2) observed for DOPAC in the presence of SDS and DA in the presence of CTAB indicate slower electrochemical kinetics due to the presence of the surfactant which confirms the observation that DOPAC and SDS molecules and DA and CTAB molecules exhibit little affinity for one another.

DAPOL is weakly retained on the CTAB-loaded column and exhibits interactions with CTAB of approximately one-tenth the strength of HQ-CTAB micelle interactions based on retention times (Table 7). This comparison implies a $K_{eq} \approx 2 \times 10^2\ M^{-1}$ for DAPOL with CTAB micelles which is slightly less than (but on the same order of magnitude as) the K_{eq} listed for DAPOL with SDS micelles (Table 7), indicating that the strength of attractive interactions of DAPOL with CTAB and of DAPOL with SDS are similar with the DAPOL-SDS interactions being slightly stronger. The electrochemical results, including slopes of log i_{pa} vs log v and plots of i_{pa} vs t_{dip}, agree with this assessment of DAPOL interactions with

CTAB and SDS. For example, slopes of log i_{pa} vs log v for DAPOL (Table 1) show that adsorption character is observed in the presence of both CTAB and SDS. However, slope values of log i_{pa} vs log v for DAPOL equal to 0.64 and 0.59 in the presence of SDS and CTAB, respectively, indicate that DAPOL responses show slightly more adsorption character in the presence of SDS. Also, plots of i_{pa} vs t_{dip} (Figure 13b) show similar reduced responses for DAPOL in the presence of both CTAB and SDS (compared to the response in pure phosphate buffer) with the less sensitive of the two responses being observed in CTAB.

This result indicates that DAPOL is more strongly attracted to an electrode coated with SDS than an electrode coated with CTAB. The equilibrium constant for HQ interactions with CTAB micelles is an order of magnitude larger than the equilibrium constant for HQ interactions with SDS micelles (Table 7), in agreement with the electrochemical data where response curves with time (i.e., plots of i_{pa} vs t_{dip}) for HQ are more sensitive in CTAB than in SDS (Figure 13d), slopes of log i_{pa} vs log v for HQ exhibit adsorption behavior in the presence of CTAB and elimination of adsorption in the presence of SDS, and electron-transfer kinetics (as measured by ΔE_p) for HQ are significantly slower in the presence of SDS than in the presence of CTAB.

Comparison of Experimental and Literature K_{eq} Values

Equilibrium constants reported in the literature (Table 8b-e) show that the K_{eq} values determined from micellar HPLC as described by equations 21-26 (Table 8a) are reasonable and consistent with the results of other investigators. Some K_{eq}

Table 8: Probe-micelle association (binding) constants for: a) the probes studied in this work, b) hydroquinone, c) selected catechols, d) selected polar organic molecules, and e) selected cyclic aromatic compounds (i.e., nonpolar organic molecules).

Probe	Molecular Weight(g/mol)	$K_{eq}(M^{-1})$ [SDS]	$K_{eq}(M^{-1})$ [CTAB]
a) Hydroquinone (HQ)[a]	110.11	2×10^2	2×10^3
DAPOL[a]	233.2	4×10^2	2×10^2 [b]
DOPAC[a]	168.1	---	1×10^5 [b]
Dopamine (DA)[a]	189.6	3×10^4	---
b) Hydroquinone[c]	110.11	21.4	---
Hydroquinone[d]	110.11	2.17×10^2	---
Hydroquinone[e]	110.11	9.00×10^2	---
c) Catechol[d]	110.11	4.34×10^2	---
4-methylcatechol[d]	124.15	1.18×10^3	---
Resorcinol[d]	110.11	4.34×10^2	---
2-chlorohydroquinone[d]	144.56	5.58×10^2	---
d) Benzylamine[c]	107.16	5.50×10^2	---
Benzamide[c]	121.14	---	9.55×10^2
Methylbenzoate[c]	136.16	---	4.898×10^3
Benzyl alcohol[c]	108.15	2.95×10^2	1.26×10^3
Nitrobenzene[c]	123.11	5.62×10^2	3.16×10^3
e) p-xylene[f]	106.17	1.6×10^4	---
Biphenyl[g]	154.21	8.5×10^4	---
Anthracene[g]	178.24	3.3×10^5	---
Pyrene[f]	202.26	1.7×10^6	---
Perylene[f]	252.30	1.7×10^7	---

[a]Values calculated from equations 21-26.
[b]Values predicted from retention time comparisons with the other probes.
[c]J.P. Foley, *Anal. Chim. Acta*, **1990**, 231, 237-247.
[d]E. Pelizzetti; E. Pramauro, *Anal. Chim. Acta*, **1985**, 169, 1-29.
[e]D.W. Armstrong, F. Nome, *Anal. Chem.*, **1981**, 53, 1662-1666.
[f]M. Almgren, F. Grieser, J.K. Thomas, *J. Am Chem. Soc.*, **1979**, 101, 279-291.
[g]M. Arunyanart, L.J. Cline-Love, *Anal. Chem.*, **1984**, 56, 1557-1561.

values for the interaction of hydroquinone (HQ) with SDS have been reported (Table 8b) which bracket the value calculated in this work, while Pelizzetti and Pramauro [44] have reported a value almost identical to the one presented herein (Table 8a and b). Equilibrium constants for interactions of DAPOL, DA, and DOPAC with SDS and CTAB and of HQ with CTAB were not found in the literature, however K_{eq} values for compounds structurally similar to those studied here were found (Table 8c and d). The four probe molecules studied in this work are polar organic molecules. DOPAC, DA, and HQ are dihydroxybenzenes and are closely related to catechol and resorcinol. HQ has hydroxy groups substituted onto the 1 and 4 carbon atoms of the benzene ring, while DOPAC and DA have hydroxy groups at the 1 and 2 carbons as well as another group of atoms substituted onto carbon 4 of the benzene ring. At pH 7, DOPAC contains a dissociated carboxyl group ($-CO_2^-$) and DA contains a protonated amine group ($-NH_3^+$) at the end of the carbon 4 substituent (Figure 3). DAPOL has a heterocyclic structure and contains a carbonyl group on one ring and two amine groups on another ring (Figure 3). K_{eq} values for catechols (Table 8c) and for polar organic molecules (Table 8d) which are structurally related to these four probe molecules have been reported. Notice that all of these K_{eq} values are on the order of 10^2-10^3 M^{-1} in good agreement with those values determined for HQ and DAPOL in this work. However, K_{eq} values determined for DA with SDS micelles and predicted for DOPAC with CTAB micelles are on the order of 10^4 and higher (Table 8a). These higher K_{eq} values for the charged probes, DOPAC and DA, can be explained based

on electrostatic interactions between the probe and surfactant molecules. Attractive interactions between neutral organic molecules, such as HQ and DAPOL, and surfactants (i.e., micelles) are due to hydrophobic interactions. These interactions are of moderate strength (since polar molecules have limited hydrophobic character) and yield K_{eq} values on the order of 10^2-10^3 M^{-1}, such as those observed for HQ, DAPOL, the catechols, and the other related neutral compounds (Table 8a, c, and d). The fact that the K_{eq} values for interactions of a given neutral probe with the negatively (SDS) and the positively (CTAB) charged surfactants are similar (i.e., differ by an order of magnitude or less) (Table 8a and d) indicates that the strength of attractive interactions of a neutral species with a surfactant is independent of the charge on the surfactant. This result confirms hydrophobic interactions as the source of attraction between neutral probes and charged surfactants. Interactions between charged organic molecules, such as DOPAC and DA, and charged surfactants, such as SDS and CTAB, involve hydrophobic as well as electrostatic effects. Probes and surfactants (i.e., micelles) having opposite charge, for example DOPAC and CTAB or DA and SDS, exhibit strong attractive interactions, leading to higher K_{eq} values than those obtained for the neutral probes (Table 8a and d). Probes and micelles having the same charge, such as DOPAC and SDS or DA and CTAB, will have very little attraction for one another and may even repel each other, leading to K_{eq} values which are small and difficult to measure (Table 7). It should be noted that large K_{eq} values may also be obtained for the interaction of nonpolar organic molecules, such as cyclic aromatic compounds (Table 8e), with

micelles due to very strong hydrophobic interactions between the nonpolar probes and the hydrophobic micelle interior. It can be seen that as nonpolar molecules become larger and consequently more hydrophobic, the strength of interactions with the surfactant (as measured by K_{eq}) increases (Table 8e). The micellar HPLC results obtained in this work provide a quantitative evaluation of probe-micelle interactions and are consistent with the findings of previous reports as well as the electrochemical data presented herein.

Equilibrium Binding Constants (K_{eq}) Determined from Electrochemical Data

From equation (20) it can be seen that a positive shift in the formal potential, i.e., $(E^{o'}_{M} - E^{o'}_{aq}) > 0$, would indicate that the reduced form of the probe interacts more strongly with surfactant aggregates than the oxidized form, while a negative shift in formal potential, i.e., $(E^{o'}_{M} - E^{o'}_{aq}) < 0$, would indicate stronger interactions for the oxidized form with surfactant aggregates than for the reduced form. Shifts in formal potentials, $E^{o'}_{M} - E^{0'}_{aq}$, observed at RPG electrodes for probe moelcules in SDS, CTAB, and Triton X-100 micellar media are listed in Table 9. $E^{o'}_{M}$ were not calculated for DAPOL since the cathodic peak for this probe cannot be measured in micellar media. Positive changes in formal potential for HQ (Table 9) show that the reduced form of the probe interacts more strongly than the oxidized form with both SDS and CTAB aggregates. The binding constants for the oxidized form of HQ, K_o (Table 9), show that the oxidized form of HQ interacts more strongly with CTAB than with SDS, similar to the behavior of the reduced probe, though the K_o values for HQ with the two surfactants differ by less than an order

Table 9: Average shifts in formal potential at RPG electrodes over the range of exposure times from 0 to 10 min for probes in surfactant concentrations above CMC[a] and equilibrium constants for the reduced and oxidized forms of the probes with surfactant aggregates; T = 25(±1)°C; v = 200 mV/s.

Probe	Surfactant	$E^{o'}_{M}$-$E^{o'}_{aq}$ (mV)	K_R[b](M^{-1})	K_o[c](M^{-1})
Hydroquinone	SDS	6.7(±6.7)	2×10^2	$1._2 \times 10^2$
	CTAB	12.2(±4.7)	2×10^3	$7._7 \times 10^2$
	Triton X-100	-19.1(±6.0)	---	---
DOPAC	SDS	23.3(±11.5)	---	---
	CTAB	0.45(±2.9)	1×10^5	$9._7 \times 10^4$
	Triton X-100	-18.2(±11.3)	---	---
Dopamine	SDS	4.7(±1.5)	3×10^4	$2._1 \times 10^4$
	CTAB	-2.3(±2.0)	---	---
	Triton X-100	-15.9(±3.9)	---	---

[a]Surfactant concentrations above CMC: 10mM SDS, 3mM CTAB, 3mM Triton X-100.
[b]Calculated from HPLC data as described by equations 21-26.
[c]Calculated from HPLC and electrochemical data as described by equations 5-20.

of magnitude. Positive shifts in formal potential for DOPAC (Table 9) show that the reduced form of the probe interacts more strongly with SDS aggregates than the oxidized form. Very small shifts in formal potential for DOPAC (Table 9) show that the oxidized and reduced forms interact with CTAB aggregates with approximately equal strength. Small positive changes in formal potential for DA indicate that interactions of the reduced form of the probe are slightly stronger than those of the oxidized form with CTAB aggregates and small negative changes in formal potential for DA indicate that interactions of the oxidized form of the probe are slightly stronger than those of the reduced form with SDS aggregates (Table 9). Comparisons of the interactions of the oxidized forms of DOPAC and DA with various surfactant aggregates, i.e., comparisons of K_o values for a given probe in different media, are not possible, since K_R, i.e., K_{eq}, was obtained for only one surfactant, CTAB, with DOPAC and one surfactant, SDS, with DA due to the limitations of the micellar HPLC data. According to shifts in formal potential (Table 9), the oxidized form of all three probe molecules interacts more strongly with Triton X-100 aggregates than the reduced form.

The most significant shift in formal potential was observed for DOPAC in SDS micellar media indicating that the electrochemical properties of the oxidized and reduced forms of DOPAC in the presence of SDS are the most distinguishable of the oxidized and reduced probes studied here. The aim of this research is to develop media in which various probe species as well as different oxidation states of probes can be differentiated using electrochemical methods. DOPAC in the

presence of SDS is a promising example of a system in which oxidation states may be selectively detected.

CHAPTER VI

RESPONSE OF HYDROPHILIC ELECTRODES IN SURFACTANT SOLUTIONS BELOW THE CRITICAL MICELLE CONCENTRATION

Deactivation of RPG Surface

Electrode Activity

In this study, SDS, CTAB, and Triton X-100 were present in the buffer at concentrations below CMC and cyclic voltammetry was used to measure probe responses at RPG electrodes. When measurements are taken immediately after placing the electrode in solution (i.e., exposure time designated as t_{dip} = 0 min), high sensitivity is observed for all probes in the presence of surfactants at concentrations below CMC (Figure 14). As the exposure time of electrode to solution is increased, the peak currents of all probes gradually decrease and in many cases level-off between exposure times of 5 and 10 minutes (Figure 14). An exception to this behavior is the response of the second oxidation peak of DAPOL in the presence of SDS below CMC which gradually increases with time similar to the response in SDS concentrations above CMC (Figure 10c).

The probe responses obtained at longer exposure times in the presence of surfactant at low concentrations are similar to those obtained in micellar media, both in magnitude and in trends of sensitivity (Figure 13 and Figure 14). For example, DA in the presence of SDS at concentrations above CMC exhibits

Figure 14: Normalized peak current (i_{pa}/AC_o) vs exposure time (t_{dip}) for: a) dopamine (DA), b) DAPOL, c) DOPAC, and d) hydroquinone (HQ) at RPG electrodes in phosphate buffer (pH 7, μ = 0.5 M) and in the indicated surfactant at concentrations below CMC; v = 200 mV/s.

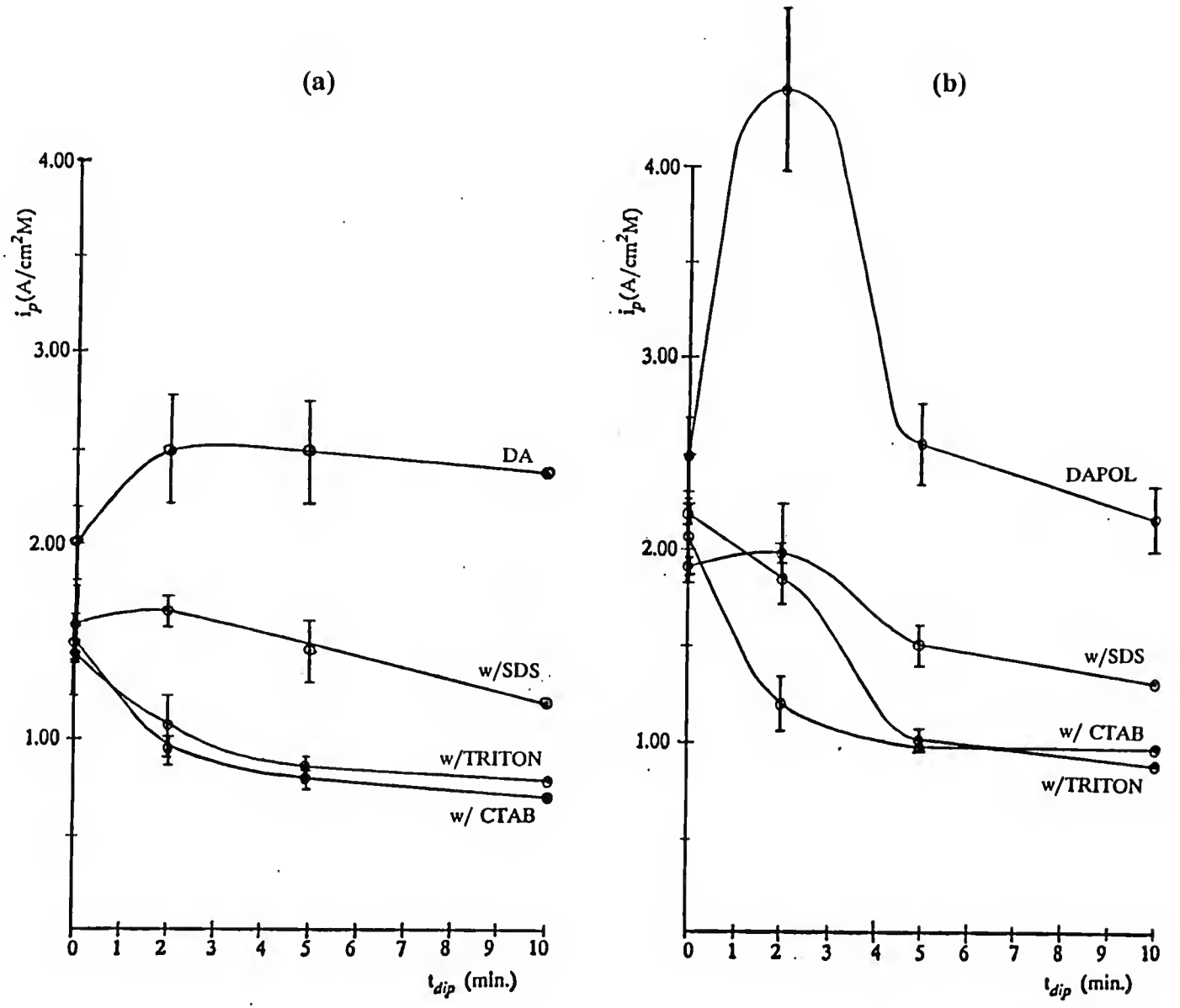
(a)
(b)
4.00
3.00
2.00
1.00
i_p(A/cm^{2}M)
DA
w/SDS
w/TRITON
w/ CTAB
DAPOL
0 1 2 3 4 5 6 7 8 9 10
t_{dip} (min.)

Figure 14: (continued) Normalized peak current (i_{pa}/AC_o) vs exposure time (t_{dip}) for: a) dopamine (DA), b) DAPOL, c) DOPAC, and d) hydroquinone (HQ) at RPG electrodes in phosphate buffer (pH 7, μ = 0.5 M) and in the indicated surfactant at concentrations below CMC; v = 200 mV/s.

(c)

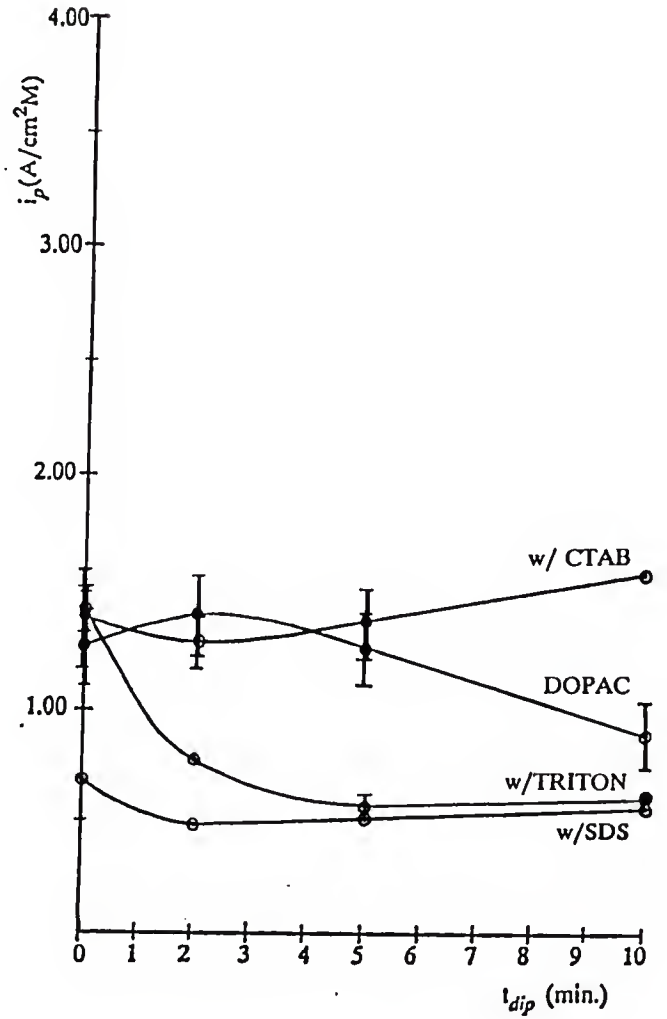
4.00
3.00
2.00
1.00
i_p(A/cm^{2}M)
w/ CTAB
DOPAC
w/TRITON
w/SDS
0 1 2 3 4 5 6 7 8 9 10
t_{dip} (min.)

(d)

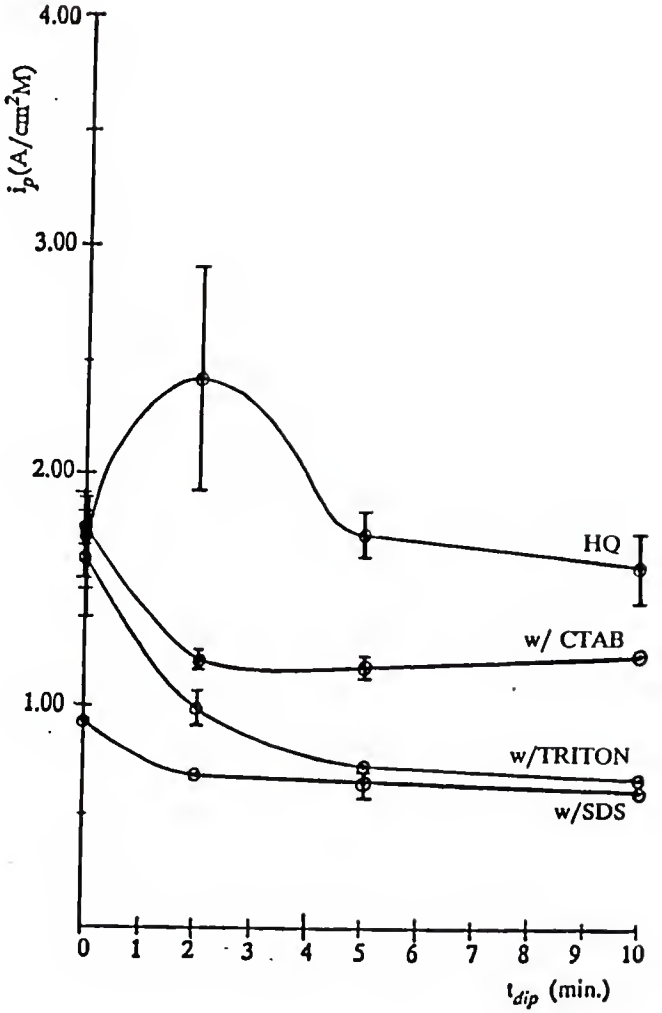
4.00
3.00
2.00
1.00
i_p(A/cm^{2}M)
HQ
w/ CTAB
w/TRITON
w/SDS
0 1 2 3 4 5 6 7 8 9 10
t_{dip} (min.)

responses which are more sensitive than those obtained in CTAB and Triton X-100 and which are less sensitive than those obtained in pure phosphate buffer (Figure 13a). This trend is also observed for DA in solutions at low surfactant concentrations (below CMC) when exposure time exceeds two minutes (Figure 14a). Likewise, DAPOL exhibits enhanced responses in the presence of SDS compared to the responses in other surfactants (Figure 13b and Figure 14b) and DOPAC and HQ exhibit enhanced responses in the presence of CTAB compared to the responses in other surfactants (Figure 13c and d; Figure 14c and d) at concentrations above and below CMC when exposure times exceed 2 minutes. All probes exhibit the most sensitive RPG responses in the absence of surfactants (i.e., in pure phosphate buffer) at all exposure times studied (Figures 13 and 14), except DOPAC which exhibits the highest responses in the presence of CTAB at long exposure times (Figures 13c and 14c).

Electron Transfer Kinetics

The effect of surfactant concentrations below CMC on electrochemical kinetics as measured by ΔE_p can be seen in Table 10. The rates of electron transfer for the probe molecules are not affected immediately by the presence of low concentrations of surfactants (below CMC). However, at longer electrode exposure times, the probe-surfactant pairs that showed little interaction in the micellar experiments exhibit marked increases in ΔE_p with time (Table 10) indicating slower electron transfer kinetics. The ΔE_p values obtained at longer exposure times in the

Table 10: Anodic to cathodic peak-to-peak potential separations (ΔE_p in mV) at RPG electrodes[a] in the presence of surfactant concentrations below CMC[b]; n = 200 mV.

t_{dip}[c] (min)	Surfactant[b]	Dopamine	DAPOL[d]	Hydro-quinone	DOPAC
0	N	33 (±4)	14 (±4)	32 (±7)	28 (±4)
2	O	30 (±0)	26 (±4)	38 (±4)	30 (±0)
5	N	33 (±5)	30 (±0)	23 (±0)	23 (±5)
10	E	30 (±0)	30 (±8)	40 (±0)	47 (±12)
0	C	40 (±7)	--	30 (±0)	23 (±8)
2	T	50 (±0)	--	43 (±5)	27 (±5)
5	A	67 (±9)	--	43 (±9)	33 (±5)
10	B	80	--	40	30
0	S	33 (±5)	--	87 (±17)	148 (±36)
2	D	50 (±8)	--	147 (±5)	313 (±17)
5	S	50 (±0)	--	163(±21)	303 (±5)
10		50	--	160	330
0	Triton	37 (±5)	--	32 (±10)	27 (±5)
2	X-100	57 (±5)	--	63 (±5)	90 (±0)
5		77 (±5)	--	113(±13)	240 (±36)
10		80	--	170	300

[a]All solutions in phosphate buffer, pH 7.0, μ = 0.5 M.
[b]Surfactant concentrations below CMC; 1mM SDS, 0.3mM CTAB, 0.106mM Triton X-100.
[c]t_{dip} - exposure time of electrode to analyte solution at an open circuit.
[d]ΔE_p values for the first oxidation peak of DAPOL (Peak I_a).

presence of surfactant concentrations below CMC (Table 10) closely resemble the ΔE_p values obtained in surfactant concentrations above CMC (Table 2).

Surface Model

The results discussed above show that similar probe responses are observed at RPG electrodes in the presence of surfactants at concentrations above and below CMC when exposure times are allowed to exceed 5 minutes. For example, the RPG electrode surface is deactivated in the presence of high and low surfactant concentrations. However, improvements in the electrochemistry for probe molecules (i.e., more sensitive peak currents and faster rates of electron transfer) in the presence of specific surfactants, compared to the results in other surfactants, are observed at surfactant concentrations above and below CMC. These improvements in the electrochemistry for specific probe-surfactant pairs indicate attractive interactions between probes and adsorbed surfactants.

To explain the probe responses obtained at RPG electrodes in surfactant concentrations above CMC it was hypothesized that surfactants adsorb onto the electrode surface in the form of two-dimensional aggregates called hemimicelles (Figure 1c). On the same hydrophilic RPG surface at surfactant concentrations below CMC, it is expected that surfactant molecules will adsorb onto the electrode in the same manner (i.e., in the form of two-dimensional aggregates with head groups oriented toward the electrode surface as well as toward the bulk solution). The similarities between probe responses in surfactant concentrations above and below CMC indicate that with time surfactants form hemimicelles at the electrode

surface in the presence of low surfactant concentrations as well as in high surfactant concentrations. Other workers [72,75-78] have also reported the formation of hemimicelles on hydrophilic surfaces in the presence of surfactant concentrations below CMC.

Electrode Reactivity and Electron Transfer Kinetics

Based on observations from plots of normalized peak currents vs time (Figure 13; Figure 14) and changes in peak-to-peak separations (Table 2 and 9), it appears that the adsorption of surfactants at concentrations above CMC occurs immediately after placing the electrode in solution while the adsorption of surfactants at concentrations below CMC is time dependent. This time dependent adsorption behavior can be explained strictly in terms of surfactant concentrations near the electrode surface. In a highly concentrated surfactant solution (above CMC), the solution is densely populated with micelles and free surfactant molecules. Therefore, when an RPG electrode is placed in a highly concentrated surfactant solution, the process of surfactant monomer adsorption onto the electrode surface and the subsequent interaction of surfactant molecules with the adsorbed surfactant occurs very quickly to form hemimicelles on the electrode surface. In dilute surfactant solutions (below CMC), surfactant molecules are dispersed throughout the solution so that surfactant monomers do not immediately encounter the electrode surface when an electrode is placed in solution. The time effect observed for the adsorption of surfactants at concentrations below CMC depends on the rate at which surfactants accumulate at the electrode surface.

Different rates of decrease in peak currents (Figure 14) and different rates of increase in ΔE_p (Table 9) for probes in SDS, CTAB, and Triton X-100 at concentrations below CMC suggest that surfactant molecules aggregate at different rates. For example, the effect of the presence of SDS at concentrations below CMC can be seen almost immediately both in normalized peak currents and ΔE_p for HQ and DOPAC (Figure 14; Table 10), indicating that assembly of SDS molecules into hemimicelles occurs relatively quickly. This result is not surprising since SDS is the mallest of the surfactant molecules studied here and has the lowest aggregation number (See CHAPTER 2, Reagents).

Probe Adsorption

Time dependent surfactant adsorption at concentrations below CMC is confirmed by changes in the dependence of peak current (i_{pa}) on scan rate (v) with increased exposure time (Table 11). At t_{dip} = 0 min, the slope values of log i_{pa} vs log v plots for all probes in all surfactants are well above 0.5 indicating probe adsorption at the electrode surface which is uninhibited by the presence of surfactant in solution. The initial slope values (i.e., t_{dip} = 0 min) obtained in the presence of SDS are slightly lower than those obtained in pure phosphate buffer while initial slope values obtained in the presence of CTAB and Triton X-100 are slightly larger than those obtained in pure phosphate buffer. The immediate decrease in probe adsorption (i.e., decrease in slopes of log i_{pa} vs log v) observed in the presence of SDS indicates that SDS molecules accumulate more rapidly at the

Table 11: SCAN RATE STUDIES: Slopes of log peak current vs log scan rate plots at RPG electrodes in the presence of surfactant concentrations below CMC[a].

Solution	Dopamine[b]	DAPOL[b]	Hydroquinone[b]	DOPAC[b]
Buffer[c]	0.62(±0.01)	0.72(±0.01)	0.69(±0.02)	0.65(±0.02)
SDS[a]				
t_{dip}[d]=0 min	0.60(±0.02)	0.66(±0.01)	0.57(±0.03)	0.61(±0.04)
t_{dip}[d]=5 min	0.56(±0.02)	0.65(±0.02)	0.42(±0.01)	0.48(±0.02)
CTAB[a]				
t_{dip}[d]=0 min	0.66(±0.02)	0.76(±0.02)	0.71(±0.02)	0.67(±0.02)
t_{dip}[d]=5 min	0.41(±0.02)	0.60(±0.02)	0.56(±0.01)	0.62(±0.03)
Triton X-100				
t_{dip}[d]=0 min	0.70(±0.03)	0.73(±0.02)	0.73(±0.04)	0.70(±0.01)
t_{dip}[d]=5 min	0.41(±0.01)	0.53(±0.01)	0.47(±0.01)	0.46(±0.01)

[a]Surfactant concentrations below CMC: 1 mM SDS, 0.3mM CTAB, 0.106mM Triton X-100.
[b]Probe concentrations: 0.5mM dopamine, 0.2mM DAPOL, 0.3mM hydroquinone, 0.5mM DOPAC.
[c]All solutions in phosphate buffer, pH 7.0, μ = 0.5 M.
[d]t_{dip} - exposure time of electrode to analyte solution at an open circuit.

electrode surface than CTAB and Triton X-100 molecules. At t_{dip} = 5 min, slope values decrease to values similar to those obtained in micellar media (Table 1 and 11). Adsorption character of responses is eliminated for the same probe-surfactant pairs that showed no interaction in the micellar studies. For example, it was observed in the micellar experiments that none of the probes interact well with Triton X-100. Likewise, at concentrations below the CMC and t_{dip} = 5 min, adsorption is eliminated in all probe-Triton X-100 solutions as indicated by the slope values of log i_{pa} vs log v plots (Table 11). The effects of low surfactant concentrations (below CMC) on the adsorption of probe molecules at RPG electrodes, as observed from slopes of log i_{pa} vs log v plots with time confirm that surfactant molecules present in solution at concentrations below CMC adsorb onto the electrode in the same form, proposed to be hemimicelles, as they do in surfactant solutions with concentrations above CMC and that surfactant adsorption at RPG electrodes is time dependent in solutions with low surfactant concentrations.

Conclusions

Based on the effects of surfactants on electrode reactivity (i.e., i_{pa} vs t_{dip} plots), electron transfer kinetics (i.e, ΔE_p values), and probe adsorption (i.e., log i_{pa} vs log v plots), it is evident that the surfactants studied here adsorb onto the RPG electrode surface in the presence of surfactant concentrations above and below CMC. The adsorption of surfactants on the RPG surface is instantaneous upon placing the electrode in solutions with surfactant concentrations above CMC, while the adsorption of surfactants on RPG occurs with time in solutions with surfactant

concentrations below CMC. Also, different rates of adsorption are observed for different surfactants at concentrations below CMC.

CHAPTER VII

RESPONSE OF HYDROPHOBIC ELECTRODES IN SURFACTANT SOLUTIONS

In order to investigate the effects of surfactant on the electrode surface, the electrochemical behavior of probe molecules in the presence of surfactants was studied at glassy carbon (GC) electrodes. In this work, SDS and CTAB were added to solutions at concentrations above and below CMC and cyclic voltammetry was used to measure probe responses. The probe responses at GC in the presence of surfactants at concentrations above and below CMC are very similar, therefore the results will be discussed simultaneously unless otherwise specified. Experiments in the presence of Triton X-100 were not performed at GC, since probe responses with time, ΔE_p values, and slopes of log i_{pa} vs log v plots at RPG electrodes indicate no interaction between the probes and Triton X-100. Based on the results at RPG, it was expected that no probe-Triton X-100 interactions would be observed at GC electrodes although the surfactant may adsorb on GC. One objective of this work is to improve electrode activity by the addition of surfactants to solution and consequently onto the electrode surface. If a surfactant, such as Triton X-100, does not show attractive interactions with any of the probes, no improvement in electrochemistry will be observed and further investigation of solutions of this surfactant will be uninformative.

Probe Adsorption

Slope values of log i_{pa} vs log v for all probes at GC electrodes are ca. 0.5 for all solution compositions (Table 3) indicating that the electrochemical processes for these probes on GC are diffusion controlled in all media studied here. That is, the presence of surfactant at the electrode surface and subsequent interaction of probes with the surfactant do not lead to adsorption behavior of the probes at GC.

Electrode Reactivity

The normalized peak current (i_{pa}) vs exposure time (t_{dip}) plots in the absence and presence of surfactants at GC electrodes are shown in Figure 15. Similarities between effects of surfactant on probe responses at GC and RPG electrodes can be seen from electrode reactivity (i.e., i_{pa} vs t_{dip} plots). For example, at GC electrodes DOPAC and HQ exhibit higher responses in the presence of CTAB at concentrations above and below CMC than in pure phosphate buffer or in the presence of SDS (Figure 15c and d). This behavior is similar to that observed at RPG (Figure 13c and d), where DOPAC and HQ responses in CTAB are enhanced compared to those obtained in SDS and approach (but typically do not exceed) the responses in pure phosphate buffer. For DA at GC, the lowest responses are obtained in the presence of CTAB at concentrations above and below CMC (Figure 15a). This behavior of DA is similar to that observed at RPG (Figure 13a and Figure 14a) where DA responses in the presence of CTAB are much lower than those obtained in the presence of SDS or in pure phosphate buffer. At GC, DA responses in pure phosphate buffer are slightly larger than those in the presence of

Figure 15: Normalized peak current (i_{pa}/AC_o) vs exposure time (t_{dip}) for: a) dopamine (DA), b) DAPOL, (c) DOPAC, and d) hydroquinone (HQ) at GC electrodes in phosphate buffer (pH 7, μ = 0.5 M) and in the indicated surfactant at concentrations above and below CMC; v = 200 mV/s.

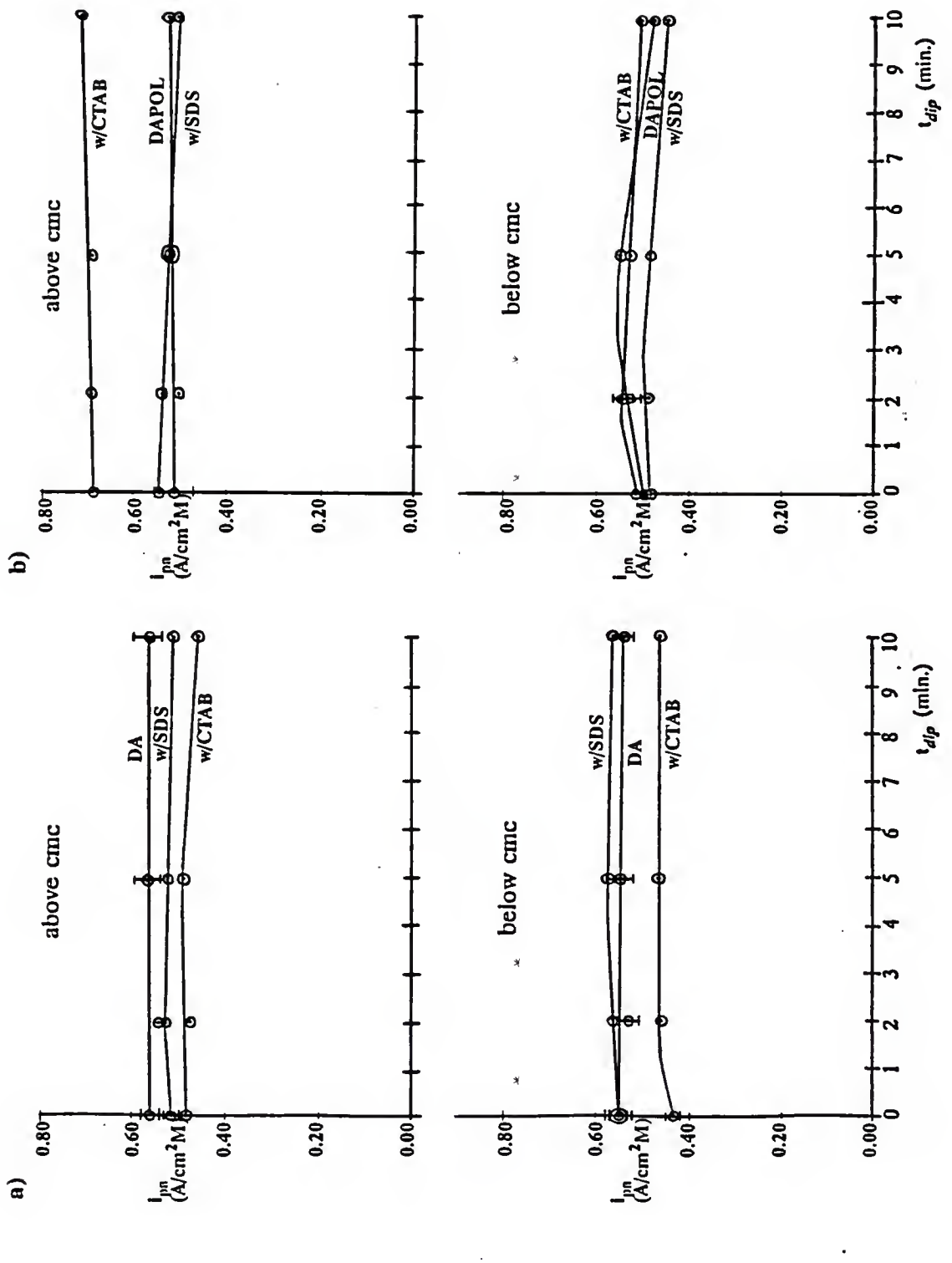
a)
above cmc
below cmc
DA
w/SDS
w/CTAB
b)
above cmc
below cmc
w/CTAB
DAPOL
w/SDS
I_{pn} (A/cm^{2}M)
t_{dip} (min.)
0.00
0.20
0.40
0.60
0.80
0
1
2
3
4
5
6
7
8
9
10

Figure 15: (continued) Normalized peak current (i_{pa}/AC_o) vs exposure time (t_{dip}) for: a) dopamine (DA), b) DAPOL, c) DOPAC, and d) hydroquinone (HQ) at GC electrodes in phosphate buffer (pH 7, μ = 0.5 M) and in the indicated surfactant at concentrations above and below CMC; v = 200 mV/s.

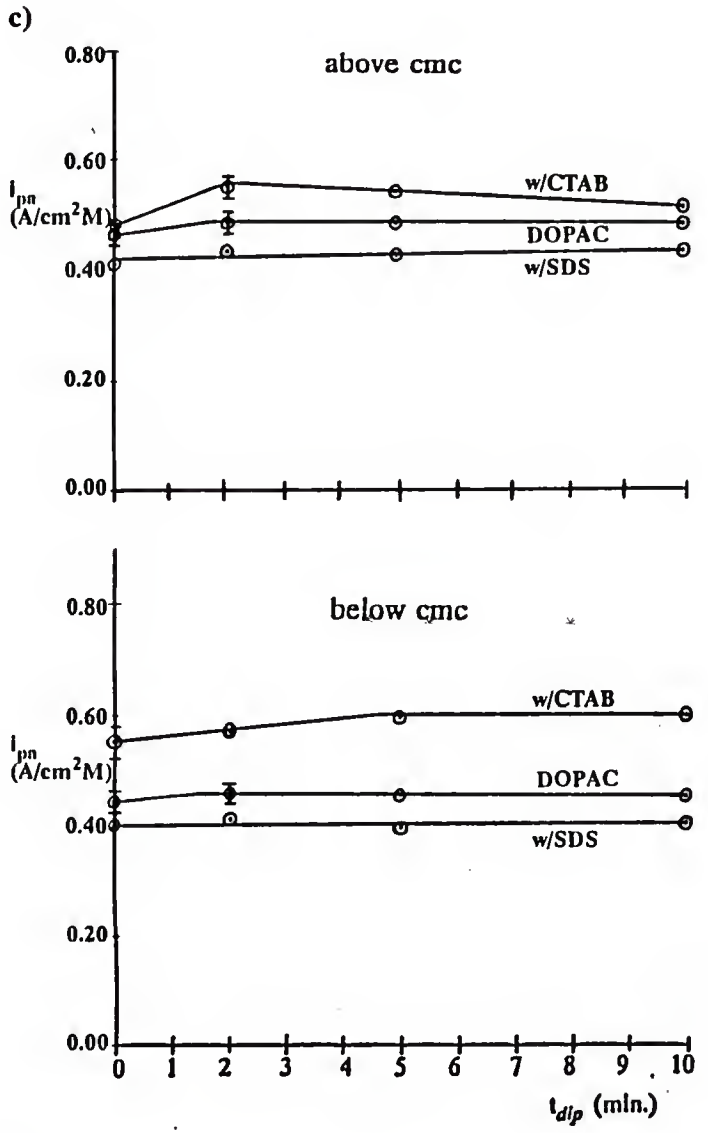
c)
above cmc
0.80
0.60
0.40
0.20
0.00
i_{pn} (A/cm^{2}M)
w/CTAB
DOPAC
w/SDS
below cmc
0.80
0.60
0.40
0.20
0.00
i_{pn} (A/cm^{2}M)
w/CTAB
DOPAC
w/SDS
0 1 2 3 4 5 6 7 8 9 10
t_{dip} (min.)

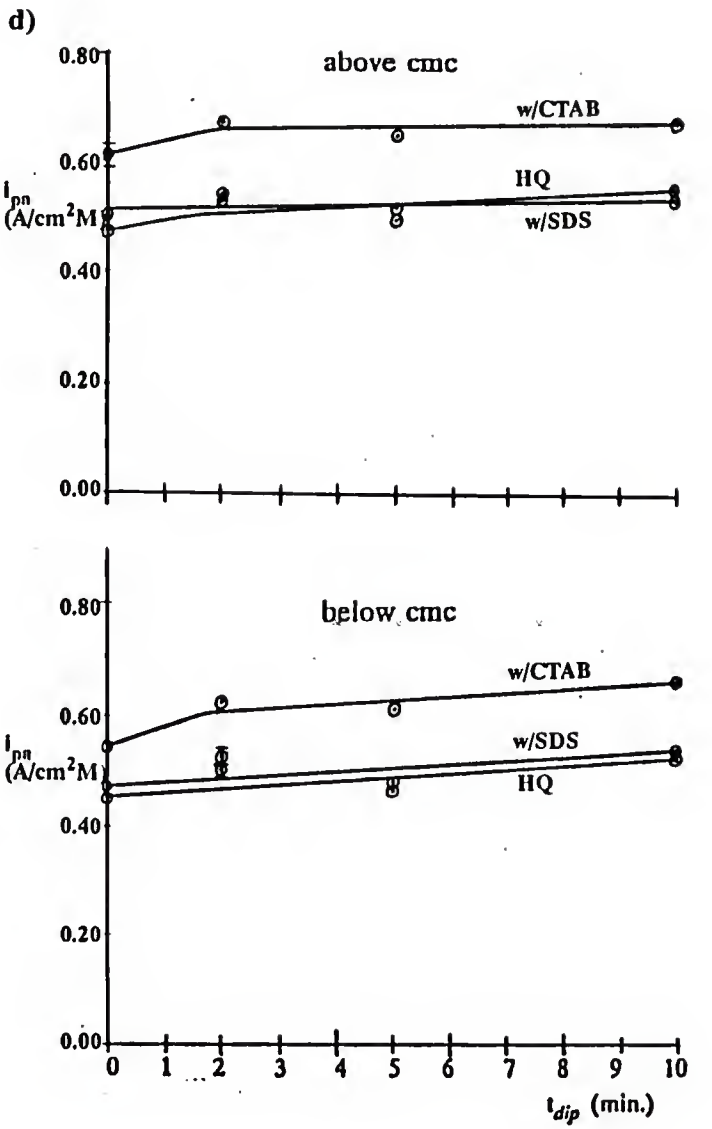
d)
above cmc
0.80
0.60
0.40
0.20
0.00
i_{pn} (A/cm^{2}M)
w/CTAB
HQ
w/SDS
below cmc
0.80
0.60
0.40
0.20
0.00
i_{pn} (A/cm^{2}M)
w/CTAB
w/SDS
HQ
0 1 2 3 4 5 6 7 8 9 10
t_{dip} (min.)

SDS at concentrations above CMC and are almost identical to those in the presence of SDS at concentrations below CMC (Figure 15a).

Differences between the effects of surfactants on probe responses at GC and RPG were observed for DAPOL. For example, the most sensitive responses for DAPOL at GC electrodes are observed in the presence of CTAB at concentrations above CMC and the least sensitive responses at GC are obtained in the presence of SDS at concentrations below CMC (Figure 15b). This behavior differs from that at RPG (Figure 13b) where the highest DAPOL response in the presence of surfactants is obtained in SDS. Also, the GC response for DAPOL in pure phosphate buffer, in SDS solutions at concentrations above CMC, and in CTAB solutions at concentrations below CMC are all very similar to each other (Figure 15b), whereas at RPG distinctive differences in sensitivity are observed in each medium (Figures 13b and Figure 14b).

Surface Models

In evaluating the similarities and differences between probe responses at RPG and GC electrodes in the presence of surfactants one feature is striking. The main difference is that probe responses in surfactants at RPG are rarely more sensitive than the responses in pure phosphate buffer, whereas the sensitivity of probe responses at GC may increase in the presence of surfactants above that obtained in pure phosphate buffer (Figure 13 and Figure 15). When discussing results at GC, enhanced and depressed responses refer to responses either above or below those obtained in pure phosphate buffer. However, enhanced responses at

RPG refer to probe responses in the presence of one surfactant which are more sensitive than probe responses in other surfactant solutions and less sensitive than probe responses in phosphate buffer. This difference and the similarities between responses at RPG and GC discussed in the previous section (i.e., enhanced responses for DOPAC and HQ in the presence of CTAB and for DA in the presence of SDS) can be explained in terms of surface models for surfactant adsorption and in terms of interactions of probe molecules with the adsorbed surfactants.

As previously described in CHAPTER 1, Systems Studied, Electrodes, GC is structurally and electrochemically different than RPG. GC is an amorphous, hydrophobic form of graphite which exhibits relatively low electrochemical reactivity [6,7,21,30,83,85] in contrast to the very ordered, hydrophilic RPG which exhibits high electrochemical reactivity [7,30,34,37]. The high activity of the RPG electrodes in phosphate buffer is largely due to probe adsorption at active sites, described in CHAPTER 1, Theories of Graphite Activity, on the active electrode surface. When an RPG electrode is placed in a surfactant solution, the surface is blocked by adsorbed surfactant in the form of hemimicelles as proposed by the model in Figure 1 and the electrode surface becomes deactivated, i.e., depressed probe responses are obtained (Figure 13). At RPG, attractive interactions between probe molecules and adsorbed hemimicelles may improve the response, but the high sensitivity observed in the absence of surfactant is not attained. On GC electrodes, probe molecules do not adsorb and low sensitivity is obtained in phosphate buffer. When a GC

electrode is placed in a surfactant solution, surfactant molecules adsorb at the electrode surface with their hydrophobic hydrocarbon chains oriented toward the electrode surface and their hydrophilic head groups extending out into the solution (Figure 2). On GC electrodes, attractive interactions between probes and adsorbed surfactants draw probe molecules to the electrode surface, increasing the rate of heterogeneous electron-transfer and leading to higher responses than those obtained in the absence of surfactants. The manner by which surfactants lower the barrier to electron transfer at GC is not well understood, however it can be seen from slope values of log i_{pa} vs log v plots below 0.5 (Table 3) that probe adsorption is not a contributing factor. At GC in aqueous media, the adsorbed surfactant molecules with their charged, hydrophilic head groups oriented toward the solution will attract neither the like charged head groups nor the hydrophobic tail groups of the free surfactants in solution. Therefore, further adsorption due to interaction between free surfactants and adsorbed surfactant molecules to form two-dimensional aggregates, as observed at RPG (Figure 1c), is not likely (Figure 2c).

At both RPG and GC electrodes, adsorption of surfactants onto the electrode results in a surfactant-covered surface with hydrophilic head groups oriented toward the solution (Figure 1c and Figure 2b). On both surfaces, attractive interactions may occur between charged probe molecules (or neutral probe molecules with a polar group) and the charged surfactant head groups. Hydrophobic interactions may also occur between probes and the surfactant hydrocarbon tails leading to partitioning of probes into the surfactant layer close to the electrode surface.

Partitioning of probes may be greater in hemimicelles at RPG surfaces than in surfactants at GC, explaining why adsorption is observed at RPG and not at GC. Based on these surface models, it is expected that attractive interactions will occur between the same probe-surfactant pairs at both RPG and GC electrodes and the results concur. For example, the responses for DOPAC and HQ in the presence of CTAB are enhanced at both RPG and GC electrodes (Figure 13c and d; Figure 15c and d).

In cases where attractive interactions do not occur between probe and surfactant molecules, probe responses at GC electrodes are either unaffected or slightly decreased from those obtained in pure phosphate buffer. Probe responses at RPG electrodes, however, are severely depressed compared to those in pure phosphate buffer due to deactivation of the electrode by the adsorbed surfactant. For example, depressed responses for probe molecules in the presence of surfactants of the same charge are observed at both RPG and GC electrodes (e.g., DOPAC with SDS or dopamine with CTAB) with the more dramatic effects of surfactant being observed at RPG (Figure 13a and c; Figure 15a and c). Also, responses of the neutral probes, HQ and DAPOL, in the presence of surfactants are depressed at RPG (Figure 13b and d) and are unaffected at GC electrodes (Figure 15b and d).

Electron Transfer Kinetics

The ΔE_p values observed at RPG (Table 2) and at GC (Tables 4 and 12) support the surface models for surfactant adsorption discussed above. Recall that ΔE_p values for diffusion controlled processes, such as the electron transfer processes

Table 12: Anodic to cathodic peak-to-peak potential separations (ΔE_p in mV) at polished GC electrodes[a] in the presence of surfactant concentrations below CMC[b]; v = 200 mV/s.

t_{dip}[c] (min)	Surfactant[b]	Dopamine	DAPOL[d]	Hydro-quinone	DOPAC
0	N	133(±21)	--	310(±29)	366(±69)
2	O	191(±5)	--	300(±18)	333(±57)
5	N	150(±22)	--	280	390
10	E	150(±22)	--	315	350
0	C	280(±8)	--	187(±5)	180(±0)
2	T	283(±13)	--	157(±5)	178(±2)
5	A	280	--	160(±8)	170
10	B	290	--	150	180
0	S	197(±2)	--	390(±0)	571(±12)
2	D	185(±4)	--	377(±13)	567 (±5)
5	S	170	--	390	570
10		175	--	380	570

[a]All solutions in phosphate buffer, pH 7.0, μ = 0.5 M.
[b]Surfactant concentrations below CMC; 1mM SDS, 0.3mM CTAB, 0.106mM Triton X-100.
[c]t_{dip} - exposure time of electrode to analyte solution at an open circuit.
[d]ΔE_p values cannot be obtained - reduction peak not observed on GC.

for the probe molecules at GC, are predicted to be 59/n (mV), where n is the number of electrons transferred, for reversible (fast) heterogeneous electron transfer [92]. All of the probes studied here undergo $2e^-/2H^+$ oxidation [5,7,42,82], so that ΔE_p values of approximately 30 mV are expected at GC for fast electron transfer kinetics. In pure phosphate buffer (Table 4), the average ΔE_p values for dopamine studied is 156(±21) mV, while the average ΔE_p values for DOPAC and HQ are 301(±13) mV and 360(±21) mV, respectively. These results indicate that the heterogeneous electron transfer kinetics for all of the probes at GC are slow (i.e., irreversible) in the absence of surfactants.

The effects of surfactants on the ΔE_p values (i.e., the heterogeneous electron-transfer kinetics) observed for the probes at GC electrodes are similar to those observed at RPG. At both GC and RPG, ΔE_p values are relatively small for DOPAC and HQ in the presence of CTAB and for dopamine in the presence of SDS, while ΔE_p values are large for DOPAC and HQ in the presence of SDS and for dopamine in the presence of CTAB (Tables 2,4, and 12). Increases in the rate of electron transfer at GC (i.e., decreases in ΔE_p) for DOPAC and HQ in the presence of CTAB and dopamine in the presence of SDS compared to the rate observed in pure phosphate buffer support attractive interactions between the same probe-surfactant pairs, i.e., DOPAC and CTAB, HQ and CTAB, and dopamine and SDS, as observed at RPG. These results confirm the surfactant adsorption models discussed above (Figure 1c and Figure 2b) which suggest that similar modification of the surface with hydrophilic head groups oriented toward the solution phase

occurs at RPG and GC in the presence of surfactants and indicate that similar attractive interactions between probe molecules and adsorbed surfactants will be observed at both electrodes. At RPG, the adsorption of surfactant molecules diminishes, but does not eliminate, probe adsorption behavior for probes which attractively interact with the adsorbed surfactant (Table 1). Therefore, attractive interactions between probes and adsorbed surfactants, such as DOPAC and CTAB, result in low ΔE_p values which are close to but still larger than the ΔE_p values obtained in pure phosphate buffer (Table 2). That is, the rates of electron-transfer for the probes at RPG are nearly the same in pure phosphate buffer and in solutions in which attractive interactions occur between the probes and the adsorbed surfactants. At GC, attractive interactions between probes and adsorbed surfactants may lead to ΔE_p values which are lower than those obtained in pure phosphate buffer, indicating an increase in the rate of electron-transfer in the presence of certain surfactants compared to those in the absence of surfactants. For example, in the presence of CTAB the average ΔE_p value for HQ at GC decreases by more than 130 mV and the average ΔE_p value for DOPAC at GC decreases by more than 180 mV compared to responses in the absence of surfactant (Tables 4 and 12). In agreement with the peak current measurements with time, the ΔE_p values in the presence of surfactants show that attractive interactions between probes and adsorbed surfactants can improve the electrochemical response of GC. At both RPG and GC electrodes, when attractive interactions do not occur between probes and adsorbed surfactants, such as DOPAC and SDS or dopamine and CTAB, ΔE_p

values are significantly larger than those observed in the absence of surfactants (Table 2, 4, and 12) indicating that the rate of electron transfer is decreased compared to that in phosphate buffer.

Surfactant Adsorption

Differences in surfactant adsorption can be seen from differences in the magnitude of probe responses at RPG and GC electrodes. The pronounced effects of CTAB on probe responses at RPG and GC indicate that CTAB adsorbs at both surfaces. Marked effects of SDS on probe responses at RPG and small effects of SDS on probe responses at GC indicate that SDS adsorbs at RPG but not at GC electrodes.

At hydrophilic RPG, CTAB and SDS appear to interact with the electrode surface and depress or enhance probe responses (i.e., i_{pa} vs t_{dip} plots) according to probe interactions with the adsorbed surfactants. For example, the presence of CTAB at RPG enhances the responses of DOPAC and HQ (Figure 13c and d), which attractively interact with CTAB, compared to responses in the presence of other surfactants. Adsorbed CTAB at RPG depresses the responses of DAPOL and dopamine (Figure 13a and b), which are not attracted to CTAB, compared to responses observed in phosphate buffer and in the presence of SDS. Also, the presence of SDS at RPG enhances the responses of dopamine and DAPOL (Figure 13a and b), which attractively interact with SDS, compared to responses in the presence of other surfactants and depresses the responses of DOPAC and HQ

(Figure 13c and d), which are not attracted to SDS. Both surfactants adsorb at RPG to yield the observed effects.

At the hydrophobic GC electrode, CTAB appears to interact with the surface and significantly affects probe responses whereas SDS appears to interact poorly and has little or no effect on probe responses. For example, the most sensitive responses for DOPAC, HQ, and DAPOL at GC are observed in the presence of CTAB (Figure 15b-d) and the least sensitive responses for dopamine are observed in the presence of CTAB (Figure 15a). On the other hand, the responses are essentially unaffected by the presence of SDS in solution (Figure 15b and d). This is for the neutral probes, DAPOL and HQ. The response of dopamine is slightly enhanced in the presence of SDS (Figure 15a) and the response of DOPAC is slightly depressed in the presence of SDS (Figure 15c). These results show that at GC, the presence of CTAB leads to large enhancement or large depression of probe responses while the presence of SDS leads to much smaller changes. The minimal effects of SDS on probe responses at GC indicate either that none of the probes attractively interact with SDS adsorbed at the electrode surface or that SDS is not adsorbed or forms a structure that is very different than on RPG. Since it has been established from the results at RPG, i.e., i_{pa} vs t_{dip} plots (Figure 13 and Figure 14), ΔE_p values (Tables 2 and 10), and slope values of log i_{pa} vs log v plots (Tables 1 and 11), and from K_{eq} values (Tables 7 and 8) that DA and DAPOL attractively interact with SDS. Therefore, the small effects of SDS on probe responses at GC indicate

that SDS adsorbtion at the GC electrode surface, if it occurs at all, produces a surface that is not significantly different than GC and very different than RPG.

On the hydrophobic GC surface, surfactant molecules adsorb onto the electrode with their hydrophobic tail groups oriented toward the electrode surface and their hydrophilic head groups oriented toward the solution (Figures 2a and b). Previous reports have shown a correlation between surfactant adsorption and chain length [73,75]. As the number of carbon atoms in the hydrocarbon tail group of a surfactant increases, the tail group becomes more hydrophobic and will adsorb onto hydrophobic surfaces. Based on probe responses at GC electrodes, it appears that the hydrophobicity of the 16-carbon CTAB tail is sufficient to promote strong interaction between CTAB and the hydrophobic GC surface, while that of the 12-carbon SDS tail is not. At the hydrophilic RPG surface, surfactant molecules adsorb with hydrophilic head groups toward the electrode surface (Figure 1) so that surfactant adsorption is independent of chain length. Probe responses (i.e., i_{pa} and t_{dip} plots; Figure 13) in the presence of CTAB and SDS at RPG indicate that both surfactants adsorb at this electrode surface.

The ΔE_p values indicate differences in the effect of SDS and CTAB molecules at GC. The effects of SDS on ΔE_p values at GC are generally less dramatic than of CTAB (Tables 4 and 12). For example, at GC electrodes the average ΔE_p values for DOPAC and HQ in the presence of CTAB decrease by 180 mV and 130 mV, respectively, indicating a substantial increase in the rate of electron transfer, while ΔE_p value for dopamine in the presence of SDS are

increases by less than 30 mV, indicating only slight improvement in the rate of electron transfer compared to that observed in pure phosphate buffer. The K_{eq} values from the micellar HPLC for interactions of these probe-surfactant pairs cannot explain the different surfactant effects, since the K_{eq} for dopamine-SDS interactions is an order of magnitude larger than the K_{eq} for HQ-CTAB interactions (Table 8a). Therefore, the differences between the effects of CTAB and SDS on probe kinetics at GC must be explained by differences in surfactant adsorption efficiency.

K_{eq} Determined from Electrochemical Data

According to Equation 23, difference between the formal potentials observed for probe molecules in phosphate buffer, $E^{o'}_{aq}$, and those observed in the presence of surfactants, $E^{o'}_{M}$, indicates which form of the probe, i.e., the oxidized or the reduced form, interacts more strongly with surfactant molecules. The shifts in formal potentials at GC for probes in the presence of surfactants, $E^{o'}_{M} - E^{o'}_{aq}$, the binding constants for the reduced probes, K_R, obtained from the micellar chromatography, and the binding constants for the oxidized probe, K_o, obtained from $E^{o'}_{M} - E^{o'}_{aq}$ and K_R according to equation 25 are listed in Table 13. Formal potentials for DAPOL at GC could not be calculated since the reduction peak of DAPOL is not well-defined on GC electrodes. For DOPAC and HQ in the presence of CTAB, substantial negative shifts in formal potentials and K_o values that are an order of magnitude larger than the K_R (Table 13) show that the oxidized forms of DOPAC and HQ interact more strongly with CTAB than the reduced

Table 13: Average shifts in formal potential at polished GC electrodes over the range of exposure times from 0 to 10 min for probes in the presence of surfactant concentrations: a) above CMC[a] and b) below CMC[b] and equilibrium constants for the reduced and oxidized forms of the probes with surfactant aggregates; T = 25(±1)°C; v = 200 mV/s.

Probe	Surfactant	$E^{o'}_M - E^{o'}_{aq}$ (mV)	$K_R{}^b(M^{-1})$	$K_o{}^c(M^{-1})$
a) Surfactant concentrations above CMC[a]				
Hydroquinone	SDS	6.5(±5.2)	2×10^2	$1._2 \times 10^2$
	CTAB	-35.2(±2.2)	2×10^3	$3._1 \times 10^4$
	Triton X-100	38.4(±6.9)	---	---
DOPAC	SDS	38.4(±6.9)	---	---
	CTAB	-32.3(±5.1)	1×10^5	$1._2 \times 10^6$
Dopamine	SDS	-4.3(±10.2)	3×10^4	$4._2 \times 10^4$
	CTAB	16.9(±10.1)	---	---
b) Surfactant concentrations below CMC[b]				
Hydroquinone	SDS	9.0(±4.2)	2×10^2	$9._9 \times 10^1$
	CTAB	-29.8(±2.2)	2×10^3	$2._0 \times 10^4$
DOPAC	SDS	35.5(±5.6)	---	---
	CTAB	-34.3(±4.8)	1×10^5	$1._4 \times 10^6$
Dopamine	SDS	-5.6(±7.3)	3×10^4	$4._6 \times 10^4$
	CTAB	14.0(±6.5)	---	---

[a]Surfactant concentrations above CMC: 10mM SDS and 3mM CTAB.
[b]Surfactant concentrations below CMC: 1mM SDS and 0.3mM CTAB.
[c]Calculated from HPLC data as described by equations 21-26.
[d]Calculated from HPLC and electrochemical data as described by equations 5-20.

forms of the probes. For HQ with SDS, small positive shifts in formal potential and moderate binding constants (Table 13) indicate that the reduced form of HQ is slightly more attracted to SDS than the oxidized form. Interactions for DOPAC with SDS and DA with CTAB are too small to be measured by micellar HPLC, so that equilibrium constants were these probe-surfactant pairs. However, the positive shifts in formal potentials for these probe surfactant pairs (Table 13) indicate that the reduced form of dopamine interacts more strongly with CTAB than the oxidized form (i.e., $K_R > K_o$ from equation 20) and the reduced form of DOPAC interacts more strongly with SDS than the oxidized form. For dopamine in the presence of SDS, small negative shifts in the formal potential and large equilibrium constants with the same order of magnitude for both forms of the probe (Table 13) indicate similar, strong interactions of the oxidized and reduced forms of the probe with SDS. The largest shifts in formal potentials at GC are the positive shift observed for DOPAC in SDS, the negative shift observed for DOPAC in CTAB, and the negative shift observed for HQ in CTAB (Table 13). These large changes in formal potentials in surfactant solutions, especially the contrasting behavior of DOPAC in SDS and DOPAC in CTAB, suggest that it may be possible to selectively detect different oxidation states of a probe using electrochemistry in the presence of a specific surfactant.

Conclusions

In summary, it appears that at GC electrodes surfactants adsorb as monomers, rather than as aggregates, with head groups oriented toward the solution

phase. Attractive interactions between probe molecules and adsorbed surfactants at GC lead to increased probe responses (i.e., i_{pa} vs t_{dip} plots) and improved electron-transfer kinetics (i.e., decreased ΔE_p values) compared to those in the absence of surfactants. Surfactant adsorption onto the hydrophobic GC surface depends on the hydrophobic character of the surfactant, i.e., the length of the surfactant hydrocarbon chain. The effects of CTAB and SDS on the probe responses at GC indicate that the 16-carbon CTAB tail interacts better with the GC surface than the 12-carbon SDS tail.

CHAPTER VIII

SUMMARY AND FUTURE WORK

It has been shown that the probes studied, DA, DOPAC, DAPOL and HQ exhibit different electrochemical behavior on different types of carbon electrodes specifically: 1) probe molecules adsorb onto RPG electrodes but do not adsorb onto GC electrodes; 2) the sensitivity of probe responses on RPG electrodes varies from species to species and changes with time for each probe, whereas probe responses on GC electrodes are nearly identical and are constant with time; and 3) probe responses on RPG electrodes exhibit better sensitivity and poorer precision than probe responses on GC.

The addition of surfactant molecules, to buffer solutions at concentrations above and below CMC affects probe responses on both RPG and GC surfaces. At RPG, surfactant molecules adsorb as hemimicelles and effectively decrease the sensitivity of probe responses and their rate of electron-transfer, increase the precision of probe responses, and, at concentrations above CMC, eliminate the changes in response with time. If attractive interactions occur between a probe molecules and adsorbed hemimicelles at RPG, the probe responses are altered less by the presence of the interacting surfactant than by the presence of non-interactive surfactants. That is, relatively sensitive responses with high precision are obtained at RPG when probe molecules attractively interact with the surfactant. At GC,

surfactants adsorb as surfactant monomers resulting in increased, decreased, or unaffected probe responses depending on the strength of probe interactions with adsorbed surfactant molecules and the strength of surfactant adsorption onto the electrode surface. Attractive interactions between a probe molecule and adsorbed surfactant at GC lead to probe responses which are more sensitive than those obtained in pure phosphate buffer, if a sufficient amount of surfactant is present at the electrode surface. For probe-surfactant pairs that attractively interact, comparisons of peak currents normalized for electrode area and probe concentration show that the improved responses at GC are less sensitive but slightly more precise than the corresponding responses at RPG. The probe responses at GC in the presence of surfactants suggest that a surfactant hydrocarbon chain having greater than 12 carbons may be necessary to ensure efficient surfactant adsorption onto the hydrophobic GC surface.

The equilibrium constants, K_{eq}, for interactions between probe and surfactant molecules, determined from micellar HPLC experiments, verify the attractive interactions observed in electrochemistry. The K_{eq} values obtained in this work agree well with literature K_{eq} values. The K_{eq} values from micellar chromatography represent the equilibrium constants for the reduced form of the probes, K_R, and the equilibrium constants for the oxidized form of the probes, K_o, were obtained from electrochemical results. Electrochemical results can also be used to detect differences in the strength of interactions between the oxidized and reduced forms of the probe molecules with surfactants when equilibrium constants are not

available. The results, especially those obtained at GC, suggest that it may be possible to selectively detect different oxidation states of a probe using carbon electrodes in combination with surfactant media.

The results discussed above indicate that the addition of surfactants to probe solutions can be used to control the electrode surface and to improve the electrochemical response. For example, the addition of surfactants creates a less sensitive but more reproducible RPG surface for the detection of probe molecules than is observed without surfactants. Also, the presence of surfactants in solution creates a more sensitive GC surface, while maintaining the high precision observed at GC in the absence of surfactants. By adding surfactants to probe solutions, electrode surfaces are modified by the adsorption of surfactants from solution. By adding the appropriate surfactant to a given probe solution, sensitive and reproducible probe responses can be obtained for specific probes. Preferential interactions between probes and surfactants may be predicted based on the structure and charge of the probe and surfactant molecules and on the results of studies like the ones presented here. These preferential interactions between probes and surfactants may be exploited in developing methods of detection for small biological materials.

Work in this area in the immediate future should be aimed at applying the knowledge presented here to developing analytically useful methods. That is, the linear dynamic range of probe concentrations which can be studied in the presence of surfactants and the feasibility of using surfactants in flowing systems, such as flow-

injection analysis (FIA), with carbon electrode detection should be investigated. Fundamental studies of the effects of surfactant chain length on the efficiency of surfactant adsorption at GC electrodes are also needed in order to optimize surface coverage by surfactants and increase sensitivity to probe responses. The next progressive step in this research would be to pursue the selective detection of one probe in the presence of other probes or in a more complicated matrix than phosphate buffer utilizing surfactant additives and carbon electrodes.

BIBLIOGRAPHY

1 P.M. Kovach; M.R. Deakin; R.M. Wightman. *J.Phys.Chem.* **1986**, 90, 4612-4617.

2 K.J. Stutts; P.M. Kovach; W.G. Kuhr; R.M. Wightman. *Anal.Chem.* **1983**, 55, 1632-1634.

3 R.M. Wightman; M.R. Deakin; P.M. Kovach; W.G. Kuhr; K.J. Stutts. *J. Electrochem.Soc.* **1984**, 131, 1578-1583.

4 D.T. Fagan; I.-F. Hu; T. Kuwana. *Anal.Chem.* **1985**, 57, 2759-2763.

5 M.R. Deakin; P.M. Kovach; K.J. Stutts; R.M. Wightman. *Anal.Chem.* **1986**, 58, 1474-1480.

6 G.W. Hance; T. Kuwana. *Anal.Chem.* **1987**, 59, 131-134.

7 L. Bodalbhai; A. Brajter-Toth. *Anal.Chem.* **1988**, 60, 2557-2561.

8 E. Hershenhart; R.L. McCreery; R.D. Knight. *Anal.Chem.* **1984**, 56, 2256-2257.

9 R.J. Bowling; R.T. Packard; R.L. McCreery. *J.Am.Chem.Soc.* **1989**, 111, 1217-1223.

10 M. Poon; R.L. McCreery. *Anal.Chem.* **1986**, 58, 2745-2750.

11 R.J. Rice; R.L. McCreery. *Anal.Chem.* **1989**, 61, 1637-1641.

12 M. Poon; R.L. McCreery. *Anal.Chem.* **1987**, 59, 1615-1620.

13 C.W. Miller; D.H. Karweik; T. Kuwana. *Anal.Chem.* **1981**, 53, 2319-2323.

14 J.F. Evans; T. Kuwana; M.T. Henne; G.P. Royer. *J.Electroanal.Chem.* **1977**, 80, 409-416.

15 J.F. Evans; T. Kuwana. *Anal.Chem.* **1977**, 49, 1632-1635.

16 I.-F. Hu; D.H. Karweik; T. Kuwana. *J.Electroanal.Chem.* **1985**, 188, 59-72.

17 D.C. Thornton; K.T. Corby; V.A. Spendel; J. Jordan; A. Robbat, Jr.; D.J. Rutstrom; M. Gross; G. Ritzler. *Anal.Chem.* **1985**, 57, 150-155.

18 G.N. Kamau; W.S. Willis; J.F. Rusling. *Anal.Chem.* **1985**, 57, 545-551.

19 M.R. Deakin; K.J. Stutts; R.M. Wightman. *J.Electroanal.Chem.* **1985**, 182, 113-122.

20 M.E. Rice; Z. Galus; R.N. Adams. *J.Electroanal.Chem.* **1983**, 143, 89-102.

21 R.C. Engstrom; V.A. Strasser. *Anal.Chem.* **1984**, 56, 136-141.

22 R. Bowling; R.T. Packard; R.L. McCreery. *Langmuir* **1989**, 5, 683-688.

23 A.A. Gewirth; A.J. Bard. *J.Phys.Chem.* **1988**, 92, 5563-5566.

24 J.-X. Feng; M. Brazell; K. Renner; R. Kasser; R.N. Adams. *Anal.Chem.* **1987**, 59, 1863-1867.

25 R.C. Engstrom. *Anal.Chem.* **1982**, 54, 2310-2314.

26 L. Falat; H.-Y. Cheng. *Anal.Chem.* **1982**, 54, 2108-2111.

27 R.E. Vasquez; H. Imai. *J.Electroanal.Chem.* **1985**, 192, 389-403.

28 L.J. Kepley; A.J. Bard. *Anal.Chem.* **1988**, 60, 1459-1467.

29 R. Bowling; R. Packard; R.L. McCreery. *J.Electrchem.Soc.* **1988**, 135, 1605-1606.

30 L. Bodalbhai; A. Brajter-Toth. *Anal.Chim.Acta* **1990**, 231, 191-201.

31 I.-F. Hu; T.Kuwana. *Anal.Chem.* **1986**, 58, 3235-3239.

32 G.E. Cabaniss; A.A. Diamantis; W.R. Murphy, Jr.; R.W. Linton; T.J. Meyer. *J.Am.Chem.Soc.* **1985**, 107, 1845-1853.

33 J.S. Mattson; H.B. Mark, Jr.; M.D. Malbin; W.J. Weber, Jr.; J.C. Crittenden. *J.Colloid Interface Sci.* **1969**, 31, 116-130.

34 R.E. Panzer; P.J. Elving. *Electrochim.Acta* **1975**, 20, 635-647.

35 R.J. Bowling; R.L. McCreery; C.M. Pharr; R.C. Engstrom. *Anal.Chem.* **1989**, 61, 2763-2766.

36 F.A. Armstrong; P.A. Cox; H.A.O. Hill; V.J. Lowe; B.N. Oliver. *J.Electroanal.Chem.* **1987**, 217, 331-366.

37 C.-W. Lee; A.J. Bard. *J.Electrochem.Soc.* **1988**, 135, 1599-1600.

38 R.A. Saraceno; A.G. Ewing. *Anal.Chem.* **1988**, 60, 2016-2020.

39 A.G. Ewing; R.M. Wightman; M.A. Dayton. *Brain Research* **1982**, 249, 361-370.

40 J.E. Baur; E.W. Kristensen; L.J. May; D.J. Wiedemann; R.M. Wightman. *Anal.Chem.* **1988**, 60, 1268-1272.

41 R. Bowling; R.L. McCreery. *Anal.Chem.* **1988**, 60, 605-608.

42 D. Astwood; C.N. D'Amico; T. Lippincott; A. Brajter-Toth. *J.Electroanal.Chem.* **1986**, 198, 283-302.

43 N. Shinozuka; S. Hayano. In *Solution Chemistry of Surfactants*, Vol. 2, K.L. Mittal (ed.), Plenum Press, New York, 1979, p.599-623.

44 E. Pelizzetti; E. Pramauro. *Anal.Chim.Acta* **1985**, 169, 1-29.

45 W.L. Hinze. In *Solution Chemistry of Surfactants*, Vol. 1, K.L. Mittal (ed.), Plenum Press, New York, 1979, p.79-127.

46 G.L. McIntire. *CRC Critical Reviews in Analytical Chemistry* **1990**, 21, 257-278.

47 L.J. Cline-Love; J.G. Habarta; J.G. Dorsey. *Anal.Chem.* **1984**, 56, 1132A-1148A.

48 E. Jacobsen. *Anal.Chim.Acta* **1966**, 35, 447-452.

49 G. Kalland; E. Jacobsen. *Acta Chem.Scand.* **1963**, 17, 2385-2390.

50 Y. Fujihira; T. Kuwana; C.R. Hartzell. *Biochem.Biophys.Res.Commun.* **1974**, 61, 538-543.

51 P. Yeh; T. Kuwana. *J.Electrochem.Soc.* **1976**, 123, 1334-1339.

52 G.L. McIntire; D.M. Chiappardi; R.L. Casselberry; H.N. Blount. *J.Phys.Chem.* **1982**, 86, 2632-2640.

53 G.L. McIntire; H.N. Blount. *J.Am.Chem.Soc.* **1979**, 101, 7720-7721.

54 G. Meyer; L.Nadjo; J.M. Saveant. *J.Electroanal.Chem.* **1981**, 119, 417-419.

55 A.E. Kaifer; A.J. Bard. *J.Phys.Chem.* **1985**, 89, 4876-4880.

56 A.E. Kaifer; A.J. Bard. *J.Phys.Chem.* **1987**, 91, 2006-2007.

57 P.A. Quintela; A.E. Kaifer. *Langmuir* **1987**, 3, 769-773.

58 T.C. Franklin; M. Iwunze. *Anal.Chem.* **1980**, 52, 973-976.

59 Y. Ohsawa; S. Aoyagui. *J.Electroanal.Chem.* **1982**, 136, 353-360.

60 M.J. Eddowes; M. Grätzel. *J.Electroanal.Chem.* **1984**, 163, 31-64.

61 M.J. Rosen. *Surfactants and Interfacial Phenomena*, John Wiley and Sons, New York, 1989.

62 J.R. Kirchhoff; E. Deutsch; W.R. Heineman. *Anal.Lett.* **1989**, 22, 1323-1340.

63 M. Almgren; F. Grieser; J.K. Thomas. *J.Am.Chem.Soc.* **1979**, 101, 279-291.

64 R. Zana. In *Surfactant Solutions: New Methods of Investigation*, R. Zana (ed.), Marcel Dekkar, Inc., New York, 1987, p. 279-285.

65 K.S. Birdi; M. Meyle; E. Stenby. In *Surfactants in Solution*, Vol. 1, K.L. Mittal and B. Lindman (eds.), Plenum Press, New York, 1984, p.645-661.

66 F.C. De Schryver; Y. Croonen; E. Geladé; M. Van der Auweraer; J.C. Dederen; E. Roelants; N. Boens. In *Surfactants in Solution*, Vol. 1, K.L. Mittal and B. Lindman (eds.), Plenum Press, New York, 1984, p.663-672.

67 Y. Ohsawa; Y. Shimazaki; S. Aoyagui. *J.Electroanal.Chem.* **1980**, 114, 235-246.

68 M. Arunyanart; L.J. Cline-Love. *Anal.Chem.* **1984**, 56, 1557-1561.

69 M. Arunyanart; L.J. Cline-Love. *Anal.Chem.* **1985**, 57, 2837-2843.

70 J.P. Foley. *Anal.Chim.Acta* **1990**, 231, 237-247.

71 P. Chandar; P. Somasundaran; N.J. Torro. *J.Colloid Interface Sci.* **1987**, 117, 31-46.

72 J.F. Scamehorn; R.S. Schechter; W.H. Wade. *J.Colloid Interface Sci.* **1982**, 85, 463-478.

73 M.D. Porter; T.B. Bright; D.L. Allara; C.E.D. Chidsey. *J.Am.Chem.Soc.* **1987**, 109, 3559-3568.

74 H.O. Finklea; S. Avery; M. Lynch; T. Furtsch. *Langmuir* **1987**, 3, 409-413.

75 P. Somasundaran; T.W. Healy; D.W. Fuerstenau. *J.Phys.Chem.* **1964**, 68, 3562-3566.

76 P. Somasundaran; D.W. Fuerstenau. *J.Phys.Chem.* **1966**, 70, 90-96.

77 J.T. Kunjappu; P. Somasundaran. *Colloids Surf.* **1989**, 38, 305-311.

78 C. Ma; C. Li. *J.Colloid Interface Sci.* **1989**, 131, 485-492.

79 B.-Y. Zhu; T. Gu. *Colloids Surf.* **1990**, 46, 339-345.

80 C.A. Widrig; C.J. Miller; M. Majda. *J.Am.Chem.Soc.* **1988**, 110, 2009-2011.

81 E. Sabatani; I. Rubinstein; R. Maoz; J. Sagiv. *J.Electroanal.Chem.* **1987**, 219, 365-371.

82 G. Dryhurst; K.M. Kadish; F. Scheller; R. Renneberg. *Biological Electrochemistry*, Vol. 1, Academic Press, New York, 1982.

83 G.M. Jenkins; K. Kawamura. *Nature* **1971**, 231, 175-176.

84 L. Bodalbhai. Ph.D. Dissertation, University of Florida, 1989.

85 C.-W. Lee; A.J. Bard. *J.Electroanal.Chem.* **1988**, 239, 441-446.

86 M.D. Hawley; S.V. Tatawawadi; S. Piekarski; R.N. Adams. *J.Am.Chem.Soc.* **1967**, 89, 447-450.

87 T. Ishimitsu; S. Hirose; H. Sakurai. *Talanta* **1977**, 24, 555-560.

88 J.A. Dean (ed.). *Lange's Handbook of Chemistry*, McGraw-Hill Book Company, New York, 1979.

89 P. Mukerjee; K.J. Mysels. *Critical Micelle Concentrations of Aqueous Surfactant Systems*, National Bureau of Standards (NSRDS-NBS 36), U.S. Government Printing Office, Washington, D.C., 1971.

90 K.L. Mittal; P. Botheral (eds.). *Surfactants in Solution*, Plenum Press, New York, 1986, p.855.

91 M. Stackelberg; M. Pilgram; V. Toome. *Z.Electrochem.* **1953**, 57, 342.

92 A.J. Bard; L.R. Faulkner. *Electrochemical Methods: Fundamentals and Applications*, John Wiley and Sons, New York, 1980, pp.213-242, 488-531, 538-546.

93 G. Gerhardt; R.N. Adams. *Anal.Chem.* **1982**, 54, 2618-2620.

94 L. Bodalbhai. Unpublished results.

95 R.N. Adams. *Electrochemistry of Solid Electrodes*, Marcel Dekker, Inc., New York, 1969, p.221.

96 F. Hine; M. Yasuda; M. Iwata. *J.Electrochem.Soc.* **1974**, 121, 749-756.

97 D.W. Armstrong; F. Nome. *Anal.Chem.* **1981**, 53, 1662-1666.

BIOGRAPHICAL SKETCH

Stacey Elizabeth Boyette was born in Hopewell, VA, on March 19, 1964. After graduating covaledictorian from Hopewell High School in 1982, she attended East Carolina University in Greenville, NC, where she played intercollegiate softball and earned a B.S. degree in chemistry. Among other academic and athletic awards received throughout high school and college, Miss Boyette was three times named Academic All-American during her career at East Carolina University. Graduating from college in May 1986, she began her graduate work at the University of Florida in the fall of that year. While completing her dissertation, Miss Boyette accepted a position as Temporary Assistant Professor at Georgia Southern University for the academic year 1990-1991. In the summer of 1991, she returned to the University of Florida for her final defense.

I certify that I have read this study and that in my opinion it conforms to acceptable standards of scholarly presentation and is fully adequate, in scope and quality, as a dissertation for the degree of Doctor of Philosophy.

Anna Brajter-Toth, Chairman
Associate Professor of Chemistry

I certify that I have read this study and that in my opinion it conforms to acceptable standards of scholarly presentation and is fully adequate, in scope and quality, as a dissertation for the degree of Doctor of Philosophy.

James D. Winefordner
Graduate Research Professor of Chemistry

I certify that I have read this study and that in my opinion it conforms to acceptable standards of scholarly presentation and is fully adequate, in scope and quality, as a dissertation for the degree of Doctor of Philosophy.

Vaneica Y. Young
Associate Professor of Chemistry

I certify that I have read this study and that in my opinion it conforms to acceptable standards of scholarly presentation and is fully adequate, in scope and quality, as a dissertation for the degree of Doctor of Philosophy.

William M. Jones
Distinguished Service Professor of Chemistry

I certify that I have read this study and that in my opinion it conforms to acceptable standards of scholarly presentation and is fully adequate, in scope and quality, as a dissertation for the degree of Doctor of Philosophy.

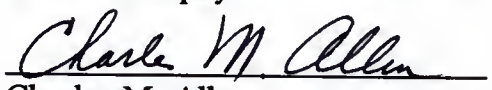

Charles M. Allen
Professor of Biochemistry and
Molecular Biology

This dissertation was submitted to the Graduate Faculty of the Department of Chemistry in the College of Liberal Arts and Sciences and to the Graduate School and was accepted as partial fulfillment of the requirements for the degree of Doctor of Philosophy.

August, 1991

_____
Dean, Graduate School